Characterisation of follicular helper T (Tfh) cells in early treated HIV-infected children: relationship to immune activation and inflammation.

by

Paulina Olifant

Thesis presented in fulfilment of the requirements for the degree of Master of Science in the Faculty of Medicine and Health Sciences at Stellenbosch University.

Supervisor: Prof Richard Glashoff

Department of Pathology. Division of Medical Microbiology. Unit of Immunology.

December 2022

Declaration

By submitting this thesis electronically, I declare that the entirety of the work contained therein is my own, original work, that I am the sole author thereof (save to the extent explicitly otherwise stated), that the reproduction and publication and publication thereof by Stellenbosch University will not infringe any third-party rights and that I have not previously in its entirety or in part submitted it for obtaining any qualification.

December 2022

Abstract

Background: South Africa has a high burden of Human Immunodefiency Virus (HIV) infection. Babies of HIV-positive pregnant women can become HIV-infected or exposed through vertical transmission. Follicular helper T (Tfh) cells have been of particular interest in HIV infection due to their preferential expansion, contribution to the HIV reservoir and dysregulation within HIV-infected individuals. The aim of this study was to investigate the Tfh cell population within children from the Children with HIV Early Antiretroviral Therapy (CHER) trial who started treatment within the first six months of life to determine whether the numbers of these cells is altered as compared to uninfected children and also whether persistent immune activation and inflammation in these children is associated with Tfh cell dysregulation.

Methodology: This retrospective cross-sectional observational study consisted of three groups, i.e., early antiretroviral-treated HIT (HIV Infected Treated), HEU (HIV Exposed Uninfected) and HUU (HIV Uninfected Unexposed), of children. Cryopreserved peripheral mononuclear blood cells (PBMCs) were stained with an 11-colour antibody panel designed and optimised for phenotypic identification and quantification of T cell populations using flow cytometry. Tfh cells populations were characterised as CD4+CXCR5+PD-1+ with/without ICOS+. CD4, CD8 and Treg cells were defined as follicular/ follicular-homing based on CXCR5+ expression and activated based on CD38+ and/or CD69+ expression. Secondary data of clinical parameters and inflammatory cytokines for each group were evaluated. Statistical comparisons between groups were made using the Mann-Whitney test to identify significant differences. Significant correlations between Tfh cells and clinical parameters, other T cell populations and inflammatory cytokines were identified using Spearman's rank order test.

Results: Phenotypic results generally indicated significantly increased proportions of CD38+ subsets in HIT group and CD69+ subsets in HEU group. Although there was no significant difference in median CD4+CXCR5+PD-1+ Tfh cell percentage between groups, the ICOS-expressing subset namely CD4+CXCR5+PD-1+ICOS+ Tfh cells was significantly higher in the HIT (33.6% vs 19.2%; $p = 0.016$) and HEU group (31.6% vs 19.2%; $p = 0.006$) compared to the HUU group. In the HIT group, CD4+CXCR5+PD-1+ Tfh cells shared significant negative correlations with a majority

of activated T cell subsets. A significant positive correlation between CD4+CXCR5+PD-1+ Tfh and CD8+PD-1+ Tc cells, general indicator of immune exhaustion, was demonstrated. Lastly, the HIT group showed the highest level of INF-α and hsCRP inflammatory cytokines and levels of IL-1β and hsCRP significantly correlated with CD4+CXCR5+PD-1+ICOS+ Tfh cells within this group.

Conclusions: Overall levels of immune activation were significantly higher in HIT and HEU groups. Several activated T cell subsets inversely correlated with CD4+CXCR5+PD-1+ Tfh cells, suggesting high levels of immune activation can lead to decreased proportions of circulating Tfh cells. Even though no significant difference in the proportion of CD4+CXCR5+PD-1+ Tfh cells was found between groups, the ICOS+ subset was significantly expanded in HIT and HEU children in comparison to HUU children. The significant positive correlation between IL-1β and ICOS-expressing Tfh cells, within the entire study population and HIT group, suggested that increased inflammation resulted in an Tfh cell increase.

Opsomming

Agtergrong: Suid Afrika het ‘n hoë las van Menslike Immuniteitsgebreksvirus (MIV) infeksie. Babas van MIV-positiewe vrouens kan MIV-besmet word of blootgestel word deur vertikale oordraging. Tfh selle is van besondere belang in MIV infeksie as gevolg van voorkeuruitbreiding, bydrae tot die MIV reservoir en wanregulering in persone wat MIV besmet is. Die doel van hierdie studie was om te ondersoek op die Tfh sel populasie, in kinders van die CHER studie wie ART begin het binne die eerste ses maande van lewe, se getalle veranderd is in vergelyking met kinders wat nie besmet is en ook of aanhoudende immuun aktivering en inflammasie in hierdie kinders geassosieer is met Tfh sel wanregulasie.

Metodes: Hierdie retrospektiwe observasie deurneestudies bestaan uit drie groepe, dit is vroegtydige ART-behandelde MIV Infeksie (sogenaamde HIT), MIV blootgestel en nie geinfekteerd (sogenaamde HEU) en MIV nie geinfekteerd en nie blootgestel (sogenaamde HUU) kinders. Gekruipreserveerde PBMCs was verwerk met ‘n elf-kleur teenliggaam paneel wat ontwerp en optimiseer is vir fenotipiese identifikasie en kwantifisering van T cell populasie deur van vloeisitometrie gebruik te maak. Tfh sel populasie was gekenmerk as CD4+CXCR5+PD-1+ met/sonder ICOS+. CD4, CD8 and Treg selle was gedefineer as follikulêre/follikulêrmigrerende gebaseer op CXCR5 uitdrukking en aktivering gebaseer op CD38+ en/of CD69+ uitdrukking. Sekondere data van kliniese parameters en inflammatoriese sitokiene vir elke groep was geevalueer. Statistiese vergelykings tussen groepe was gemaak deur die Mann-Whitney toets te gebruik om betekenisvolle verskille te identifiseer. Die Spearman’s rank orde toets was gebruik om betekenisvolle vergelykings tussen Tfh selle en kliniese parameters, ander T sel populasies en inflammatoriese sitokiene te identifiseer.

Resultate: Finotipiese resultate het in die algemeen ‘n aansienlikke verhoogde proporsie van CD38+ substel in die HIT groep en CD69+ substel in die HEU groep getoon. Alhoewel daar nie n aansienlikke verskil in mediaan CD4+CXCR5+PD-1+ Tfh selle persentasie tussen die groepe was nie, was die ICOS-uitdrukking substel naamlik CD4+CXCR5+PD-1+ICOS+ Tfh sel aansienlik hoër in die HIT groep (33.6% vs 19.2%; p = 0.016) en HEU groep (31.6% vs 19.2%; p = 0.006) in vergelyking met die HUU groep. In die HIT groep, CD4+CXCR5+PD-1+ Tfh selle het n aansienlike

negatiewe korrelasie met die meerderheid geaktiveerde T cell subgroup. ‘n Aansienlikke positiewe korrelasie tussen CD4+CXCR5+PD-1+ Tfh selle en CD8+PD-1+ Tc selle, ‘n algemene aanwyser van immuun uitpitting, was gedemonstreer. Ten laaste, die HIT groep het die hoogste vlak van INF-α en hsCRP inflammatoriese sitokiene getoon en vlakke van IL-1β en hsCRP het negatief gekorreleer met CD4+CXCR5+PD-1+ICOS+ Tfh selle binne hierdie groep.

Gevolgtrekking: Die algehele vlakke van immuun aktivering was beduidend hoër in die HIT en HEU groepe. Verskeie geaktiveerde T sel substelle het omgekeerd gekorreleer met CD4+CXCR5+PD-1+ Tfh selle, suggererend dat hoë vlakke van immuun aktivering kan lei tot n verlaagde proporsie van Tfh selle. Tfh selle word gereguleer deur CD8 T selle, Tfc en Tfr selle. Uitbreiding van CD8 T selle, CD38-geaktiveerde Tfc selle en Tfr selle in die HIT groep korreleer negatief met CD4+CXCR5+PD-1+ Tfh selle. Die negatiewe korrelasie tussen hsCRP en ICOS-uitdrukking Tfh selle, het verhoog in die HIT groep, wat suggereer dat inflammasie wat in HIT kinders voortgaan lei tot ‘n afname in Tfh selle. Hierdie stuudie demonstreer die uitbreiding van ICOS-uitdrukking Tfh selle (mees algemeen beskou as ware perifere Tfh selle) in vroeg behandelde HIT kinders wat aansienlik gereguleer was deur immuun aktivering en inflammasie.

Acknowledgements

Several individuals greatly contributed to the completion of this thesis and I would like to express my sincerest gratitude to all those people.

Firstly, and above all, my project supervisor Dr Richard Glashoff for his unyielding support, guidance and patience. I appreciate all the effort and time you have invested in directing and encouraging me through the course of my Master's studies, especially at times when I was feeling frustrated and demotivated. Your insight and knowledge considerably fostered my interest in immunology and helped shape this thesis.

Dr Shalena Naidoo and Dr Rozanne Adams, I would like to thank you for being such inspirations and mentors, and for always teaching and assisting me with techniques and concepts that were completely new to me with such a kindly attitude.

I thank my fellow immunology students, Ansia van Coller and Christine Evert, for their motivation, encouragement and willingness to always lend a helping hand.

Dr Andrea Gutschmidt, Nazma Mansoor and Timothy Reid for all your advice and instruction in flow cytometry and for assisting me with the design and set up of my flow cytometric experiments.

I would also like to thank my colleagues at the Division of Medical Microbiology for providing such a positive and friendly work environment that encourages growth, learning and enhanced my passion for research, as well as for assisting me whenever I needed it.

I extend my gratitude to our collaborators from the CHER trial, the Division of Medical Virology and those involved in the Reservoir Study for laying the groundwork for my research project.

I thank my friends and family, and especially my fiancé, Jamie, for their support and driving me to finish my Master's studies. I also especially thank my father for helping me write the Afrikaans portion of this thesis.

Lastly, I would like to give acknowledgement to the funders, without whom this research would not have been possible: National Research Foundation (NRF) and Poliomyelitis Research Foundation (PRF).

Table of Contents

List of Tables

List of Figures

List of Abbreviations

.fcs	Flow Cytometry Standard File
Ab	Antibody
AIDS	Acquired Immunodeficiency Syndrome
APC	Allophycocyanin
APC-H7	Allophycocyanin-H7
APCs	Antigen presenting cell
ART	Antiretroviral therapy/treatment
BB515	Brilliant Blue 515
BP	Band-pass filter
BV510	Brilliant Violet 510
BV605	Brilliant Violet 605
CAF	Central Analytic Facility
cART	Combination antiretroviral therapy
CD	Cluster of differentiation
CHER	Children with HIV Early Antiretroviral Therapy
CS&T	Cytometer Setup and Tracking
DMSO	Dimethyl sulfoxide
EDTA	Ethylenediaminetetraacetic acid
FBS	Foetal Bovine Serum
FDC	follicular dendritic cell
FMO	Fluorescence Minus One
FSC	Forward scatter
FVS700	Fixable Viability Stain 700

GC	Germinal centre
HEU	HIV-exposed uninfected
HIT	HIV-infected treated
HREC	Human Research Ethics Committee
hsCRP	high-sensitivity C-reactive protein
HUU	HIV-uninfected unexposed
I/C	Intracellular
IFN	Interferon
IFN-α	Interferon-alpha
IFN-γ	Interferon-gamma
Ig	Immunoglobulin
IgG	immunoglobulin G
IL	Interleukin
IL-1β	Interleukin 1 beta
IQR	Interquartile range
LP	Long-pass filter
mAb	monoclonal antibody
MFI	Median Fluorescent Intensity
MTCT	Mother-to-child transmission
NCAM	Neural cell adhesion molecule
NK	Natural killer
PBS	Phosphate Buffered Saline
PE	Phycoerythrin
PE-CF594	Phycoerythrin-CF594

PE-Cy7	Phycoerythrin-Cyanine 7
Percp-Cy5.5	Peridinin-chlorophyll protein-Cyanin5.5
PMT	Photomultiplier tubes
PMTCT	Prevention of mother-to-child transmission
PREDICT	Randomized Early versus Deferred Initiation in Cambodia and Thailand
r	Spearman correlation coefficient
RCF	Relative Centrifugal Force
rSD	Robust standard deviation
rSD_{EN}	Robust standard deviation of the electronic
S/N	Signal-to-noise ratio
SI	Stain Index
SLO	secondary lymphoid organ
SSC	Side scatter
START	Strategic Timing of Antiretroviral Therapy
Tfc	T follicular cytotoxic
Tfh	Follicular helper T
Tfr	T follicular regulatory
TNFα	Tumor necrosis factor alpha
Treg	Regulatory T
USA	United States of America
V450	Violet 450
WHO	World Health Organisation

Markers denoted with a “+” or “-” superscript indicated intracellular or cell surface expression of cell populations. Positive expression (+) indicated the marker was present, whereas negative expression (-) indicated the marker was absent.

Chapter 1 – Introduction

Presently, the pandemic of HIV infection continues to be a global health issue impacting millions of people with new infections occurring every year. South Africa has a high burden of HIV infection and paediatric HIV infection is still a prevalent concern for HIV-positive pregnant women.

However, with the advent of antiretroviral therapy (ART), new paediatric HIV infections have declined over the years due to a decrease in mother-to-child transmissions from HIV-positive pregnant women. However, a small percentage of children still acquire HIV through vertical transmission or become exposed to the virus in utero.

Several studies have proved that both HIV-infected and HIV-uninfected exposed children have higher morbidity and mortality rates, regardless of ART and early interventions (Ekali et al., 2019). In contrast to infants born to HIV negative mothers, HIV-infected/exposed children encounter a wide variety of phenotypic and functional dysregulations in immune responses early on in life (Afran et al., 2014).

Tfh cells are crucial for the production of virus-specific antibody responses and viral clearance in both acute and chronic infections. This cell population has been of special interest with regards to the development of novel vaccination strategies against HIV, especially because of its association with the generation of broadly neutralizing HIV antibodies. However, in the context of HIV infection it was discovered that Tfh cells also constitute a significant portion of the latent reservoir, allowing HIV persistence and immune evasion. In this way, Tfh cells are beneficial but can also play a pathologic role in HIV infection. Several studies of HIV-positive adults have investigated Tfh cells in respect to immune dysregulation, weakened vaccine responses and disease progression, however not many studies have investigated the impact of Tfh cells in children (McCarty et al., 2018).

The implication of immunological impairment in HIV-infected and HIV-uninfected exposed children is of significant public health relevance. Investigations into the mechanisms of immune dysregulation and deficiencies may aid in preventing faster disease progression and serious defects in children whose immature immune systems evolved in the presence of HIV (Muema et al., 2017; Afran et al., 2014).

Chapter 2 – Literature Review

2.1 Human Immunodeficiency Virus

Infection with HIV is a lifelong disease that targets and weakens the body's immune system making it more susceptible to opportunistic infections. HIV is incurable and without effective treatment measures it can develop into Acquired Immunodeficiency Syndrome (AIDS), an advanced stage of infection characterised by severe clinical manifestations, infections and even cancer development (Leong et al., 2017).

HIV primarily infects and induces the degradation of CD4 helper T cells, which actively play a key role in adaptive immune responses. After a cell is directly infected with HIV, productive HIV replication occurs and the cell's ability to function becomes impaired through processes of cytotoxicity and apoptosis. Additionally, HIV can elicit further damage to neighbouring uninfected cells causing dysfunction or even cell death (Deeks et al., 2004).

Furthermore, the decline of CD4 T cells results from direct or indirect cytopathic effects by the virus as well as the destruction of infected cells by cytotoxic CD8+ T cells. The hallmark decline of CD4 T cells in HIV-infected individuals, especially in children, makes them prone to acquiring opportunistic infections. Additionally, the underlying inflammation and inadequate responses of the immune system introduce notable health challenges and immune dysfunction, especially in patients with chronic infection. Without treatment, the frequency of CD4 T cells drops below a critical level and an immunocompromised individual may die due to AIDS-related complications (Kinter et al., 2007; Leong et al., 2017).

The progression of HIV disease is the result of generalized and persistent T cell activation as well as a prolonged and amplified rate of T cell turnover. HIV infection causes the rate of T cell proliferation, expansion as well as death to increase. Additionally, it impairs the production of new progenitor cells so that the population of cells cannot be replenished. Several studies suggest that the increased T cell turnover is linked to immune exhaustion which hinders the regenerative capacity of the immune system (Deeks et al., 2004). Therefore, a key characteristic of HIV infection is the development of chronic immune activation which precedes immune exhaustion as well as the dysregulation and depletion of B and T cells (Ruffin et al., 2012).

2.1.1 The HIV Epidemic and Vertical Transmission

Human Immunodeficiency Virus (HIV) infects millions of individuals across the world. According to a 2021 UNAIDS report, in 2020 there were approximately 37.7 million people living with HIV of which 1.7 million were children below the age of 15 years. It was estimated that 85% of HIV-infected pregnant women had access to antiretroviral treatment for the prevention of mother to child transmission and new infections in children have decreased by 53% from 2010 to 2020. However, in 2019 (the year before), it was estimated that there were 150 000 children (<15 years) newly infected with HIV and 95 000 children (<15 years) that died due to AIDS-related illnesses (UNAIDS, 2021).

Globally there are about 4 500 new infections of HIV a day and 59% of those new infections occur in sub-Saharan Africa. South Africa has proven to be one of the countries to host the highest number of people living with HIV. UNAIDS estimated that in 2019 there were 7 500 000 HIV-infected people living in South Africa and within this population 340 000 were children below the age of 15 years (UNAIDS, 2020)

The principal mode of HIV transmission to infants is through mother-to-child transmission, which occurs in approximately 25% - 30% of pregnancies of infected woman. Mother-to-child transmission (MTCT) of HIV is described as the transfer of the virus from an infected mother to her child during pregnancy, labour, delivery, or through breastfeeding. Without intervention the rate of transmission is between 15% - 45%, however with the use of successful interventions (such as the early administration of antiretroviral drugs) this can be decreased to less than 5% (Clerici et al., 2000).

According to UNAIDS as of 2019, approximately 97% of HIV-infected pregnant women, living in South Africa, were seeking antiretroviral therapy (ART) or prophylaxis to prevent the spread of the virus to their infants through vertical transmission (UNAIDS, 2020).

It was estimated that 52% of infants, in sub-Saharan Africa, who are infected with HIV die before turning two years old when no therapeutic intervention is provided. This indicates the importance of diagnosing infants early in life and the immediate initiation of ART for the reduction of HIV-related mortality as well as long-term morbidity (Alvarez et al., 2017).

Regarding HIV infection in pregnant women, foetal exposure to the virus in utero can either result in the child becoming infected with the virus or exposure without infection. Exposure that does not lead to infection and the likelihood of the virus or viral particles traversing the placental barrier without foetal infection is experimentally substantiated (Clerici et al., 2000).

With increased access to paediatric antiretroviral therapy and better prevention of mother-to-child transmission (PMTCT) services and modifications to WHO (World Health Organisation) guidelines there has been a decrease in new infections among children born to HIV-positive mothers and therefore, an increase in the percentage of children exposed to HIV as a foetus.

2.1.2 The effects of foetal HIV exposure or infection

When foetal development occurs in a microenvironment contaminated with either whole virus or viral particles or both the immune system of the foetus develops in the background of the viral infection, leading to the development of complex immune defects (both quantitative and qualitative) (Clerici et al., 2000). Therefore, vertical transmission of HIV has implications on the development of immunity to pathogens in children born to HIV-positive mothers leading to either low or the absence of immune responses (Muema et al., 2017).

Immune defects may include abnormal proportions of T lymphocytes, a decreased CD4/CD8 ratio as well as a reduction in the percentage of naïve CD8+ T cells (Clerici et al., 2000). During foetal exposure, viral antigens may also trigger high levels of immune activation and cellular apoptosis (Nielsen et al., 2001; Miyamoto et al., 2010). This especially relates to the CD4 T cell compartment, which has been shown to be qualitatively defective, with cells expressing elevated levels of activation markers. Paradoxically, CD4 T cells also display reduced responsiveness to stimulation which is linked to an increase in the levels of lymphocyte exhaustion due to the upregulation of inhibitory markers (Muema et al., 2017).

Since CD4 T cells function to aid B cells, defects in the CD4 T cell compartment may lead to the development of HIV-induced B cell defects due to the decline of CD4 T cells or stimulation by qualitatively defective CD4 T cells. Defects in the B cell compartment leads to an increased susceptibility to opportunistic infections that would normally be supressed by antibody (Ab) responses. Therefore, HIV-infected patients

that encounter routine vaccines and common infections display weak antibody and memory B cell responses. In children, especially, weak B cell response could cause them to be more susceptible to repeated infections irrespective of previous exposure and immunisation. This is of significant importance in vertically HIV-infected children as it may cause them to experience more rapid disease progression and develop severe defects. Even though there have been several in-depth studies of the B cell defects affecting HIV-infected adults, research of the same magnitude is limited and lacking for HIV-infected children (Muema et al., 2017).

A higher morbidity and mortality are also prevalent within HEU children. These children experience increased hospitalisations, diarrhoeal diseases and acute respiratory tract infections. Additionally, they may have considerable developmental impairment and increased risk for growth impairment as a result of maternal HIV and ART exposure (Ekali et al., 2019).

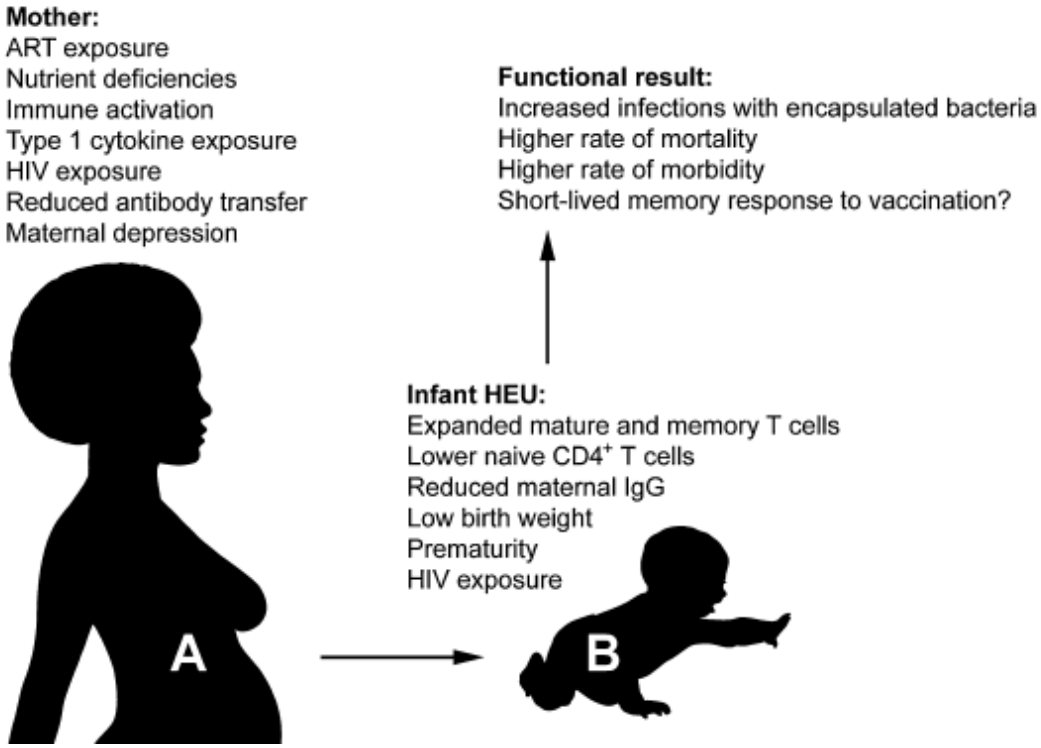

Figure 2.1: The effects of HIV and anti-retroviral therapy (ART) exposure on the immune system of infants exposed to HIV-1 via vertical transmission. As demonstrated in the figure HIV-exposed uninfected (HEU) children experience several immune defects as well as flawed physical growth, resulting in increased mortality and morbidity (Afran et al., 2014).

The majority of untreated HIV-infected children die within 2 years of life most likely due to an inadequacy in their development of immune responses. A greater understanding of the immunological defects that afflicts them could aid in the design of improved interventions to help them survive (Muema et al., 2017).

2.1.3 Antiretroviral treatment of HIV

Combination antiretroviral therapy (cART) consists of drugs that function to target and inhibit the action of several components, such as reverse transcriptase, protease and integrase, of the viral replication cycle and thereby suppresses production of the virus by host cells. Additionally, they may target host co-receptors, such as CCR5, to prevent entry of the virus (Leong et al., 2017). Through the action of cART, the replication cycle of HIV is dramatically disrupted, and the level of plasma HIV RNA decreases to a limit where it cannot be detected by commercial assays (below 50 copies/ml). In addition, treatment with cART impedes the development of AIDS by restoring CD4 T cell counts in the blood and thereby improving immune function and survival of the infected individual. However, there is a percentage of virally supressed cART-treated patients (approximately 25%) in which CD4 T cell counts are not fully restored to a level comparable to that of a healthy control (Luo et al., 2017; Pérez et al., 2019).

In most HIV-infected patients, treatment with a cART regimen effectively reduces plasma viremia to the point where it is undetectable and suspends progression of the disease. However, a major limitation of ART is that it cannot eliminate integrated HIV provirus within host cells and the termination of treatment unavoidably results in reactivation and rebound of the virus (Leong et al., 2017).

Additionally, ART is unable to restore serological memory in HIV-infected patients (Titanji et al., 2006). The long-term use of antiretrovirals is also associated with a risk of developing drug resistance, drug toxicity as well as poor adherence to the antiretrovirals, which has been linked to a reduced effectivity in viral suppression (Alvarez et al., 2017).

However, the positive effects of early ART in HIV-infected adults were demonstrated in a 2015 clinical trial called Strategic Timing of Antiretroviral Therapy (START). In this trial, participants displayed a reduction in AIDS-related events as well as major non-AIDS related illnesses (The INSIGHT START Study Group, 2015). This emphasised

the benefits of immediate initiation of ART following HIV diagnosis in adults. In recognition of this study, in 2016, the WHO amended their guidelines and recommended that ART be administered to all HIV-positive diagnosed individuals despite symptom presentation or clinal stage. However, there is limited research about the impact of this recommendation on children and adolescents infected perinatally with HIV. However, irrespective of clinical and immunological status or CD4 count, the WHO has recommended ART for all children below the age of 5 years due to their faster disease progression and increased mortality compared to older populations (Alvarez et al., 2017).

A randomised trial investigating the impact of early ART initiation on infants and children, the Children with HIV Early Antiretroviral Therapy (CHER) trial, found that asymptomatic perinatally HIV infected infants (between the age of 6 and 12 weeks) that had immediate ART initiation displayed a decrease in infant mortality as well as progression of HIV infection compared to infants with deferred treatment (treatment initiation when CD4 levels reached <20% or categorised WHO stage 3 or 4) (Violari et al., 2008). In contrast, another randomised clinical trial, the Randomized Early versus Deferred Initiation in Cambodia and Thailand (PREDICT) trial, discovered no significant difference in the mortality and AIDS-free survival of ART early treated (CD4 levels 15-24%) and ART deferred (CD4 levels <15%) HIV-positive children between the ages of 1 and 12 years old. However, in the PREDICT study there was a reduced overall mortality and elevated AIDS-free survival rates within both cohorts and therefore this study was insufficiently powered to identify a difference (Puthanakit et al., 2012). Therefore, due to the need for substantial supporting evidence on the influence of early ART initiation, the updated 2016 WHO treatment guidelines, for which clinical and immunological status are irrelevant, were considered to be conditional recommendations for children/adolescents between 1-19 years old (Alvarez et al., 2017).

2.1.4 Latent infection of HIV

In cART-treated HIV-infected individuals the viral load is reduced to a level where it is undetectable by commercial assays. However, cART cannot eradicate the virus completely due to the life-long persistence of latently infected cells that constitute a fairly small but stable HIV reservoir. In this way the virus persists regardless of successful cART, goes unnoticed and is even protected against responses of the

immune system. This reservoir of cells hosts replication-competent provirus and is able to generate infectious virus upon reactivation by antigens (Ags) and cytokines or the discontinuation of cART, contributing to viral rebound (Mouquet, 2017; Pérez et al., 2019).

It has been demonstrated that these viral reservoirs are established during the initial stages of infection and even the administration of intense ART treatment early after infection does not help to eliminate them (Moukambi et al., 2017). It is suggested that by targeting and eliminating these cellular reservoirs of HIV it may be possible to prevent viral rebound and ultimately cure patients of the infection (Leong et al., 2017).

2.2 T cell-driven immunity against HIV

2.2.1 Germinal centres

Germinal centres (GCs) are anatomical structures with a specialised function that develop in response to T-dependent antigens. They form within B cell follicles which are located in secondary lymphoid organs (SLOs). Antibody-forming cells are generated and vital processes such as class-switch recombination (CSR), somatic hypermutation (SHM) as well as high-affinity B cell selection occur in GCs. Within the GC sites, antigen-specific naïve B cells interact directly with T cells which help drive T cell-dependent Ab responses (Linterman et al., 2011; King et al., 2008).

The reactions that occur in GCs are heavily reliant on signalling from antigen-specific T cells that migrate into the follicle, especially CD4+ T cells, that trigger the differentiation of high-affinity antigen-selected GC B cells into plasma cells and memory B cells. With the supply of developmental cues provided by CD4+ T cells the GC reaction sustains long-term humoral immunity against the pathogen (King et al., 2008). Somatic hypermutation within GCs involves the mutation of V-region genes of the B receptor cell after which the selection of high affinity B cells leads to the generation of high-affinity memory B cells and antibody-producing plasma cells. Dysfunction of the selection process in the germinal centre reaction causes autoantibody production and a disruption in self-tolerance. GC tolerance is critically regulated by Tfh cells, which select for cognate GC B cells. Autoimmunity develops because of dysregulation in the population of Tfh cells. This emphasizes the need for a controlled regulation of positive selection occurring in GCs (Linterman et al., 2011).

Within the microenvironment of the GC there is intense collaboration between multiple cell populations, including Tfh cells, GC B cells, follicular dendritic cells (FDCs), T follicular regulatory (Tfr) cells and tangible body macrophages to produce a robust response against a pathogen (Linterman & Hill, 2016). This collaboration is examined in figure 2.2 below (Pissani & Streeck, 2014).

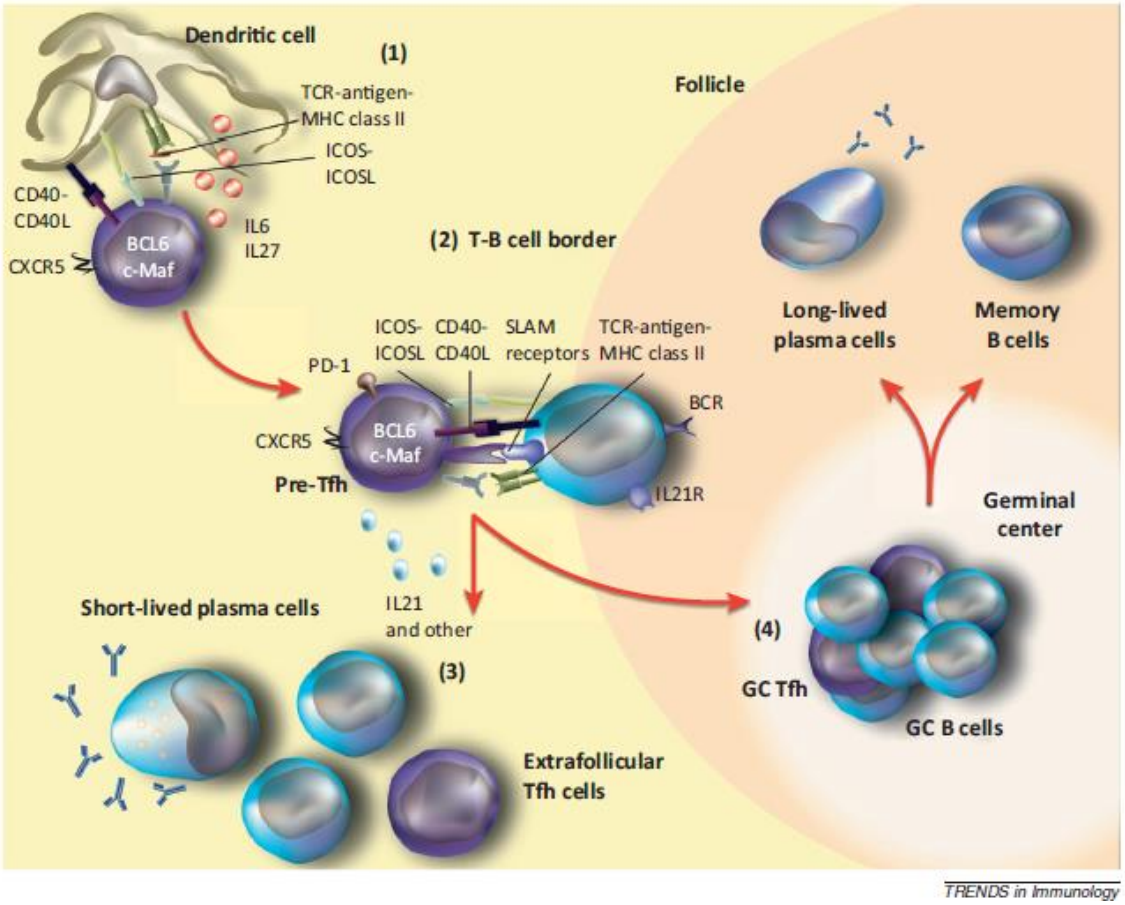

Figure 2.2: The germinal centre (GC) reaction. (1) Activation of naïve CD4 T cells occurs after contact with Ag-primed dendritic cells. Tfh cell differentiation is triggered through the interaction of CD40 and CD40L, ICOS and ICOS-L as well as TCR and MHC class II coupled with Ag. Cytokines, IL6 and IL27, derived from DCs and B cells further stimulate the development of Tfh cells, and as a result BCL6, c-MAF and CXCR5 (Tfh cell transcription factors) are upregulated. (2) Pre-Tfh cells express CXCR5, which controls their migration to the T-B cell border where cognate pre-Tfh and B cells interact via molecular signalling, incl. ICOS:ICOSL, CD40:CD40L, SLAM receptors and TCR:MHC-11 interactions, additionally various cytokines, such as IL-21. IL-21 supports Bcl6 and c-MAF expression which induces the expression of surface receptors on Tfh cells. Concurrently, B cells are subject to a range of signals that activate their maturation into either extrafollicular or GC B cells. (3) Short-lived plasma cells, derived from extrafollicular activated B cells, then secrete Abs with or without

the aid of extrafollicular Tfh cells. (4) The GC is maintained by the prolonged co-stimulation between germinal centre Tfh (GC Tfh) cells and GC B cells, which re-establishes the commitment to the Tfh cell lineage. Additionally, with the help of GC Tfh cells, GC B cells undergo somatic hypermutation and antibody class-switch recombination, which leads to the formation of memory and long-lived plasma cells (Pissani & Streek, 2014).

2.2.2 Helper T (Th) cells

CD4+ T cells, commonly known as Helper T (Th) cells, possess the vital function of coordinating and mediating the responses of the adaptive immunity. Several cell populations of distinct effector helper T cells with various functional capabilities have been discovered in the presence of pathogenic infection. The impact of helper T cells on the coordination of humoral immune responses is related to their effect on other immune cell populations (Read et al., 2016). One of the most crucial functions of CD4+ T cells is their assistance to B cells and Ab responses (Crotty, 2019).

The CD4 molecule on Th cells is known to be HIV's primary receptor and as a result this cell population is the primary cellular target for infection. Throughout infection, the amount of Th cells is negatively correlated with plasma viral load (Gulzar & Copeland, 2004; Kitchen et al., 2004).

2.2.2.1 Follicular helper T (Tfh) cells

Follicular helper T (Tfh) cells are a heterogenous, specialised subset of CD4 T cells that provide help to B cells and stimulate the formation of GCs within SLOs (Xu et al., 2017). From the different subsets of CD4+ T cells, Tfh cells are primarily responsible for producing potent antibody-mediated responses due to their close interaction with B cells (Read et al., 2016). They enable Ab responses to combat a range of bacterial, viral, fungal and even parasitic infections (Crotty, 2019).

The initial cognate interaction between Tfh cells and B cells occurs mechanistically at the T-cell-B-cell border of SLOs, e.g., lymph nodes and spleen. The formation of GCs is triggered because of this cognate interaction and results in the generation of neutralizing antibodies (Read et al., 2016). Through the maintenance of the GC reaction, Tfh cells play a significant role in mediating high affinity antibody responses to antigens as well as the production of memory B cells (Gensous et al., 2018). Not only are Tfh cells needed for GC responses to infection but also somewhat for pre-GC extrafollicular Ab responses (Crotty, 2019). Tfh cells regularly produce IL-21, a

cytokine that stimulates B cell differentiation and antibody production (Perdomo-Celis et al., 2017).

Through the aid of B cells, Tfh cells critically contribute to the development of antigen-specific antibody responses. Tfh cells play a crucial role in the affinity maturation of antibodies by supporting processes, such as somatic hypermutation as well as immunoglobulin class switching (i.e., CSR), and encourage the differentiation and preservation of B cells. This is all enabled by the GC-reaction, in which GC Tfh cells and Ag-specific B cells interact and adhere to a stringent regulatory program (Pissani & Streeck, 2014).

Tfh cells have demonstrated a positive association with the production of broadly neutralizing HIV-1 antibodies (bNAbs) and consequently Tfh cells have been of particular significance in HIV-related research (Crotty, 2019 ; Moukambi et al., 2017).

Tfh cell differentiation

Tfh cells have a unique differentiation program, transcription profile, phenotype and function distinct from other CD4 T cell subsets (Linterman & Hill, 2016). The differentiation process of Tfh cells is intricate and involves multiple stages that are maintained by many extrinsic and intrinsic cell factors (Read et al., 2016). The specific differentiation program of Tfh cells is triggered by immunisation and requires several cycles of antigen presentation and cytokine signalling (Linterman & Hill, 2016).

The standard Tfh cell differentiation program necessitates interaction with two types of antigen presenting cells (APCs), namely DCs and B cells, at different stages. Early Tfh cell differentiation is triggered by DCs whereas later events and complete GC-Tfh cell maturation is controlled by interactions with B cells (Crotty, 2019). Similarly, to the developmental processes of other known Th cell subsets, the development of Tfh cells is positively and negatively regulated by certain cytokines as seen in Figure 2.3 (Read et al., 2016).

Tfh cell differentiation is controlled by the transcriptional repressor B-cell lymphoma-6 (Bcl-6), which functions to antagonise the differentiation of other helper T cell subsets and mediate the migration and role of Tfh cells (Leong et al., 2017). The identification of Tfh cells is relatively new compared to other T cell populations and was a result of the discovery of a CD4 T cell subpopulation, detected in lymphoid follicles, formed

through Bcl-6 transcription. Bcl-6 is therefore the key transcription factor encoding for Tfh cells, which have a very different gene-expression profile compared to other CD4 T cell subsets i.e., Th1, Th2 and Th17 cells (Perdomo-Celis et al., 2017).

Upon the Ag-dependent activation of naïve CD4+ T cells, the differentiation of Tfh cells is stimulated by specific environmental signals, such as cytokine signalling. Resulting in an increased expression of Bcl-6 and the consequent up-regulation of genes which are characteristic of the Tfh cell programme. This includes expression of the cell surface receptors CXC chemokine receptor 5 (CXCR5), inducible T-cell co-stimulator (ICOS) as well as programmed cell death protein 1 (PD-1) (Read et al., 2016).

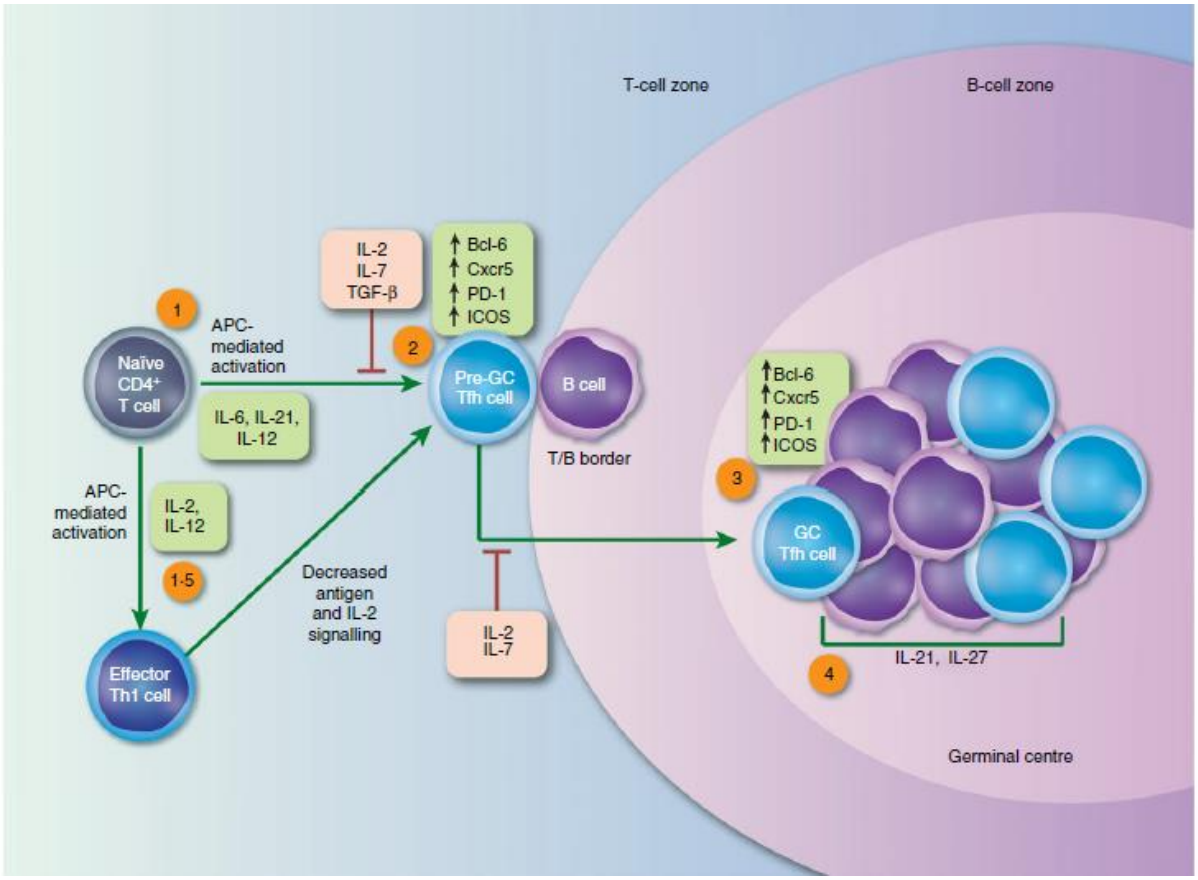

Figure 2.3: The development of Tfh cells and the influence of cytokine signalling. Depicted in this schematic are the various stages of Tfh cell differentiation. Highlighted in red and green are the respective negative and positive impacts of cytokine signalling on the development of Tfh cells in murine models. (1) In the presence of specific cytokines, the initiation of Tfh cell development is triggered upon the activation (mediated by APCs) of naïve CD4+ T cells. (2) As a result, the transcription factor, Bcl-6, is up-regulated along with other Tfh-lineage defining genes such as CXCR5, PD-1 and ICOS. Pre-germinal center (Pre-GC) Tfh cells then migrate to T/B cell border and engage in cognate interactions with B cells.

(3) The Tfh cell gene expression patterns of BCL-6, CXCR5, PD-1 and ICOS is then further up-regulated. (4) Ensuing T and B cell interactions results in the development of the GC and the preservation of the GC Tfh cell phenotype (Read et al., 2016).

Tfh cell phenotype

As mentioned previously, the induction of Bcl-6 stimulates CXCR5 expression on Tfh cells (Leong et al., 2017). The localisation of Tfh cells to follicular areas within lymphoid tissues is controlled by its CXCR5 expression, which is attracted to chemokine ligand 13 (CXCL13) expressed on B cells (Gensous et al., 2018). The high levels of CXCR5 expression are crucial for migration and entry into B cell zones of SLOs (i.e., the B cell follicle) (Perdomo-Celis et al., 2017). Allowing Tfh cells to assist B cells in the generation of humoral responses against infection.

The close proximity to B cells within follicles and the expression of costimulatory surface Ags, particularly ICOS molecule, helps facilitate the interaction between B and Tfh cells for the formation of GCs. ICOS-expression on activated T cells in the presence of IL-6 encourages the secretion of IL-21, a principal Tfh cell cytokine. Therefore, ICOS is of particular interest in the study of Tfh cells because of its dual function as a migration receptor as well as a costimulatory molecule.

Additionally, GC Tfh cells express high levels of PD-1. The inhibitory receptor, PD-1, helps maintain the GC reaction by inhibiting the suppressive activity of regulatory T cells. Additionally, PD-1 inhibits CXCR3 expression on Tfh cells, which like CXCR5 controls follicular localisation. In comparison to Tfh cell populations that express low levels of PD-1, GC Tfh cells secrete higher levels of IL-21 and provide the most help to B cells (Leong et al., 2017; Crotty, 2019). Table 2.1 below demonstrates the positive or negative expression of certain phenotypic markers expressed on various follicular cells, including Tfh cells.

Table 2.1: Phenotypic markers of Tfh cells (CD4+) and other follicular cells: follicular cytotoxic T cells (Tfc) (CD8+) and follicular B cells (CD19+) (adapted from Perdomo-Celis et al., 2017).

Marker	Expression in follicular cells			Function
	CD8+ T cells	CD4+ T cells	CD19+ B cells	
CD3	+	+	-	Associated with the T cell receptor and required for its signal transduction

CD8	+	-	-	Co-receptor for major histocompatibility complex (MHC) class I molecules
CD4	-	+	-	Co-receptor for MHC class II
C-X-C chemokine receptor type 5 [CXCR5 (CD185)]	+/High	+/High	+/High	Receptor for the chemokine CXCL13. It enables the migration of T cells to B cell zones in secondary lymphoid tissues
Programmed death [PD-1 (CD279)]	+	+	-	Regulates T cell activation and tolerance mechanisms
Inducible T cell costimulator (ICOS)	+	+	-	Costimulator of T cells through the binding to ICOSL in B cells

Tfh cell action as a latent HIV reservoir

Within the CD4+ Th cell population, Tfh cells have been identified as a major cell type for latent HIV infection (Leong et al., 2017; Lindqvist et al., 2012). Tfh cells are targeted by HIV for infection, replication and production due to their low inclination for apoptosis. By being a continuous regenerating source for HIV to target, Tfh cells are capable of establishing a lasting viral reservoir within lymphoid tissues, in which they are protected from the action of CTLs (Pissani & Streeck, 2014). Additionally, ART has no effect on latently infected cells, which undergo homeostatic proliferation and have the ability to secrete productive virus after stimulation (Siliciano & Greene, 2011).

Germinal center (GC Tfh) vs circulating Tfh (cTfh) cells

Tfh cells are preferentially most abundantly located in lymphoid follicles where they stimulate B cells through a range of cytokine and CD40L signalling (Perdomo-Celis et al., 2017). Tfh cells remain within SLOs in order to aid B cells, which is their primary function, whereas non-Tfh effector cells i.e., cytotoxic CD4 T cells, Th1, Th2, Th9 and Th17 cells, for the most part depart from SLOs and migrate to areas of inflammation or infection. However, GC Tfh cells are also capable of migrating out of GCs through the down-regulation of CXCR5 expression (Crotty, 2019).

These extrafollicular Tfh cells function outside of GCs, providing signals to B cells or memory B cells located in the T-B cell border (during initial immune responses) or migrating to distant sites away from the follicle and T-B cell border. Populations of Tfh cells (CXCR5+PD-1+ICOS+/-) that exist in blood are referred to as circulating Tfh (cTfh)/peripheral (pTfh) cells. This may include recently activated Tfh cells as well as

resting memory Tfh cells, likely derived from GC Tfh cells. The majority of cTfh cells is comprised of resting memory Tfh cells that frequently recirculate in peripheral blood (Crotty, 2019).

Because Ag-specific GC-Tfh cells are confined to SLOs they are difficult to access and study in vivo (Crotty, 2019). For this reason, many studies have utilised the GC-Tfh cell counterpart found in blood, cTfh cells, as an indicator of Tfh cell responses in infection. As mentioned previously, cTfh cells are presumed to be derived from GC-Tfh cells because of their strong phenotypic and functional characteristic resemblance to Tfh cell populations found in GCs. Like GC-Tfh cells, they express the characteristic markers: CXCR5, PD-1 and ICOS as well as the transcriptional repressor Bcl6, additionally demonstrating a memory phenotype.

Moreover, the analysis of CXCR3- cTfh cells isolated from human blood has indicated that they are the major functional equivalent of GC Tfh cells on account of their effective induction of naïve B cells for Ab production in in vitro experiments. CXCR3+ cTfh cells, however, were insufficient possibly due to PD-1, which mentioned previously inhibits CXCR3 expression. Indeed, it has been reported that cTfh cells (with a CXCR5+CXCR3-PD-1+ memory phenotype) displayed a high level of functionality and is associated with the generation of bNAbs in HIV+ donors (Zhang et al., 2019).

Studies have shown that healthy individuals have a reduced frequency of Tfh cells in their peripheral blood (Moukambi et al., 2017). These cells are mostly located within GCs or in close proximity to GCs of secondary lymphoid organs, however Tfh memory cell populations have been found to circulate via blood (Xu et al., 2017)**.**

2.2.2.2 Regulatory T (Treg) cells

Regulatory T (Treg) cells, characterised as CD4+CD25+ T cells, function to suppress the activation and proliferation of T cells as well as cytokine production. Additionally, they prevent immune responses to self-Ags and control inflammation triggered by pathogens of chronic infection. They function to restrain the responses of effector Th cells and CTL in the presence of chronic infection, such as HIV. These cells are also capable of migrating to and assembling in lymphoid tissues where they contribute to immunosuppression (Nilsson et al., 2006).

Natural CD25+FOXP3+ Treg cells play a crucial role in immune surveillance and the control of autoimmunity. However, Treg cells have been implicated in inflicting their suppressive activity on appropriate immune responses to foreign antigens and thereby encouraging viral persistence in vivo (Kinter et al., 2007).

Within asymptomatic HIV-infected individuals Treg cells, characterised by a CD4+CD25+FoxP3+ phenotype, have demonstrated significant suppressor activity in peripheral blood by quelling HIV-specific immune responses, such as those of HIV-primed CD4+ and CD8+ T cells. This limits the immune system and as a result it is unable to effectively control viral replication (Nilsson et al., 2006).

It would be of great importance to investigate the suppressive activity of Treg cells in HIV-infection. Identifying whether they can be used as an immunotherapeutic target for the amplification of HIV-specific immune responses and whether this approach is more efficient at certain stages of disease progression (Kinter et al., 2007).

2.2.2.3 Follicular regulatory T (Tfr) cells

A recently identified cell population, namely follicular regulatory (T) cells has been found to possess shared characteristics with both conventional regulatory T cell populations and Tfh cells (Xu et al., 2017). Even though Tfr cells share transcriptional and phenotypic similarities with Tfh cells, they have a suppressive function and therefore resemble conventional Treg cells to a greater extent (Linterman & Hill, 2016). In the same way that Tfh cell development is influenced by Bcl-6, CD28, SLAM-associated proteins (SAP) and B cells so is the production of Tfr cells. However, Tfr cells are derived from Foxp3+ precursors formed in the thymus, and not naïve or Tfh cells (Gensous et al., 2018).

It has been suggested that Tfr cells are a subset of CD4+FoxP3+ regulatory T cells which also express CXCR5 and therefore migrate to GCs where they regulate the frequency of Tfh cell and GC B cell populations to limit the magnitude of the GC response (Gensous et al., 2018). The limitation of autoreactive B cell generation is the key physiological role of Tfr cells. Therefore, in Ag-specific immune responses Tfr cells act to prevent the development or eliminate SHM-generated autoreactive B cells (Crotty, 2019).

Besides the regulatory marker, FoxP3, Tfr cells also express CD25, IL-10, CTLA-4 and glucocorticoid-induced TNFR-related protein. To achieve immune homeostasis, it

is important that there is a balance in the regulation of both Tfr cell and Tfh cell populations and their activity. In vivo a reduced frequency of Tfr cells has been linked to an amplified GC reaction. The impairment of the Tfr cell compartment leads to the enhancement of Tfh cell activity, which in turn can result in the development of autoreactive B cells and the generation of autoantibodies (Gensous et al., 2018; Xu et al., 2017). However, it is not clear whether Tfr cells have the capacity to directly regulate populations of Tfh cells under certain physiological conditions in vivo as it is rare that Tfr cells will be present in GCs and therefore Tfr exerting their function on GC-Tfh cells directly is unlikely (Crotty, 2019).

2.2.3 Cytotoxic T cells (Tc/CTLs)

CD8+ T cells, also known as cytotoxic T lymphocytes (CTLs/ Tc cells), are a heterogenous subset of antigen-specific T cells that carry out various effector functions against pathogenic infections, incl. Epstein-Barr virus (EBV), cytomegalovirus (CMV) and HIV-1 (Demers et al., 2013). During infection, Ag-specific CTLs are primed within the T cell zone of SLOs, after which they undergo differentiation into effector T cells that kill infected cells.

The cell mediated immune responses of CTLs are essential for the control of viral replication. These responses may be lytic or non-lytic, and include the secretion of chemokines, cytokines and cytolytic effector molecules as well as Ag-specific targeting and lysis of infected cells (Demers et al., 2013; Gulzar & Copeland, 2004). The optimal function of Tc cells is not only dependent on their capacity for cytotoxic effector function but also on localisation to infected sites or sites of tumour formation, which is a prerequisite.

In unresolved infections, including HIV infection, or cancer the differentiation of Ag-specific T cells leads to a state of T cell exhaustion, due to an increased expression of several inhibitory receptors, such as PD-1. As a result, there is a reduction in the effector function of Tc cells, clonal deletion and impairment in the development of memory T cells (Leong et al., 2016).

CD8+ cytotoxic T cells have a critical function in antiviral immunity through the secretion of antiviral cytokines and direct destruction of HIV-infected cells (Kitchen et al., 2004).

It is well understood that Tc cells are typically excluded from B cell follicles, however not a lot is known about antigen-specific Tc cell populations that are able to gain entry into B cell follicles for infection control (Leong et al., 2016).

2.2.3.1 Follicular cytotoxic T (Tfc) cells

Tc cells that express the phenotypic marker CXCR5, and have the ability to migrate to and enter B cell follicles, where they eliminate virally-infected Tfh and B cells, are termed follicular cytotoxic T cells (Tfc cells). This recently discovered population of cells is the product of a tightly regulated process of CXCR5 transcription, not usually characteristic of Tc cells, during Tc cell differentiation (Leong et al., 2016).

Studies have indicated that Tfc cells are a distinct effector-type subset of Tc cells and are transcriptionally, phenotypically and functionally different to conventional effector Tc cells. Phenotyping as well as transcriptional profiling of Ag-specific Tfc cells has demonstrated that Tfc cells are more characteristically similar to Tfh cells and to a lesser degree memory Tc cell populations (Leong et al., 2016).

The possession of Tfh cells characteristics can be attributed to the expression of Bcl6 during CD8 T cell differentiation into Tfc cells. The upregulation of Bcl6 results in the suppression of granzyme B expression. Concurrently Blimp1, a transcription factor that induces CD8 T cell differentiation into effector and memory subsets, is repressed resulting in the generation of Tfc cells that have reduced cytotoxic function (Perdomo-Celis et al., 2017).

However, in a study by Leong et al, the characterisation of Tfc cells demonstrated elevated expression of markers associated with memory, i.e., CD62L, TCF-1 and IL-7R. Even though the expression of effector molecules, such as granzymes and perforin was reduced in Tfc cell populations, they demonstrated a specialised function in viral control within follicles as well as a markedly reduced exhaustion phenotype compared to conventional Tc cells during chronic infection (Leong et al., 2016).

This is demonstrated through the absence of exhaustion markers: T-cell immunoglobulin (TIM)-3 and CD244 (2B4) along with the finding that PD-1 expression is higher in CXCR5- Tc cells compared to CXCR5+ Tc cells in SLOs. Even so, the prolonged Ag exposure within lymphoid follicles in times of chronic infection or tumour development may possibly cause dysfunction in T cell responses due to prolonged activation (Perdomo-Celis et al., 2017).

A small percentage of human Tfc cells (CXCR5+CD8+ T cells) also circulate via peripheral blood but are phenotypically different to Tfc cell populations located in lymphoid follicles. This suggests that Tfc cells are capable of downregulating follicle homing markers, such as CXCR5, exiting the follicle and entering the circulation, perhaps in order to migrate to sites of inflammation, with a lowered phenotype of activation (Perdomo-Celis et al., 2017).

All together CXCR5+ CD8 T cells develop following Ag exposure when naïve CD8+ T cells are primed and supplied with specific cytokine signals by APCs (i.e., DCs) aided by Th cells. This initiates Bcl-6 and CXCR5 expression, along with additional chemokine receptors, activation as well as exhaustion markers, and homing to lymphoid follicles. Antigenic persistence and additional APC signalling finally leads to differentiation into Tfc cells possessing an effector memory phenotype that very possibly constitutes a pool of long-lived memory T cell precursors (Perdomo-Celis et al., 2017).

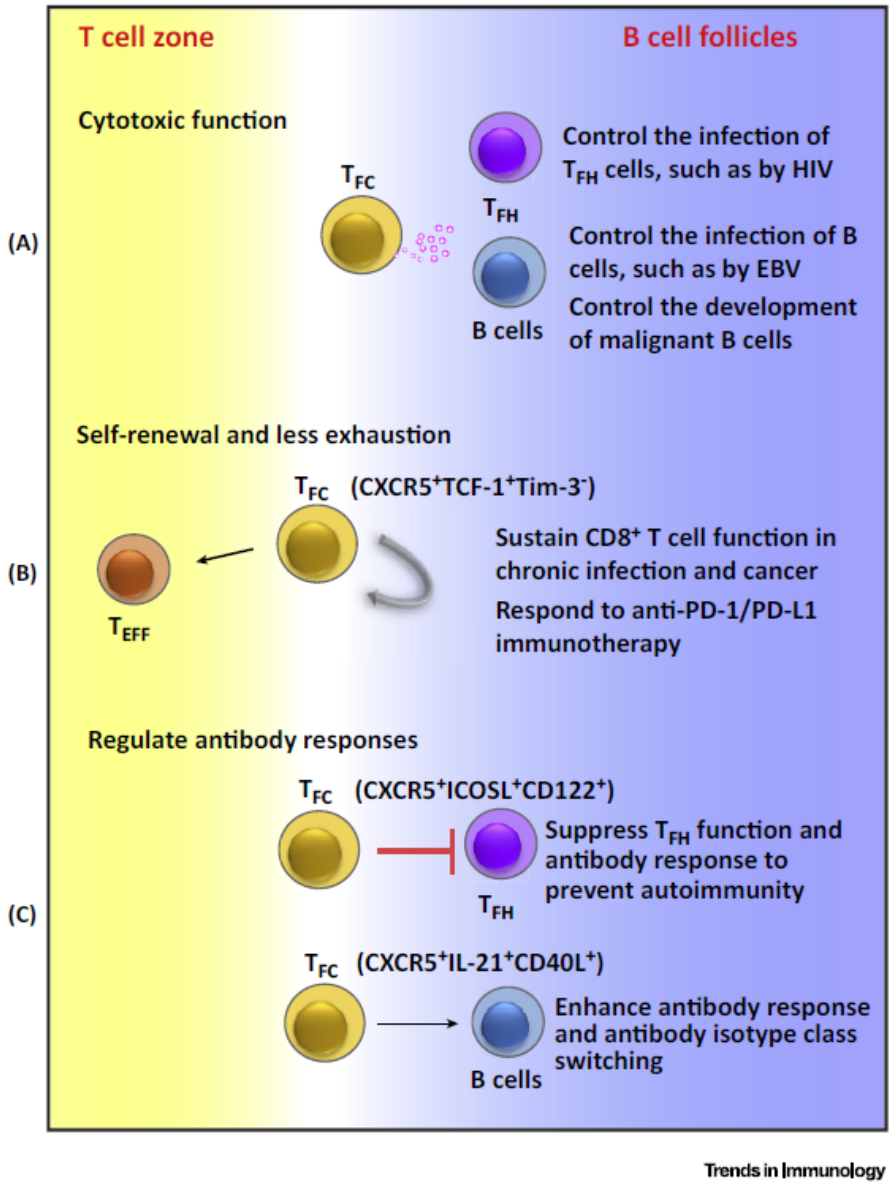

Figure 2.4: The role of CXCR5+CD8+ cytotoxic T (Tfc) cells. A) Through the immunosurveillance of B cell follicles, Tfc cells target and eradicate HIV-1 infected Tfh cells as well as Epstein-Barr virus (EBV) infected B cells. EBV infection is classically associated with B cell lymphomas and therefore Tfc cells play a role in the prevention of cancer cell proliferation. B) Equipped with capability of self-renewal and a less-exhausted phenotype (in comparison to non-Tfc effector cells) Tfc cells play a crucial role in maintaining cellular immunity during chronic viral infections and select cancers, in which there is prolonged Ag exposure. Following anti-PD-1/PD-L1 blockade immunotherapy CXCR5+ Tfc cells are able to differentiate into CXCR- non-Tfc effector cells and thereby produce a proliferative burst of CD8 T cells. C) Tfc cells may have the capacity to supress or enhance Ab responses, presumably depending on the type of immune reaction (Yu & Ye, 2018).

In line with their potential to support B cells and Ab responses, Tfc cells help maintain the architecture of GCs by exercising their cytotoxic functions. Indeed, self-reactive B cells develop following interactions with auto-antigens as a result of immune evasion by viral pathogens/tumour cells because of a lack of Tc cells and regulatory cell subsets in follicles. Their assistance in GC formation and B cell activation may be attributed to the expression of CD40L, which also reinforces their phenotypic similarity to Tfh cells (Perdomo-Celis et al., 2017).

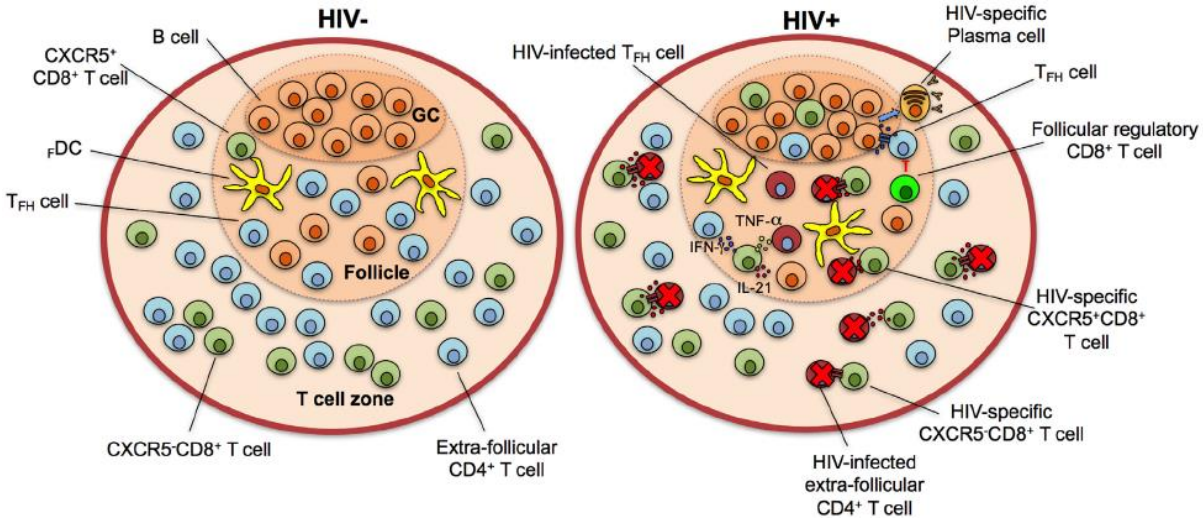

Figure 2.5: The control of HIV infection in lymphoid follicles by CXCR5+CD8+ T (Tfc) cells. Within HIV-negative individuals CD8+ T cells predominantly localize outside of the follicle, in the T cell zone, and only a small proportion are located inside the follicle. However, in HIV+ individuals there is an increase in CXCR5+CD8+ T cell populations in the lymphoid follicle (and germinal centers) in which Ag-specific Tc cells destroy infected Tfh cells. This can occur through the secretion of cytotoxic granules as well as receptor-mediated apoptosis. The secretion of TNF-α, IFN-γ and IL-21 by CXCR5+CD8+ T cells also leads to the development of an antiviral state through Tfh and B cell stimulation. Additionally, Tfh cells are inhibited by follicular regulatory CD8+ T cells which aid B cell differentiation for high-affinity, isotype class-switched Ab production (Perdomo-Celis et al., 2017)**.**

Several studies suggest that the abundance of HIV-infected Tfh cells in ARV-treated HIV+ individuals is partly due to the inadequate follicular localisation of Tc cells. A clearer understanding of Tc cell differentiation into B cell follicle-homing Tfc cells is crucial for the development of a cure strategy that targets and eliminates HIV-infected cells harbouring within lymphoid follicles (Leong et al., 2016).

2.2.4 Immunopathogenic responses to HIV infection

In both HIV-infected adults and children many non-AIDS related morbidities are linked to chronic inflammation (Bourke et al., 2019). Inflammation is a defence mechanism that helps protect the body against endogenous danger signals and invading pathogens, however if it is uncontrolled and persists over time inflammation may cause pathology. Studies have shown that there are elevated levels of inflammation in HIV infected individuals, regardless of viral suppression by cART. The parameters of inflammation, like C-reactive protein as well as pro-inflammatory cytokines, i.e., interleukin (IL)-6, tumor necrosis factor alpha (TNF-α) and B-cell activating factor (BAFF) stay elevated over time and are used as predictors for a multitude of clinical conditions. Combined these clinical conditions/co-morbidities are known as serious non-AIDS events (SNAEs), and include neurological disease, cardiovascular disease, liver disease, cancer, and subsequent death (Pérez et al., 2019).

Infection with HIV leads to systemic inflammation due to chronic enteropathy (CE). The reduction in villous architecture as well as the diminution of mucosal CD4+ T cells, characteristic of CE, during the early stages of HIV infection leads to an increase in gut permeability. This allows microbial translocation and the infiltration of leukocytes, such as monocytes and macrophages which release proinflammatory molecules. Along with a rise in pathogen carriage, this causes changes in the microbiome. Altogether this contributes to the development of systemic inflammation (Bourke et al., 2019; Pérez et al., 2019).

The elevation of inflammatory cytokines has also been linked to a reduction in immunoregulatory responses and development of lymphoid tissue fibrosis in HIV-infected individuals. Primary contributors to irregular levels of inflammation, and immune activation, includes continuous HIV replication in untreated individuals and residual viral replication in treated virologically controlled individuals, as well as exposure to other pathogenic microbes causing co-infections, such as human cytomegalovirus (HCMV) (Pérez et al., 2019).

In HIV infection, mortality and morbidity is precipitated by inflammation. As described, various mechanisms may be responsible for the development of chronic inflammation. A deeper understanding of these mechanisms may lead to the discovery of novel

targets to minimize the high risk of SNAEs and improve clinical outcomes in HIV-infected individuals (Ekali et al., 2019; Pérez et al., 2019).

2.2.4.1 Immune activation

One critical component of HIV pathogenesis is the occurrence of widespread immune activation (Pissani & Streeck, 2014). It has been proposed that patients with chronic infection may have uncontrolled immune activation that plays a significant role in the depletion of CD4 T cells and represents a potent clinical predictor of cell death (Eggena et al., 2005).

In untreated HIV-infected individuals, the rate of depletion of CD4+ T cells and progression of disease is predicted by T cell activation markers along with T cell turnover. However, after the initiation of ART there is a decline in the T cell turnover rate and level of widespread T cell activation. This suggests that generalised T cell activation is the cause of HIV disease progression and the ongoing high level of T cell turnover, linked with the immune system's inability to create additional progenitor T cells, ultimately leads to a gradual reduction in peripheral CD4 T cells (Deeks et al., 2008).

Even though chronic T cell activation is significantly less with ART treatment, years later residual T cell activation may persist in HIV-infected patients regardless of continuous treatment (Luo et al., 2017). Extreme levels of T cell activation in chronically HIV-infected patients, including HIV-infected infants, can be caused by the circulation of gut translocated microbial products (Alvarez et al., 2017).

Marker of immune activation: CD38

In the earliest phase of activation, the multifunctional transmembrane glycoprotein, CD38, is up-regulated on T cells. It has been demonstrated that the activation of T cells, indicated by the expression of CD38 on CD8+ CTLs is a much stronger prognostic indicator for disease progression than CD4 T cell count at various stages of HIV infection (Alvarez et al., 2017).

Marker of immune activation: CD69

Following activation of T cells, CD69 is also expressed early on. CD69 is therefore involved in the earliest stages of T cell activation. The surface expression of the glycoprotein CD69 is maintained several days after its induction and is therefore

relatively stable. The functional involvement of CD69 elevates the frequency of proliferation of T cells. In addition to T cells CD69 can be expressed on several other hematopoietic originating cells, such as B and NK cells and is also amplifies their proliferation (Ziegler et al., 1994).

2.2.4.2 Immune exhaustion

When CD8+ T cells interact with their cognate antigen, T cell inhibitory molecules are up-regulated to manage the subsequent T cell activation as well as prevent autoimmunity. However, antigen persistence can interfere with this homeostatic mechanism and as a result CD8+ T cells may become permanently exhausted or dysfunctional (Hoffmann et al., 2016).

Immune exhaustion decreases the regenerative capacity of the immune system. T cells that are exhausted cannot effectively lyse infected cells, undergo proliferation, or produce antiviral cytokines. As a result, the virus is not effectively cleared by the immune system and persists leading to the development of chronic infection (Fahey et al., 2011).

In the setting of HIV-1 infection, up-regulation of immune checkpoint receptors (ICRS) such as the surface molecule, PD-1, has been linked to T cell exhaustion (Hoffmann et al., 2016).

2.2.4.3 Inflammation

In both HIV-infected adults and children many non-AIDS related morbidities are linked to chronic inflammation (Alvarez et al., 2017). Inflammation is a defence mechanism that helps protect the body against endogenous danger signals and invading pathogens, however if it is uncontrolled and persists over time inflammation may cause pathology. Studies have shown that there are elevated levels of inflammation in HIV infected individuals, regardless of viral suppression by cART. The parameters of inflammation, like C-reactive protein as well as pro-inflammatory cytokines, i.e., interleukin (IL)-6, tumor necrosis factor alpha (TNF-α) and B-cell activating factor (BAFF) stay elevated over time and are used as predictors for a multitude of clinical conditions. Combined these clinical conditions/co-morbidities are known as serious non-AIDS events (SNAEs), and include neurological disease, cardiovascular disease, liver disease, cancer, and subsequent death (Pérez et al., 2019).

Infection with HIV leads to systemic inflammation due to chronic enteropathy (CE). The reduction in villous architecture as well as the diminution of mucosal CD4+ T cells, characteristic of CE, during the early stages of HIV infection leads to an increase in gut permeability. This allows microbial translocation and the infiltration of leukocytes, such as monocytes and macrophages which release proinflammatory molecules. Along with a rise in pathogen carriage, this causes changes in the microbiome. Altogether this contributes to the development of systemic inflammation(Bourke et al., 2019; Pérez et al., 2019).

The elevation of inflammatory cytokines has also been linked to a reduction in immunoregulatory responses and development of lymphoid tissue fibrosis in HIV-infected individuals. Primary contributors to irregular levels of inflammation, and immune activation, includes continuous HIV replication in untreated individuals and residual viral replication in treated virologically controlled individuals, as well as exposure to other pathogenic microbes causing co-infections, such as human cytomegalovirus (HCMV) (Pérez et al., 2019).

In HIV infection, mortality and morbidity is precipitated by inflammation. As described, various mechanisms may be responsible for the development of chronic inflammation. A deeper understanding of these mechanisms may lead to the discovery of novel targets to minimize the high risk of SNAEs and improve clinical outcomes in HIV-infected individuals (Bourke et al., 2019; Pérez et al., 2019).

2.2.4.4 Dysregulation of the humoral immune response

HIV infection causes the gradual development of abnormalities in the humoral immune system. Dysregulation in B cell phenotype and function is demonstrated early in infection and is never completely restored even with the administration of long-term ART (Lindqvist et al., 2012). Defects such as hyperactivation of B cells (i.e., hypergammaglobulinemia), increased spontaneous antibody secretion and increased activation marker expression as well as the development of B cell lymphomas can manifest in HIV-infected patients (Titanji et al., 2006).

Some studies suggest that the differentiation of naïve and memory B cells play a role in the development of B cell dysfunctions during HIV infection. In the peripheral blood of patients with chronic infection, decreased proportions of circulating memory B cells have been observed. In HIV-infected patients, both treated and untreated, the reduced

frequency of memory B cells and rise in the transitional B cell phenotype is associated with the expansion of Tfh cells (Miles & Connick, 2016).

In HIV-infected patients, components involved in the development and control of HIV-specific memory B cells may be dysregulated or non-functional. This is demonstrated by the absence of HIV-specific antibodies in antiretroviral treated patients. It is suggested that compromised responses of memory B cells as well as reduced levels of high affinity, HIV-specific antibodies may result in a higher risk of contracting infections in HIV-positive patients as well as children born to infected mothers (Titanji et al., 2006).

In summation, Tfh cells play a major role in the humoral immunity against HIV infection. They interact with several other lymphocyte populations, especially B cells that reside in GCs, and contribute to the development/maintenance of said GCs and the production of high affinity antibody responses. However, in the context of HIV infection Tfh cells may also become a hindrance, as it is preferentially targeted by HIV for infection, by enlarging the HIV reservoir for latent infection. Additionally, dysregulation in the Tfh cell compartment my lead to the development of dysfunctional immune responses and immunopathogenesis. In order to gain a clearer insight into the impact of Tfh cells within HIV-infected individuals, the dynamics between Tfh cells and other key cell populations, known to play a role in HIV immunity, needs to be investigated.

Study Rationale

South Africa has one of the highest burdens of HIV infection, with regards to both new infections and people already living with HIV. Even with improved access to antiretroviral treatments, MTCT of HIV is still a cause of paediatric infections in South Africa. Children born to HIV-infected pregnant women may acquire HIV consequently through vertical transmission or experience exposure to the virus and remain uninfected. The immature immune systems of these children, i.e., HIV-exposed infected and HIV-exposed uninfected, develop in the presence of HIV and according to several studies become dysfunctional/dysregulated, resulting in increased mortality and morbidity, susceptibility to infections, production of weak antibody responses to vaccination and several other defects, when compared to that of unexposed uninfected children. There is abundant research investigating immunopathology as a result of HIV infection in HIV-infected adults, however research on its impact on children is lacking.

Tfh cells have become of particular interest in HIV research and investigation because of their significant role in the production of effective humoral immune system responses and generation of broadly neutralizing antibodies, for the clearance of HIV. However, they have also been found to be preferentially target by HIV for infection and make up a major part of the HIV reservoir, contributing to latent infection.

The goal of this study was to identify the frequency of Tfh cells (among other cell subsets commonly researched in HIV immunopathology) within early-treated HIV-infected children who were part of the CHER trial and assessed between the ages of 8 – 12 years, as well as HIV-exposed uninfected and HIV-unexposed uninfected children. In addition, to investigate levels of immune activation (and subsequent exhaustion) as well as inflammation by identifying the frequency of cell populations expressing markers of activation and exhaustion, and inflammatory cytokines, respectively. Having a better understanding of the dynamics of Tfh cells with other cell populations within the T cell compartment and its relationship to immune activation and inflammation could help to provide a better understanding of the immune status of early treated HIV infected children.

Aims and Objectives

The aim of this study was to investigate the Tfh cell population in children from the CHER study who began ART within the first six months of life to ascertain whether any ongoing immune activation and inflammation in these children translated into immune dysregulation in the Tfh cell compartment.

The objectives of this study were to:

I. Phenotypically characterise Tfh cells and determine their relative proportions (%) in early treated HIV-infected and HIV-exposed uninfected children.
II. Determine the relative proportions (%) of total T cells, CD4 T cells and CD8 T cells as well as specific subset populations.
III. Asses the relationship between the frequency of Tfh cells and clinical parameters, such as absolute CD4 count, absolute CD8 count and CD4:CD8 ratio.
IV. Determine the relative proportions (%) of T cell subsets expressing CXCR5 (marker of follicular homing) and asses their relationship to Tfh cells.
V. Determine the relative proportions (%) of T cell subsets expressing CD38 and CD69 (markers of activation) as well as CD8 T cells expressing PD-1 (marker of exhaustion).
VI. Assess the impact of immune activation (and exhaustion) as well as inflammation on the frequency of Tfh cells.

Chapter 3 – Methodology

3.1 Participant recruitment and initial investigations

The research documented in this thesis formed part of a larger collaborative study called the Reservoir study conducted by the Division of Medical Virology and Medical Microbiology in the Department of Pathology of Stellenbosch University as well as FAMCRU in the Department of Paediatrics. The Reservoir study was a collaborative National Institutes of Health (NIH)-funded study that focused on children enrolled in the CHER trial.

The aim of the Reservoir study was to analyse the short and long-term virological, neurological as well as immunological impact of early antiretroviral treatment on children with vertically acquired HIV infection. Samples obtained were from children, between the age of 8 – 12 years, enrolled in the CHER trial. The study was approved by the Health Research Ethics Committee (HREC), Faculty of Medicine and Health Sciences at Stellenbosch University (M14/07/029; PI: Prof MF Cotton). This study formed part of a section titled “immune investigations”. All parents/guardians of the patients (as they were underage at the time) provided informed consent for the larger study which included a clause for the storage of cells and further immune characterisations.

The participants of this study consisted of three cohorts of age (approximately 8 - 12 years old) and community (residing in the same areas with a similar socio-economic background) matched children. The three cohorts were comprised of children infected with HIV through vertical transmission who were given ART from birth either with or without treatment interruption (i.e., HIV Infected Treated), children who were exposed to the virus as a foetus but not infected (HIV Exposed Uninfected), as well as children that were HIV unexposed and therefore uninfected (HIV Unexposed Uninfected). All of the HIV-infected children were placed on ART from an early age. It is uncertain whether infection occurred in-utero, intrapartum or post-partum. Some of the children within this group had treatment interrupted 40 weeks after birth while others had no treatment interruption.

3.2 Study Design

This study was a retrospective cross-sectional observational assessment using three study cohorts, i.e., HIT, HEU and HUU, for the characterisation and quantification of Tfh cells and other T lymphocyte cell subsets as well as the analysis of immune cell activation and inflammation.

3.3 Secondary data

CD4 T cell count, CD8 T cell count and CD4:CD8 ratio (i.e., clinical parameters) data was obtained using lymphocyte counts of EDTA whole blood samples collected from participants. IL-1β, IFN-γ, TNFα, IFN-α and hsCRP (i.e., inflammatory cytokines) data was obtained using Luminex® Multiplex Assays. These experiments and acquisition of this data was performed by a colleague at the Division of Medical Virology, Faculty of Medicine and Health Sciences at Stellenbosch University, and was related to another study which also formed part of the Reservoir Study. Although these were not tested for in the process of this study, the data of these parameters for each sample selected (i.e., representing an individual study participant) was available for use.

3.4 Sample selection

Peripheral blood mononuclear cell (PBMC) samples, previously isolated from the whole blood drawn from participants at approximately 8-12 years of age, and stored in a liquid nitrogen dewar were selected based on the availability of PBMC containing cryovials, which had matched plasma containing cryovials stored, and collected. In this study at least two cryovials (each containing approximately 2,5 million cells) were required for the assay.

The number of samples collected for each group were as follows:

Cohort	Number of samples
HIT	20 (10 no ART interruption; 10 ART interruption)
HEU (control group)	19
HUU (control group)	20

3.5 PBMC Isolation and Cryopreservation

After the collection of whole blood from participants, PBMCs were isolated within 24 hours using the Ficoll-gradient method. The whole blood of each participant was transferred from ethylenediaminetetraacetic acid (EDTA) tubes into either 15ml/50ml falcon tube depending on the blood volume. A blood volume below 7ml was transferred to a 15ml falcon tube whereas a blood volume above 7ml was transferred into a 50ml falcon tube. The whole blood was then centrifuged at 3000 revolutions per minute (rpm) for 10 minutes with the break and acceleration set to the highest setting using either a Jouan b4i or Rotanta 460R centrifuge. After centrifugation, the top plasma layer was collected and aliquoted into 2ml cryovials for viral load testing. The remaining blood was diluted with phosphate-buffered saline (PBS; Lonza BioWhitakker, WhiteSci, SA) equal to that of the volume of plasma that was removed. Using a bulb pipette the diluted blood was mixed and carefully layered onto 6ml (for blood volumes between 7ml) or 15ml (for blood volumes above 7ml) of Ficoll Histopaque-1077 (Sigma-Aldrich, Merk, SA) in a separate falcon tube, which was centrifuged at 2000 rpm for 30 minutes. The lowest settings for break and acceleration were used, as well as for all centrifugation steps thereafter. After centrifugation, the PBMC layer was collected, transferred to a falcon tube containing PBS, topped up with PBS (until 13ml in a 15ml tube or 40ml in a 50ml tube) and centrifuged at 1600 rpm for 17 minutes. For smaller blood volumes this wash step was performed once however for larger blood volumes (>25ml) this wash step was repeated. The supernatant was discarded, and the pellet resuspended in PBS for cell counting. Blood volumes ≤10ml were reconstituted in 5ml PBS whereas blood volumes >25ml were reconstituted in 20ml of PBS. To determine the cell concentration and viability a cell count was performed using a 1:1 dilution of cell suspension and Trypan blue and processed using a TC20™ cell counter (Bio-Rad Laboratories, USA). The detection gate on the cell counter was set to 6 – 17µM. After obtaining the cell count (performed in quadruplicate and averaged), the cell suspension was centrifuged once more at 1600 rpm for 10 minutes, after which the supernatant was discarded. The pellet was then resuspended in cryopreservation media. The cryopreservation media was prepared using 90% Heat Inactivated Fetal Bovine Serum (FBS; Gibco, ThermoFischer Scientific, SA) and 10% Dimethyl Sulfoxide (DMSO; Sigma-Aldrich, Merk, SA), which was added in a dropwise manner while swirling cells gently in the

tube so that the final cell concentration was approximately 2,5 million cells per ml. The cell suspension was aliquoted into 2ml cryovials and placed in a Mr Frosty (Thermo Fischer Scientific, California, USA) to be stored overnight at -80°C and thereafter transferred to a liquid nitrogen dewar for long-term storage.

3.7 General protocol for surface and intracellular staining of PBMCs

3.7.1 Sample preparation

PBMC cryovials of selected participants were collected from a liquid nitrogen dewar and transported on dry ice to a bead bath set to 37°C for rapid thawing of samples. Within a disinfected laminar flow hood, 1ml of warmed wash media (made up of RPMI 1640 with L-Glutamine and Heat Inactivated FBS) was added dropwise to each cryovial containing thawed PBMCs so that the volume within the cryovial was doubled. This cell suspension was transferred to a 15ml falcon tube and filled with 7ml of wash media. Another 1ml of wash media was added to each cryovial to wash excess cells residing at the bottom of the cryovial and transferred to the 15ml falcon tube as well. The total volume of diluted cell suspension within the 15ml falcon tube (=10ml) was then centrifuged at 1500 rpms for 7 minutes with the break and acceleration set to the highest setting. Following the centrifugation step, the supernatant was carefully discarded, and the pellet resuspended in 1ml of staining media (made up of PBS and Heat Inactivated FBS) for cell counting. A cell count was performed to determine the cell concentration and viability of the cell suspension. 10µl of cell suspension was mixed with 10µl of Trypan Blue (1:1 dilution) and processed with a TC20™ cell counter (Bio-Rad Laboratories, CA, USA). Following the cell count, cell suspension was centrifuged at 1500 rpms for 5 minutes. Thereafter, the supernatant was discarded, and the pellet resuspended in 100µl of staining media.

3.7.2 Staining for T cells and immune activation

100µl of cell suspension of each sample was aliquoted into separate 14ml polystyrene round bottom non-pyrogenic falcon tubes (BD Falcon™) and stained with a pre-made cocktail of fluorochrome-conjugated antibodies. The tubes were vortexed and incubated in the dark at room temperature for 30 minutes. 500µl of staining media was then added to each tube and tubes were centrifuged at 1500 rpm for 10 minutes. After centrifugation, the supernatant was decanted, and the pellet resuspended in 100µl of Fix/Perm media. Tubes were then vortexed and incubated in the dark at room temperature for 20 minutes. Thereafter, 1ml of permeabilization wash buffer was

added to each tube and centrifuged at 1500 rpm for 5 minutes. The supernatant was discarded, and the pellet resuspended in 100µl of perm wash buffer after which the cell suspension was stained with the anti-FoxP3 V450 antibody and incubated in the dark at room temperature for 30 minutes. After incubation, 500µl of perm-wash media was added to each tube and centrifuged at 1500 rpm for 5 minutes. The supernatant was discarded, and the pellet resuspended in 500µl of formaldehyde for the fixation of cells. The tubes were then incubated at room temperature for 10 minutes and centrifuged at 2000 rpm for 10 minutes. After discarding the supernatant, 200µl of staining media was added to each tube, which were then stored in the dark at 4°C overnight for FACS acquisition, via a BD LSR II flow cytometer (BD Biosciences, CA, USA), the next day.

3.7.3 Panel Design

An eleven-colour (i.e., multicolour) staining panel was designed for the phenotypic identification of T lymphocytes. All the antibodies used in this study were obtained from BD (BD Biosciences, CA, USA). The antibody panel (i.e., T cell panel) included the following fluorochrome-conjugated monoclonal antibodies (mAbs): CD3-Brilliant Violet 510 (BV510); CD4-Brilliant Blue 515 (BB515); CD8-Allophycocyanin-H7 (APC-H7); CD185 (CXCR5)-Peridinin-chlorophyll protein-Cyanin5.5 (PerCP-Cy5.5); CD279 (PD-1)-Allophycocyanin (APC); CD278 (ICOS)-Phycoerythrin (PE); CD25-Phycoerythrin-Cyanine 7 (PE-Cy7); FoxP3-Violet 450 (V450), an intracellular staining antibody; CD38-Brilliant Violet 605 (BV605); CD69-Phycoerythrin-CF594 (PE-CF594) as well as Fixable Viability Stain 700 (FVS700), a fixable amine-reactive viability marker.

These antibodies were carefully selected based on the configuration of the instrument (i.e., flow cytometer: BD LSR II (BD Biosciences, CA, USA)) used, the availability of clones for each fluorochrome-conjugated antibody, the relative dimness and brightness of each fluorochrome-conjugated antibody, the density and class (i.e., primary, secondary or tertiary) and co-expression of specific antigens (i.e., surface or intracellular markers) on target cells.

The availability of clones was determined using the BD FACSELECT™ Multicolour Reagent Selector (BD Biosciences 2018, https://www.bdbiosciences.com/in/paneldesigner/index.jsp). Using the BD Biosciences Relative Fluorochrome Brightness chart

(https://www.bdbiosciences.com/documents/Fluorochrome-Chart-Relative-Brightness.pdf) highly expressed markers were paired with dim fluorochromes and lowly expressed markers with bright fluorochromes. Additionally, the BD Horizon™ Guided Panel Solution (GPS) tool (BD Biosciences 2018, https://www.bdbiosciences.com/en-us/applications/research-applications/multicolor-flow-cytometry/product-selection-tools/horizon-gps-tool) was used to create a preliminary gating strategy to broadly analyse the co-expression of different classes of antigens and the relationship of cell populations and subpopulations of interest. During this antibody panel design stage, BD Spectrum Viewer (BD Biosciences 2018, https://www.bdbiosciences.com/en-us/applications/research-applications/multicolor-flow-cytometry/product-selection-tools/spectrum-viewer) was also used to determine the spectral overlap that would be encountered using combinations of selected fluorochromes, which would need to be compensated for. Table 3.1 below shows a summary of the clone, isotype, and reactivity information of the mAbs used in this study.

Table 3.1: Summary of information of mAbs used for T cell panel in this study.

Monoclonal Antibody (mAb)		Clone	Isotype	Reactivity	BD Catalogue Number	Target cells
Marker	Fluorochrome					
CD3	BV510	HIT3a	Mouse IgG2a, κ	Human	564713	T cells
CD4	BB515	RPA-T4	Mouse IgG1a, κ	Human	564419	T helper cells
CD8	APC-H7	SK1	Mouse (BALB/c) IgG1, κ	Human	560179	T cytotoxic cells
CD185 (CXCR5)	PerCP-Cy5.5	RF8B2	Rat (LOU) IgG2b, κ	Human	562781	Follicular T cells
CD279 (PD-1)	APC	MIH4	Mouse IgG1, κ	Human	558694	T follicular helper cells/ Exhausted T cells
CD278 (ICOS)	PE	DX29	Mouse IgG1, κ	Human	557802	T follicular helper cells
CD25	PE-Cy7	M-A251	Mouse (BALB/c) IgG1, κ	Human	557741	T regulatory cells
FoxP3 (I/C)*	V450	259D/C7	Mouse IgG1	Human	560459	T regulatory cells
CD38	BV605	HB7	Mouse IgG1, κ	Human	562665	Activated T cells
CD69	PE-CF594	FN50	Mouse IgG1, κ	Human	562617	Activated T cells
FVS700 (a dye, not a mAb)	Intracellular amine reactive dye with emission detectable in 720/40 BP filter)	N/A	N/A	Mammalian	564997	Non-viable (dead) cells

N/A – Not Applicable
*FoxP3 (I/C) is an intracellular cell marker.

3.8 Optimisation of Assay

3.8.1 Instrument Set-up

Flow cytometric data acquisition was performed on a BD LSR II (BD Biosciences, CA, USA) flow cytometer using BD FACSDiva™ software (Version 8.0.1) at the BD Flow Cytometry training centre of the Central Analytical Facility (CAF) at Stellenbosch University, Tygerberg Medical Campus and at the Institute of Infectious Disease and Molecular Medicine (IDM) Flow Cytometry Core Facility at the University of Cape Town. Both cytometers were equipped with Blue (488 nm), Violet (405 nm) and Red (633 nm) lasers and emission filters for PE-Cy7 (Long-pass filter [LP]: 735, Band-pass filter [BP]: 780/60), PerCP-Cy5.5/BB700 (LP: 685, BP: 695/40), PerCP/PE-Cy5 (LP: 635, BP: 670/14), PE-CF594 (LP: 600, BP: 610/20), PE (LP: 550, BP: 575/26), FITC/BB515 (LP: 505, BP: 530/30), BV605 (LP: 555, BP: 605/40), BV605 (LP: 555, BP: 605/40), BV510 (LP: 505, BP: 525/50), BV421/V450 (LP: -, BP: 440/40), APC-H7 (LP: 735, BP: 780/60), APC-R700 (LP: 690, BP: 720/40) and APC (LP: -, BP: 660/20).

To ensure quality control the flow cytometer was calibrated with BD cytometer setup and tracking (CS&T) beads (BD Biosciences, CA, USA) on each day that an experiment was performed in order to ensure optimal performance of fluidics and optics systems of the instrument. Basic daily maintenance also included cleaning and priming of the instrument.

Additionally, Rainbow Calibration Particles (8 peaks) (Sphero™, BD Biosciences, USA) were processed before each experiment. This was done to align instrument settings by checking photomultiplier tubes (PMT) sensitivity, resolution as well as linearity of the flow cytometer. Rainbow particles contain a combination of fluorophores and have an emission spectra compatible with various common fluorophores that are used in immunofluorescent staining. These rainbow particles were used to create application settings to be used for each experiment to ensure consistent and reproducible results between experiments. For each parameter, within each antibody panel, a histogram was created on FACSDiva™ software (Version 8.0.1) and using an interval gate the 7th peak was gated on when running particles. The Median Fluorescent Intensity (MFI) of peak 7 for each parameter was recorded and with every subsequent experiment if the peak were to fall outside of the interval gate and if the MFI was too low or too high (i.e., not similar to the original), the voltage for that

parameter was slightly adjusted. Therefore, any subtle changes in fluorescent levels between experiments could be detected and resolved.

3.8.2 Monoclonal Antibody Titrations

Antibody titration experiments were performed for each monoclonal antibody used in this study, including antibody stock with the same catalogue number but different lot numbers. This was done to identify the optimal volumes of antibody to be used for the staining of cells in experiments. Titrations indicate the optimal concentration that can be used in an assay to produce an optimal fluorescent signal to accurately discriminate between positive and negative cell populations. In multiparametric flow cytometry it is important to maximise the fluorescent signal while minimising the noise (fluorescent background) produced by the flow cytometer, autofluorescence as well as the non-specific binding of antibodies.

In this study, the signal-to-noise ratio (S/N) was used to determine the optimal concentration and was calculated by dividing the median fluorescence intensity (MFI) of the positive population by the negative population for each antibody dilution. The S/N measured the sensitivity of the assay and the ability to discriminate between positive (stained) and negative (unstained) populations.

Additionally, in order to measure the relative brightness of a specific fluorochrome-conjugated antibody, the Stain Index (SI) was calculated (as per the formula depicted below) by dividing the difference between the MFI of the positive and MFI of the negative population by the robust standard deviation (rSD) of the negative population multiplied by two.

$$\text{Stain Index} = \frac{MFI_{pos} - MFI_{neg}}{2\sigma_{neg}}$$

MFI = Mean Fluorescence Intensity
σ = Standard Deviation

The higher the S/N the better the discrimination between positive and negative cell populations and the higher the SI the better the relative brightness of the fluorochrome-conjugated antibody compared to a negative (unstained) control. Therefore, using

these measures the optimal staining volume for each antibody was determined accordingly.

Antibody titration experiments were performed under the same conditions as experiments for samples and made use of thawed PBMCs which were cryopreserved isolated from a healthy volunteer. All antibodies were titrated using the optimised standard surface staining protocol except for FoxP3 V450, for which fixation and permeabilization steps were included for intracellular staining. The viability dye, FVS700, was used as per the manufacturers recommended staining concentration.

After thawing, PBMCs were stained with fluorochrome-conjugated antibodies at decreasing concentrations. For antibodies with a recommended staining volume of 5µl (concentration of 1:20), PBMCs were stained with a doubling dilution series of 1:20, 1:40, 1:80 and 1:160. Whereas antibodies with a recommended staining volume of 20µl (concentration 1:5), PBMCs were stained with a doubling dilution series of 1:5, 1:10, 1:20 and 1:40.

Before acquisition of stained samples for titration experiments, an unstained sample was processed for the voltage adjustment of forward scatter (FSC) and side scatter (SSC) detection to standardise light scatter for the differentiation of major leucocyte subpopulations. The unstained sample was also used to adjust the voltage for each fluorescent parameter so that the rSD measured was ≥ 2.5 times the rSD of the electronic noise (rSD_{EN}).

After processing the series of PBMC samples stained with multiple concentrations of antibody, the data was collected for each antibody and exported to FlowJo software (version 10.3), in which the MFI of the negative and positive population for each dilution, as well as the signal to noise ratio and stain index was calculated and thereafter exported to Microsoft Excel. Table 3.2 shows the selected dilution factor that produced the highest S/N and SI.

Table 3.2: Optimal staining dilutions for T cell panel based on antibody titration experiments. For antibodies that have more than one optimal titrated staining dilution factor, these antibodies produced different results because they were from a different lot number even though the catalogue number was the same.

Monoclonal Antibody (mAb)		Manufacturer Recommended Staining Dilution Factor	Titrated Staining Dilution Factor
Marker	**Fluorochrome**		
FVS700	Intracellular amine reactive dye with emission detectable in 720/40 BP filter)	1:1000	N/A
CD3	BV510	1:20	1:40/1:50
CD185 (CXCR5)	PerCP-Cy5.5	1:20	1:80
CD38	BV605	1:20	1:80/1:160
CD69	PE-CF594	1:20	1:20/1:80
CD4	BB515	1:20	1:40
CD8	APC-H7	1:20	1:80
CD279 (PD-1)	APC	1:5	1:20
CD278 (ICOS)	PE	1:5	1:20
CD25	PE-Cy7	1:20	1:80
FoxP3 (I/C)*	V450	1:20	1:100

*FoxP3 (I/C) is an intracellular T cell marker.

3.8.3 Fluorescence Compensation for Spectral Overlap

Fluorescence spillover occurs when the measured signal of a specific fluorochrome is emitted in the detector of another fluorochrome. Fluorescence compensation is therefore performed to correct for emission spectral overlap and ensure that the fluorescence detected in a particular detector derives from the fluorochrome being measured. This ensures that the background signal produced as a result of spillover is subtracted in all detectors (Cossarizza et al., 2017).

Figure 3.1 shows a visual representation of the spectral overlap incurred by the selected fluorochromes for all three lasers (i.e., blue, violet and red). These images were created using the online tool BD Fluorescence Spectrum Viewer (BD Biosciences 2018, https://www.bdbiosciences.com/en-us/applications/research-applications/multicolor-flow-cytometry/product-selection-tools/spectrum-viewer).

In this study compensation controls were made using anti-immunoglobulin capture beads, namely Anti-Mouse Ig, κ chain (for antibodies with a mouse isotype) and Anti-Rat Ig, κ chain (for antibodies with a rat isotype) and Negative control compensation particles (BD CompBeads; BD Biosciences, CA, USA).

The advantage of using capture beads in this study was that no biological material (i.e., PBMCs) was needed, controls were easy and less time consuming to prepare and didn't degrade easily over time and therefore the same controls could be used for multiple experiments.

Compensation controls were prepared for each different fluorochrome-conjugated antibody. Additionally, a control was prepared using thawed PBMCs for the FVS700 viability dye, as it does not bind with BD CompBeads, to accurately distinguish between live and dead cells. Compensation controls were prepared and processed for each experiment to ensure standardisation and quality control.

Compensation controls, for each fluorochrome-conjugated antibody, were prepared as per the manufacturer's protocol (BD CompBeads; BD Biosciences, CA, USA). For each antibody one full drop of either BD CompBeads anti-mouse Ig or BD CompBeads anti-rat Ig (depending on the isotype of the antibody) and one drop of BD CompBeads negative control were added to a 14ml polystyrene round bottom non-pyrogenic falcon tubes (BD Falcon™) containing 100µl of staining buffer. 20µl of prediluted antibody stock – dilution was determined using the optimal staining concentration as per titration experiments mentioned previously – was then added to the appropriate tube and incubated at room temperature, protected from direct light, for 30 minutes. After incubation, 2ml staining buffer was added and the tubes centrifuged at 200 RCF for 10 minutes. After this washing step, the supernatant was discarded, and the pellet resuspended in 500µl of staining buffer.

Compensation controls, for FVS700, were prepared as per the surface staining protocol used to stain thawed PBMC samples in this study. A positive control, in which cells were killed with 70% EtOH, and a negative control, without the 70% EtOH kill, was prepared due to FVS700 binding of dead and not live cells.

For each experiment, before the processing of cohort samples, compensation controls were processed and acquired. Both a negative and positive peak was gated on for each antibody in the panel, compensation was calculated and then applied to cohort

samples on FACSDiva software. The compensation was also checked and reapplied to sample data during data analysis on FlowJo software (version 10.3).

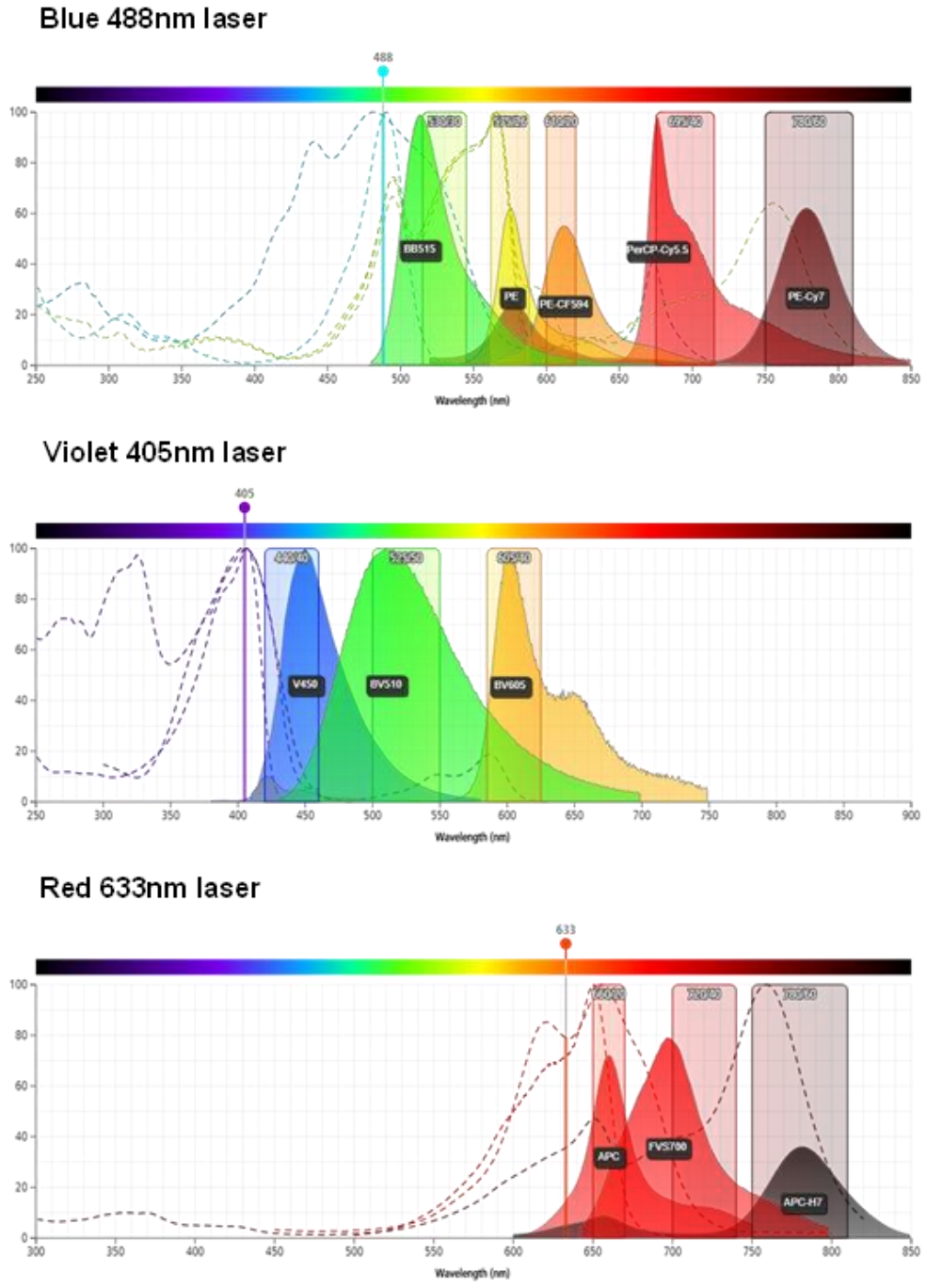

Figure 3.1: Spectral overlap encountered between selected fluorochromes. The emission spectrum (demonstrated by solid lines and coloured peaks) as well as the absorption spectrum (demonstrated by dotted lines) are shown for each fluorochrome in T cell panel for the blue 488nm, violet 405nm and red 633nm lasers. Rectangles represent band-pass filters that determine which parts of the spectrum are detected in the flow cytometer. Spectral overlap occurs where the emission spectra of one fluorochrome overlaps with that of an adjacent

fluorochrome within the bandpass filter. This spillover needs to be compensated for in a multicolour staining experiment in order to eliminate the possibility of false positive results caused by the detection of the incorrect fluorochrome.

3.8.4 Fluorescence Minus One Controls for gating strategy

Fluorescence Minus One (FMO) controls were processed in order to accurately distinguish negative and positive cell populations for specific markers of interest. This is especially useful for experiments in which marker expression is low. FMO controls provide a threshold for positively stained cell populations and a measure of the fluorescent spread of other fluorochromes into the channel of interest (Cossarizza et al., 2017).

In the FMO control, all antibodies within the antibody panel are included except for the antibody that is controlled for. For example, in the CD3 FMO control tube cells were stained with all antibodies in the panel except for the CD3 mAb, i.e., CD3 BV510. FMO controls were made for each fluorochrome-conjugated antibody using PBMCs from a healthy adult volunteer.

FMO controls were made using thawed cryopreserved samples, which were stained as per the standard staining protocol used in this study. When acquiring these FMO control stained samples, the same procedure for samples of participants was applied. A preliminary gating strategy was created on FACSDiva software to ensure that all fluorescent markers could be detected. Additionally, a fully stained sample of the same cryopreserved cells was acquired. During data analysis, FMO controls were used to create population gates, which would define cell populations based on the phenotypic expression of specific markers of interest.

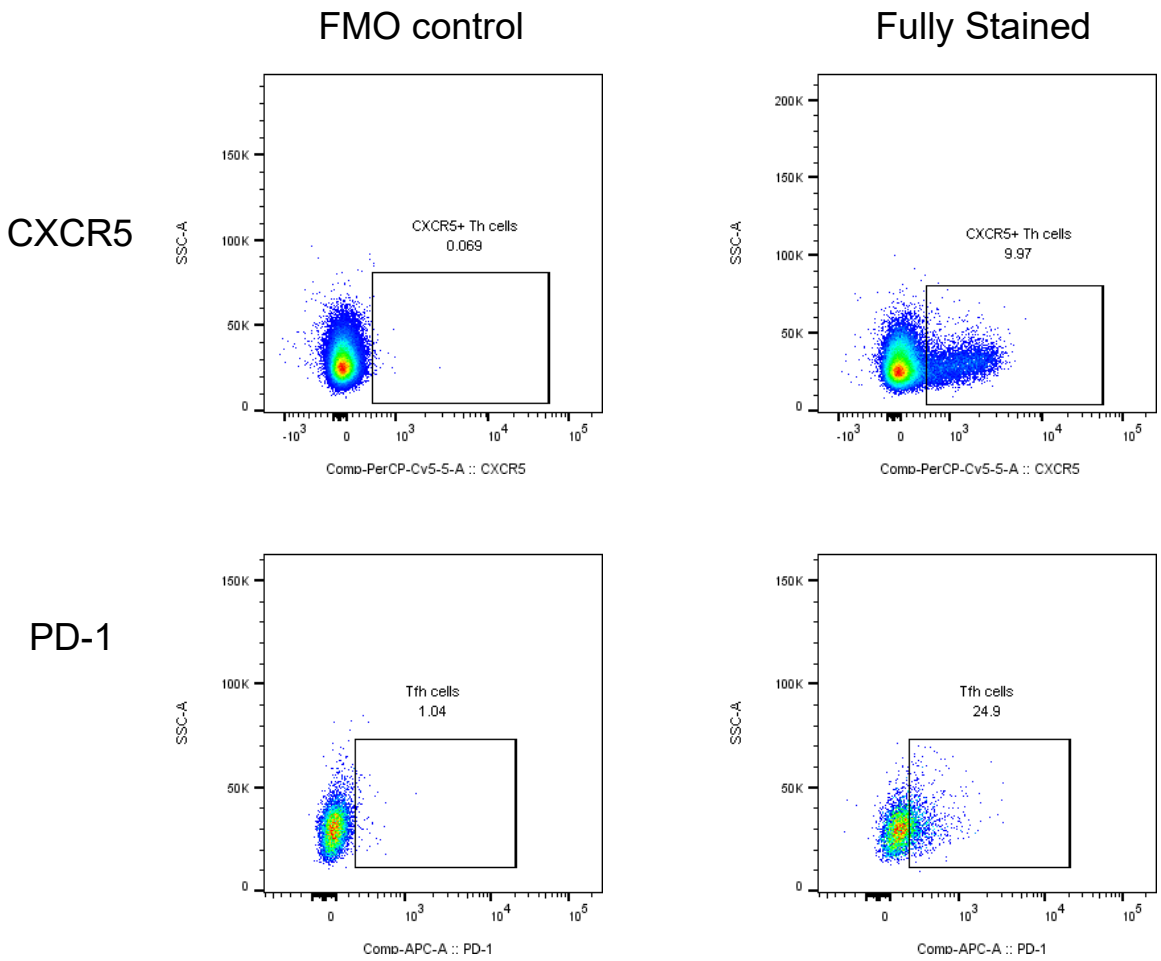

Figure 3.2: Fluorescence Minus One (FMO) gating control and fully stained dot plots for CXCR5 and CD279 (PD-1). Dot plots were generated in FlowJo (version 10.3). In the plot each dot represents a single cell and where they cluster indicates a distinct cell population. Red and yellow areas are where the cells are densest (i.e., highest percentage of cells). Squares within the plot represent region gates designed to discriminate between marker-specific positive and negative cells. Side scatter (SSC) is demonstrated on the y-axis whereas the parameter (i.e., marker of interest) is demonstrated on the x-axis. “Comp” indicates that the data was compensated. FMO control do not contain the antibody used to stain cells for that specific marker which is why region gates are empty, whereas the fully stained sample does and positive cells for that marker are displayed within the region gate.

3.9 Sample Processing and Data Acquisition

Stained samples were processed using a BD LSR II flow cytometer (BD Biosciences, CA, USA) located in the BD Central Analytical Facility (BD-CAF) at Stellenbosch University’s Tygerberg Campus as well as in the Institute of Infectious Disease and

Molecular Medicine (IDM) Flow Cytometry Core Facility at the University of Cape Town. Before each experiment (i.e., processing of stained participant samples) CS&T beads were run to check the performance of the cytometer, thereafter 8 peak rainbow calibration particles were run for standardisation as well as all compensation controls for the elimination of spectral overlap. After applying compensation, samples were processed by the cytometer using a low flow rate. Before running, each sample was vortexed to ensure resuspension of cells. Cell acquisition was performed using BD FACSDiva™ (BD Biosciences) software. A forward scatter (FSC) vs side scatter (SSC) gate was used to define lymphocytes from total events acquired. For the elimination of debris, the threshold was set to 20 000 events. An acquisition “stopping gate” was used for each panel. After a specified number of events are acquired and recorded within the stopping gate the cytometer stops processing the sample and no further data is acquired. The stopping gate was set to acquire 200 000 events for each sample stained with a cocktail of fluorochrome-conjugated antibodies. The preliminary hierarchal gating strategy used on BD FACSDiva™ (BD Biosciences) software was as follows: SSC-A vs FSC-A (lymphocytes – Population 1); SSC-A vs FVS700 (live lymphocytes – Population 2); FSC-H vs FSC-A (singlets – Population 3); SSC-A vs CD3 (CD3- and CD3+ cells – Population 4).

3.10 Data Analysis: Defining Lymphocyte Populations (Gating Strategy)

In this study lymphocyte populations of interest were identified based on specific marker (i.e., antigen) expression. Table 3.3 depicts the immunophenotyping criteria used for the discrimination of major lymphocyte populations. Additionally, markers of activation including CD38 and CD69 were analysed on these cell populations to determine levels of immune activation. PD-1, a marker of exhaustion, was also analysed on the CD8 T cell population to determine the levels of immune exhaustion. A summary of the phenotypic characterisation used for the identification of cell populations of interest are described in Table 3.3.

Data that was acquired from the LSR II flow cytometer using BD FACSDiva™ (BD Biosciences) software was exported to FlowJo™ software (Version 10.0, FlowJo, LCC, USA) in the form of Flow Cytometry Standard data files (.fcs) files and further analysed.

Table 3.3: Summary of the phenotypic characterisation of T lymphocyte populations of interest based on marker expression.

Cell population	Immunophenotype (markers for identification)
T cells	CD3+
Follicular T cells	CD3+CXCR5+
CD38+ activated T cells	CD3+CD38+
CD69+ activated T cells	CD3+CD69+
Helper T (Th) cells	CD3+CD4+
CD38+ activated Th cells	CD3+CD4+CD38+
CD69+ activated Th cells	CD3+CD4+CD69+
Follicular Th cells	CD3+CD4+CXCR5+
CD25+ Th cells	CD3+CD4+CD25+
Follicular helper T (Tfh) cells	CD3+CD4+CXCR5+PD-1+ICOS-/+
CD38+ Tfh cells	CD3+CD4+CXCR5+PD-1+CD38+
CD69+ Tfh cells	CD3+CD4+CXCR5+PD-1+CD69+
Regulatory T (Treg) cells	CD3+CD4+CD25+FoxP3+
CD38+ activated Treg cells	CD3+CD4+CD25+FoxP3+CD38+
CD69+ activated Treg cells	CD3+CD4+CD25+FoxP3+CD69+
Follicular regulatory T (Tfr) cells	CD3+CD4+CXCR5+CD25+FoxP3+
CD38+ activated Tfr cells	CD3+CD4+CXCR5+CD25+FoxP3+CD38+
CD69+ activated Tfr cells	CD3+CD4+CXCR5+CD25+FoxP3+CD69+
Cytotoxic T (Tc) cells	CD3+CD8+
CD38+ activated Tc cells	CD3+CD8+CD38+
CD69+ activated Tc cells	CD3+CD8+CD69
CD38+CD69+ activated T cells	CD3+CD8+CD38+CD69+
PD-1 exhausted Tc cells	CD-3+CD8+PD-1+
Follicular cytotoxic T (Tfc) cells	CD3+CD8+CXCR5+
CD38+ activated Tfc cells	CD3+CD8+CXCR5+CD38+
CD69+ activated Tfc cells	CD3+CD8+CXCR5+CD69+

Because FMO controls discriminate between positive and negative marker expression, FMO control analyses were carried out and used to design a gating strategy to accurately identify and distinguish cell populations of interest.

A graphical representation of the hierarchal gating strategy is displayed below in Figure 3.3.

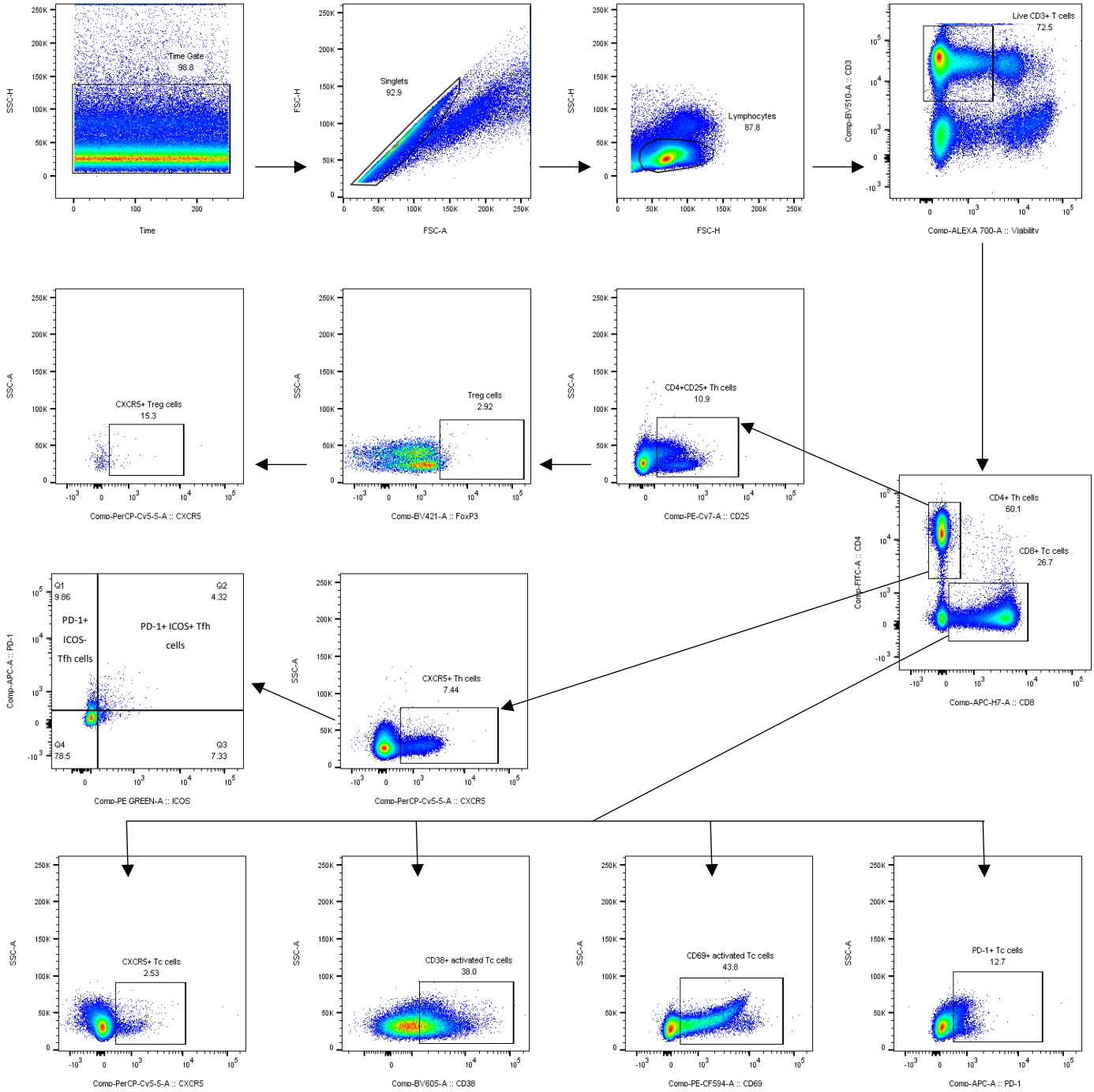

Figure 3.3: Gating strategy for T cell panel. All gates were created according to FMO controls. In the figure, SSC indicates side scatter whereas FSC indicates forward scatter. A time gate (SSC-H vs Time) was used to gate on total events. From which singlets (FSC-H vs FSC-A) were gated on for the exclusion of doublets. From singlets, the total lymphocyte population (SSC-H vs FSC-H) was gated on and subsequently live CD3+ T cells (CD3 vs Viability) through the exclusion of dead cells using the viability dye. From total live CD3+ T

cells, CD4+ helper T and CD8+ cytotoxic T cell populations (CD4 vs CD8) were gated on. From CD4+ Th cells the CD25+FoxP3+ regulatory T cells (SSC-A vs CD25 and subsequently SSC-A vs FoxP3) were gated as well as the CXCR5+ Tregs subset (SSC-A vs CXCR5). Additionally, from CD4+ Th cells the total CXCR5+ Th cells (SSC-A vs CXCR5) were gated on and from this PD-1+ICOS- and PD-1+ICOS+ Tfh cell subsets (PD-1 vs ICOS). From CD8+ Tc cells, CXCR5+ Tc (SSC-A vs CXCR5), CD38+ activated Tc (SSC-A vs CD38), CD69 activated Tc (SSC-A vs CD69) and PD-1+ exhausted Tc (SCC-A vs PD-1) cell subsets were gated on.

3.11 Statistical Analysis

Cell acquisition data was exported from FlowJo™ and saved to a Microsoft Excel database in the form of cell percentage data. Percentage data was that of cell populations that had been gated on and identified based on the expression of specified cell markers. Statistical analysis of the data was performed using GraphPad Prism software for Windows (Version 7.0, GraphPad, CA, USA).

Before any statistical analysis tests were performed, the D'Agostino-Pearson omnibus test was used to determine whether the data was normally distributed. Although a majority of the parameters passed the normality test, there was a considerable proportion that did not. Data that was not normally distributed demonstrated a p-value less than the α value (a.k.a. p-value threshold; alpha = 0.05). For this reason, non-parametric data was not normalised and non-parametric tests were performed on the full data set. The following statistical tests were applied on the data set.

3.11.1 Comparative analysis of HIT, HEU and HUU groups

Study groups were compared to each other using the Mann-Whitney test in the following manner: HIT vs HEU; HIT vs HUU; HEU vs HUU. Non-parametric data for cell populations of interest was described using median percentage data and interquartile ranges (IQR). Median percentages obtained for each of the three cohorts were compared and tested for significance. The results were considered significant when p-values were less than 0.05 ($p < 0.05$).

Tables were used to depict the descriptive statistics (i.e., median and IQR) of each group and indicate whether a significant difference was observed for a specific parameter (i.e., clinical marker, cell population of interest or inflammatory cytokine)

between groups. For cell populations of interest, the parent cell population from which the specific cell population of interest was gated (i.e., is a subset thereof) was also indicated.

Box-and-whisker plots were used to graphically depict a comparison of the data sets of the three cohorts (HIT vs HEU vs HUU). In each box-and-whisker plot the box indicated the interquartile range (IQR: 25-75% confidence interval). The horizontal line inside the box represented the median and the vertical lines (whiskers) outside of the box indicated the 10-90% confidence interval of the data. Dots within each plot represented outliers. Significant P-values were depicted as asterisks symbols in graphs and interpreted as follows:

Symbol	Symbol meaning
*	$P \leq 0.05$
**	$P \leq 0.01$
***	$P \leq 0.001$
****	$P \leq 0.0001$

3.11.2 Correlation analysis between Tfh cells and other parameters

Tfh cells were correlated with other lymphocyte cell populations of interest, clinical parameters (i.e., absolute CD4 count, CD8 count and CD4:CD8 ratio) and inflammatory cytokines. Non-parametric Spearman's rank order test was used to identify significant relationships between Tfh cell populations within each cohort with the parameters listed above.

Scatter plots were used to graphically depict the data. In each plot, a dot represented a patient sample. The line within the plot showed the linear regression, as either a negative or positive correlation. The correlation coefficient (r-value) and significance (p-value) were also depicted in each plot. Results were considered significant when p-values were less than 0.05 ($p < 0.05$). The degree of association between cell populations/parameters were determine using the r-value and interpreted as follows:

Value of r	Interpretation
1.0	Perfect correlation
0 to 1	The two variables tend to increase or decrease together
0.0	The two variables do not vary together at all
-1 to 0	One variable increases as the other decreases
-1.0	Perfect negative or inverse correlation

Chapter 4 – Results

4.1 Comparative analysis of HIT, HEU and HUU groups

4.1.1 Clinical parameters

As indicated in Figure 4.1A, no significant differences were identified between groups with regards to the absolute CD4 T cell count. In regards to absolute CD8 T cell count, as indicated in Figure 4.1B, the HIT group demonstrated a significantly higher median of cells/µl (median: 907 cells/µl, IQR: 627.5 – 1173 cells/µl) in comparison to both the HEU group (median: 592 cells/µl, IQR: 464 – 776 cells/µl) (p = 0.003) and HUU group (median: 627.5 cells/µl; IQR: 480.5 – 773.3 cells/µl) (p = 0.001). The HIT group also demonstrated a significantly lower median CD4:CD8 ratio (median: 1.11, IQR: 0.79 – 1.42) in relation to the HEU group (median: 1.59, IQR: 1.17 – 1.8) (p = 0.006) and HUU group (median: 1.64, IQR: 1.39 – 1.93) (p = 0.0002), respectively (Figure 4.1C).

Table 4.1: Descriptive statistics and comparison of clinical parameters.

Clinical marker	HIT group Median (IQR)	HEU group Median (IQR)	HUU group Median (IQR)	P-value HIT vs HEU	P-value HIT vs HUU	P-value HEU vs HUU
Absolute CD4 T cell count	**998** (797 – 1244)	**972** (814 – 1101)	**1024** (758 – 1292)	0.627	0.868	0.536
Absolute CD8 T cell count	**907** (627.5 – 1173)	**592** (464 – 776)	**627.5** (480.5 – 773.3)	0.003	0.001	0.967
CD4:CD8 ratio	**1.11** (0.79 – 1.42)	**1.59** (1.17 – 1.8)	**1.64** (1.39 – 1.93)	0.006	0.0002	0.333

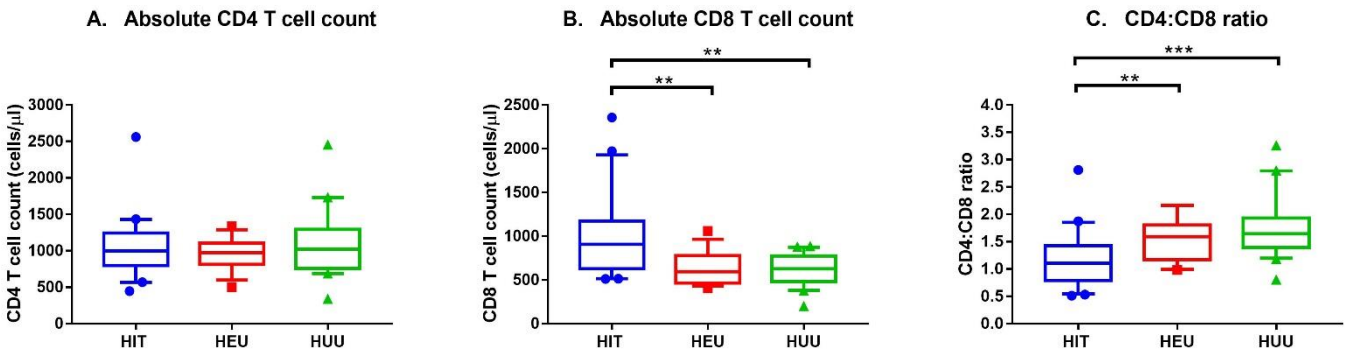

Figure 4.1: Box-and-whisker plots showing the comparison of clinical parameters between HIT, HEU and HUU groups.

4.1.2 Total lymphocytes and CD3 T cells

As indicated in Figure 4.2A, the HEU group demonstrated a significantly higher median percentage of total lymphocytes (median: 87.8%; IQR: 83.2 – 92.4%) in comparison to the HIT group (median: 79.4%, IQR: 73.5 – 87.13%) (p = 0.013) and HUU group (median: 81.3, IQR: 75.23 – 87.23%) (p = 0.004), respectively. The HUU group displayed a significantly higher median percentage of CD3+ T cells (median: 71.45%, IQR: 62.38 – 77.08%) compared to the HEU group (median: 65.6, IQR: 27.3 – 71.6%) (p = 0.061) (Figure 4.2B). As a proportion of CD3+ T cells, no significant differences were observed for CXCR5+ T cells (follicular-homing T cells) between the three groups (Figure 4.2C). However, significant differences in median percentage of CD38+ and CD69+ CD3 T cell subsets were observed. As indicated in Figure 4.2D, CD38+ T cells were significantly expanded in the HIT group (median: 65.15%, IQR: 53.53 – 66.48%) compared to the HEU group (median: 50.5, IQR: 41.8 – 61.2%) (p = 0.008). Additionally, as shown in Figure 4.2E, there was a significantly increased percentage of CD69+ T cells in the HEU group (median: 16.5%, IQR: 13 – 21.2%) in comparison to both the HIT group (p = 0.023) and HUU group (p < 0.0001) respectively, and a significantly higher median percentage in the HIT group (median: 9.56%, IQR: 6.12 – 18.58%) in comparison to the HUU group (median: 6.94, IQR: 4.12 – 7.85%) (p = 0.037).

Table 4.2: Descriptive statistics and comparison of total lymphocytes and CD3 T cell populations.

Cell population	Parent cell population	HIT group Median (IQR)	HEU group Median (IQR)	HUU group Median (IQR)	P-value HIT vs HEU	P-value HIT vs HUU	P-value HEU vs HUU
Total lymphocytes	Single cells	**79.4** (73.5 – 87.13)	**87.8** (83.2 – 92.4)	**81.3** (75.23 – 87.23)	0.013	0.867	0.004
CD3+ T cells	Total lymphocytes	**64.6** (58.85 – 71.9)	**65.6** (27.3 – 71.6)	**71.45** (62.38 – 77.08)	0.972	0.075	0.061
CD3+CXCR5+ T cells	CD3+ T cells	**7.13** (5.47 – 8.59)	**6.89** (5.09 – 8.28)	**5.94** (4.25 – 8.85)	0.765	0.204	0.482
CD3+CD38+ T cells		**65.15** (53.53 – 66.48)	**50.5** (41.8 – 61.2)	**55.15** (48.88 – 65.08)	0.008	0.08	0.211
CD3+CD69+ T cells		**9.56** (6.12 – 18.58)	**16.5** (13 – 21.2)	**6.94** (4.12 – 7.85)	0.023	0.037	<0.0001

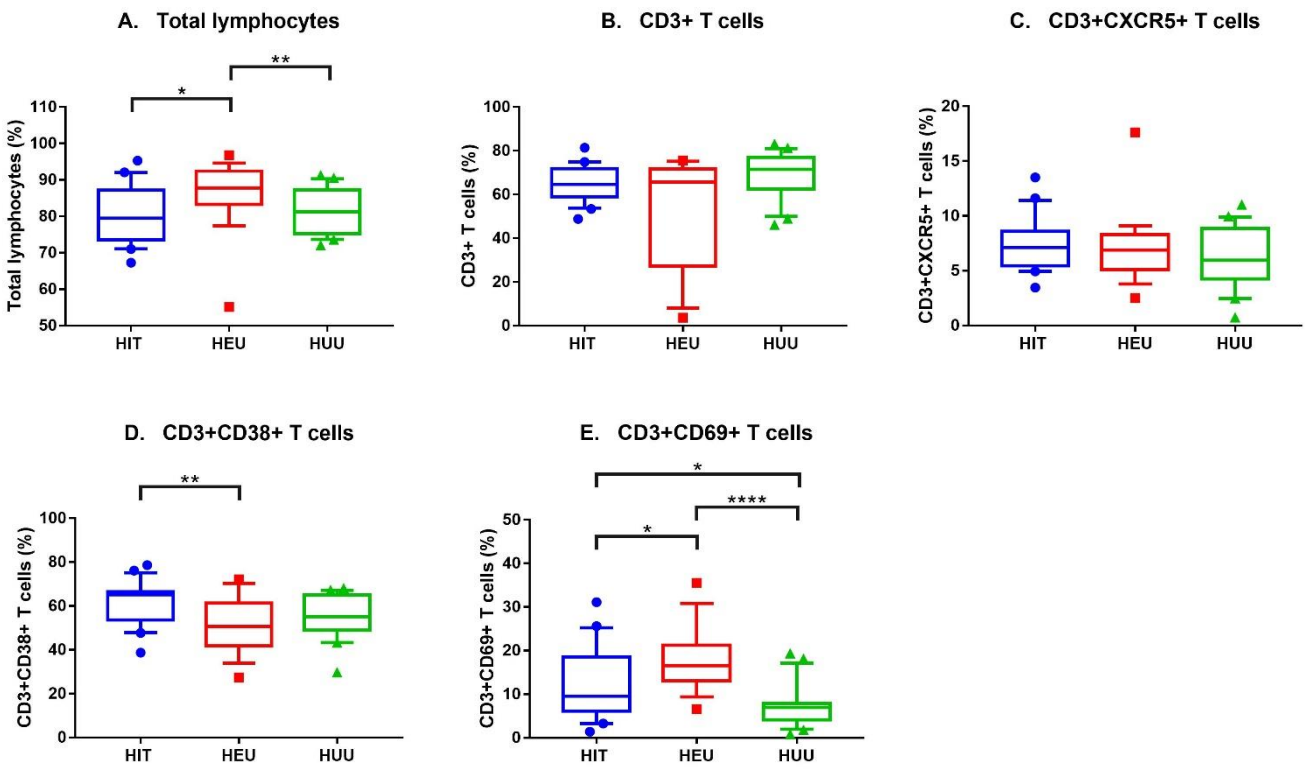

Figure 4.2: Box-and-whisker plots showing the comparison of total lymphocytes and CD3 T cell populations between HIT, HEU and HUU groups.

4.1.3 CD4 Th cells

As indicated in Figure 4.3A, CD4+ Th cells, a subset CD3+ T cells, was significantly increased in the HUU group (median: 63.05%, IQR: 58.68 – 69.93%) in comparison to the HIT group (median: 53.7%, IQR: 47.8 – 57.98%) ($p = 0.003$). A significantly higher median percentage of CD38-activated CD4 T cells, namely CD38+ Th cells, was demonstrated by the HIT group (median: 70.05%, IQR: 63.2 – 73.48%) in comparison to both the HEU group (median: 56.2%, IQR: 48.5 – 69%) ($p = 0.0051$) and HUU group (median: 60.15%, IQR: 55.88 – 67.53%) ($p = 0.008$) (Figure 4.3B). In contrast, as depicted in Figure 4.3C, a significantly higher median percentage of CD69-activated CD4 T cells, namely CD69+ Th cells, was demonstrated by the HEU group (median: 17.5%, IQR: 13.3 – 21.7%) in comparison to both the HIT group (median: 9.54%, IQR: 3.69 – 13.3%) ($p < 0.0001$) and HUU (median: 6.43%, IQR: 3.40 – 7.91%) ($p < 0.0001$), respectively. No significant differences in CXCR5+ Th cells, as a proportion of CD4+ Th cells, were identified between the three groups (Figure 4.3D). However, significant differences in the median percentage of CD38+ and CD69+ subsets of CXCR5+ Th cells was identified. As indicated in Figure 4.3E, the median

percentage of CD38+CXCR5+ Th cells was significantly higher in the HIT group (median: 67.1%, IQR: 58.78 – 76.73%) compared to both the HEU group (median: 51.9, IQR: 47.5 – 63.7%) (p = 0.0017) and HUU group (median: 60.3%, IQR: 54 – 66.33%) (p = 0.028). As depicted in Figure 4.3F, the proportion of CD69+CXCR5+ Th cells was significantly higher in the HEU group (median: 28%, IQR: 22 – 35.8%) compared to both the HIT (median: 13.8%, IQR: 5.08 – 23.78%) (p = 0.0006) and HUU groups (median: 6.5%, IQR: 4.64 – 10.68%) (p < 0.0001). The HEU group also had a significantly higher median percentage (median: 16.5%, IQR: 4.96 – 24.5%) of CD4+CD25+ Th cells compared to the HIT group (median: 5.34%, IQR: 4.11 – 6.38%) (p = 0.0021) (Figure 4.3G).

Table 4.3: Descriptive statistics and comparison of CD4 Th cells and follicular Th cell populations.

Cell population	Parent cell population	HIT group Median (IQR)	HEU group Median (IQR)	HUU group Median (IQR)	P-value HIT vs HEU	P-value HIT vs HUU	P-value HEU vs HUU
CD4+ Th cells	CD3+ T cells	**53.7** (47.8 – 57.98)	**57.8** (51 – 67.9)	**63.05** (58.68 – 69.93)	0.149	0.0003	0.149
CD4+CD38+ Th cells	CD4+ Th cells	**70.05** (63.2 – 73.48)	**56.2** (48.5 – 69)	**60.15** (55.88 – 67.53)	0.0051	0.008	0.527
CD4+CD69+ Th cells		**9.54** (3.69 – 13.3)	**17.5** (13.3 – 21.7)	**6.43** (3.40 – 7.91)	<0.0001	0.199	<0.0001
CD4+CXCR5+ Th cells		**10.28** (8.66 – 14.2)	**10.1** (7.1 – 12)	**8.81** (5.56 – 13.03)	0.227	0.163	0.835
CD4+CXCR5+CD38+ Th cells	CD4+CXCR5+ Th cells	**67.1** (58.78 – 76.73)	**51.9** (47.5 – 63.7)	**60.3** (54 – 66.33)	0.0017	0.028	0.095
CD4+CXCR5+CD69+ Th cells		**13.8** (5.08 – 23.75)	**28** (22 – 35.8)	**6.5** (4.64 – 10.68)	0.0006	0.097	<0.0001
CD4+CD25+ Th cells	CD4+ Th cells	**5.34** (4.11 – 6.38)	**16.5** (4.96 – 24.5)	**7.82** (6.09 – 9.97)	0.0021	0.0002	0.376

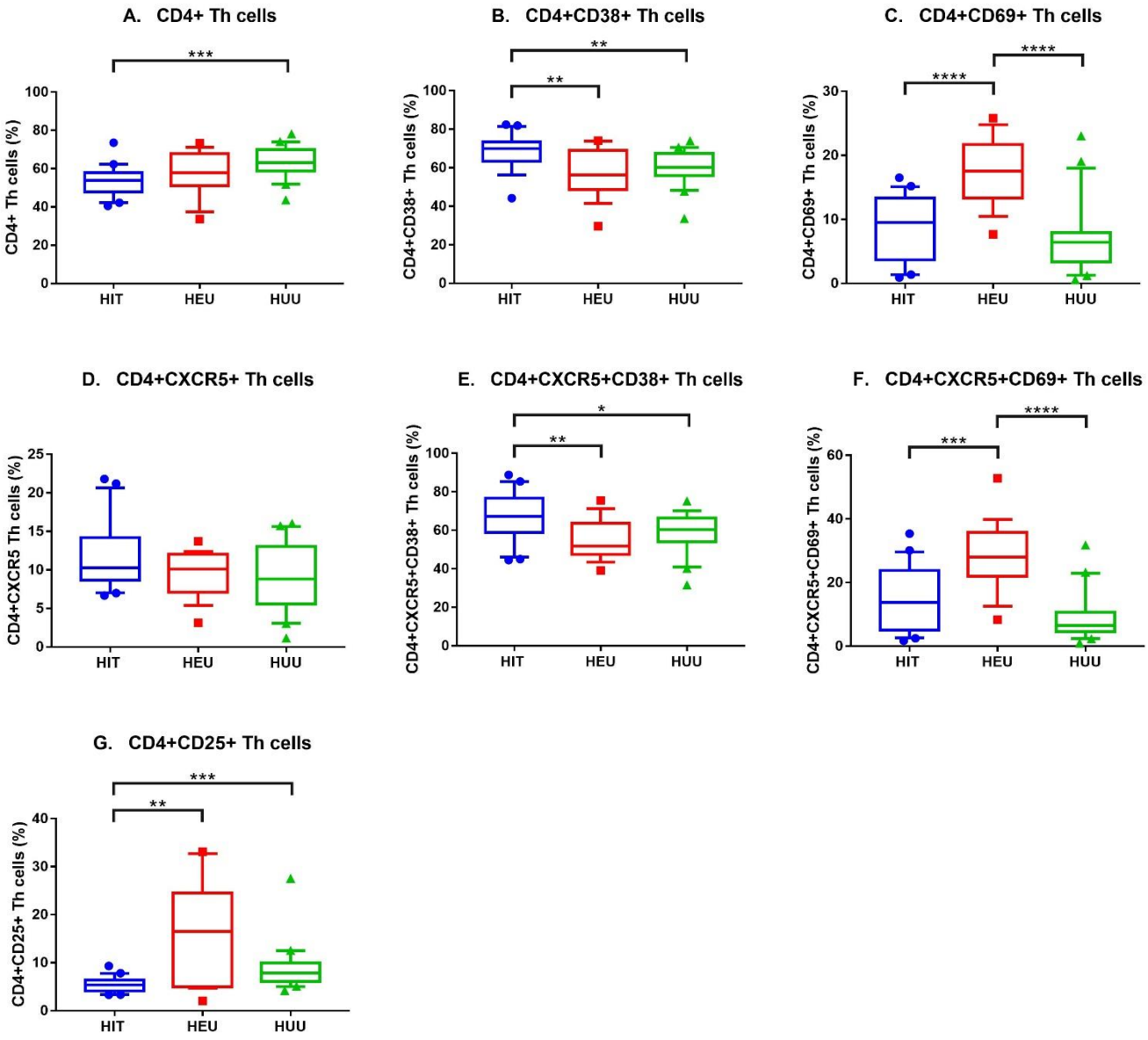

Figure 4.3: Box-and-whisker plots showing the comparison of CD4 Th cells and follicular Th cell populations between HIT, HEU and HUU groups.

4.1.4 Treg cells

As depicted in Figure 4.4A, no significant differences in CD4+CD25+FOXP3+ Treg cells was observed between groups. However, the CD38+ subset of these Treg cells (i.e., CD25+FOXP3+CD38+ Treg cells) was significantly increased in the HIT group (median: 73.45%, IQR: 65.33 – 79.48%) in comparison to the HEU (median: 46.8%, IQR: 38.4 – 60%) and HUU group (median: 51.1%, IQR: 41.45 – 56.45%) with a significance of $p < 0.0001$ (Figure 4.4B). The median percentage of CD25+FOXP3+CD69+ Treg cells was significantly lower in the HUU group (median: 23.6%, IQR: 17.13 – 28.3%) compared to the HIT group (median: 31.1%, IQR: 22.78

-46.55%) (p = 0.012) and HEU (median: 41.2%, IQR: 31.8 – 50%) (p < 0.0001) respectively (Figure 4.4C). Lastly, CXCR5+ Treg cells was significantly increased in the HIT group (median: 22.85%, IQR: 13.48 – 31.28%) in comparison to both the HEU (median: 14.4%, IQR: 10.1 – 20.6%) (p = 0.028) and HUU (median: 9.95%, IQR: 5.97 – 15.45%) (p = 0.0006) groups (Figure 4.4D).

Table 4.4: Descriptive statistics and comparison of Treg cell populations.

Cell population	Parent cell population	HIT group Median (IQR)	HEU group Median (IQR)	HUU group Median (IQR)	P-value HIT vs HEU	P-value HIT vs HUU	P-value HEU vs HUU
CD4+CD25+FOXP3+ Treg cells	CD4+CD25+ Th cells	**5.18** (2.88 – 22.89)	**7.92** (3.74 – 10.3)	**4.75** (2.52 – 9.14)	0.478	0.57	0.222
CD25+FOXP3+CD38+ Treg cells	CD4+CD25+ FOXP3+ Treg cells	**73.45** (65.33 – 79.48)	**46.8** (38.4 – 60)	**51.1** (41.45 – 56.45)	<0.0001	<0.0001	0.797
CD25+FOXP3+CD69+ Treg cells		**31.1** (22.78 – 46.55)	**41.2** (31.8 – 50)	**23.6** (17.13 – 28.3)	0.184	0.012	<0.0001
CD25+FOXP3+CXCR5+ Treg cells		**22.85** (13.48 – 31.28)	**14.4** (10.1 – 20.6)	**9.95** (5.97 – 15.45)	0.028	0.0006	0.085

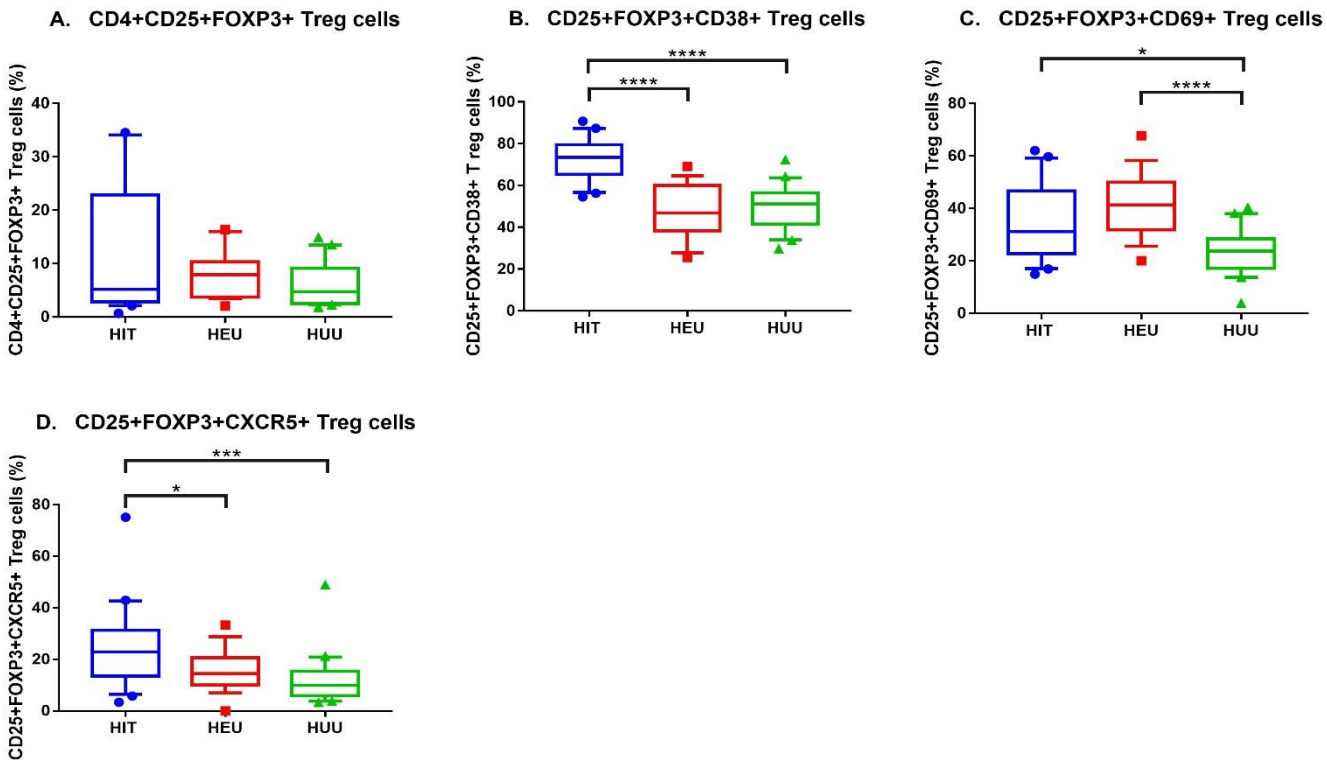

Figure 4.4: Box-and-whisker plots showing the comparison of Treg cell populations between HIT, HEU and HUU groups.

4.1.5 Tfh cells

As indicated in Figure 4.5A, no significant difference was found for CD4+CXCR5+PD-1+ Tfh cells between the groups. However, as indicated in Figure 4.5B, the further characterised ICOS+ subset of this cell population, classified as CD4+CXCR5+PD-1+ICOS+ Tfh cells, was found to be significantly higher in the HIT group (median: 33.6%, IQR: 11.18 – 40.58%) in comparison to the HUU group (median: 19.2%, IQR: 5.35 – 28.93%) ($p = 0.016$). Additionally, the HEU group also had a significantly higher ($p = 0.006$) median percentage of CD4+CXCR5+PD-1+ICOS+ Tfh cells (median: 31.6%, IQR: 21.3 -37.6%) compared to the HUU group. CD4+CXCR5+PD-1+CD38+ Tfh cells, as a subset of CD4+CXCR5+PD-1+ Tfh cells, was significantly higher in the HIT group (median: 70.3%, IQR: 63.55 – 76.98%) in comparison to both the HEU (median: 59.7%, IQR: 55.4 – 71.4%) ($p = 0.025$) and HUU groups (median: 62.65%, IQR: 58.1 – 68.4%) ($p = 0.018$) (Figure 4.5C). As indicated in Figure 4.5D, CD4+CXCR5+PD-1+CD69+ T cells, as a subset of CD4+CXCR5+PD-1+ Tfh cells, was observed to be significantly increased higher in the HEU group compared to both the HIT (median: 25%, IQR: 13.15 – 38.15%) ($p<0.0001$) and HUU (median: 15.2%, IQR: 11.6 – 22.85%) ($p< 0.0001$) groups. respectively.

Table 4.5: Descriptive statistics and comparison of Tfh cell populations.

Cell population	Parent cell population	HIT group Median (IQR)	HEU group Median (IQR)	HUU group Median (IQR)	P-value HIT vs HEU	P-value HIT vs HUU	P-value HEU vs HUU
CD4+CXCR5+PD-1+ Tfh cells	CD4+CXCR5+ Th cells	**39** (31.13 – 57.58)	**40.2** (32 – 48.2)	**45.3** (37.35 – 52.43)	>0.9999	0.274	0.312
CD4+CXCR5+PD-1+ ICOS+ Tfh cells	CD4+ CXCR5+PD-1+ Tfh cells	**33.6** (11.18 – 40.58)	**31.6** (21.3 – 37.6)	**19.2** (5.35 – 28.93)	0.749	0.016	0.006
CD4+CXCR5+PD-1+ CD38+ Tfh cells		**70.3** (63.55 – 76.98)	**59.7** (55.4 – 71.4)	**62.65** (58.1 – 68.4)	0.025	0.018	0.662
CD4+CXCR5+PD-1+ CD69+ Tfh cells		**25** (13.15 – 38.15)	**46.1** (39.1 – 51.6)	**15.2** (11.6 – 22.85)	<0.0001	0.122	<0.0001

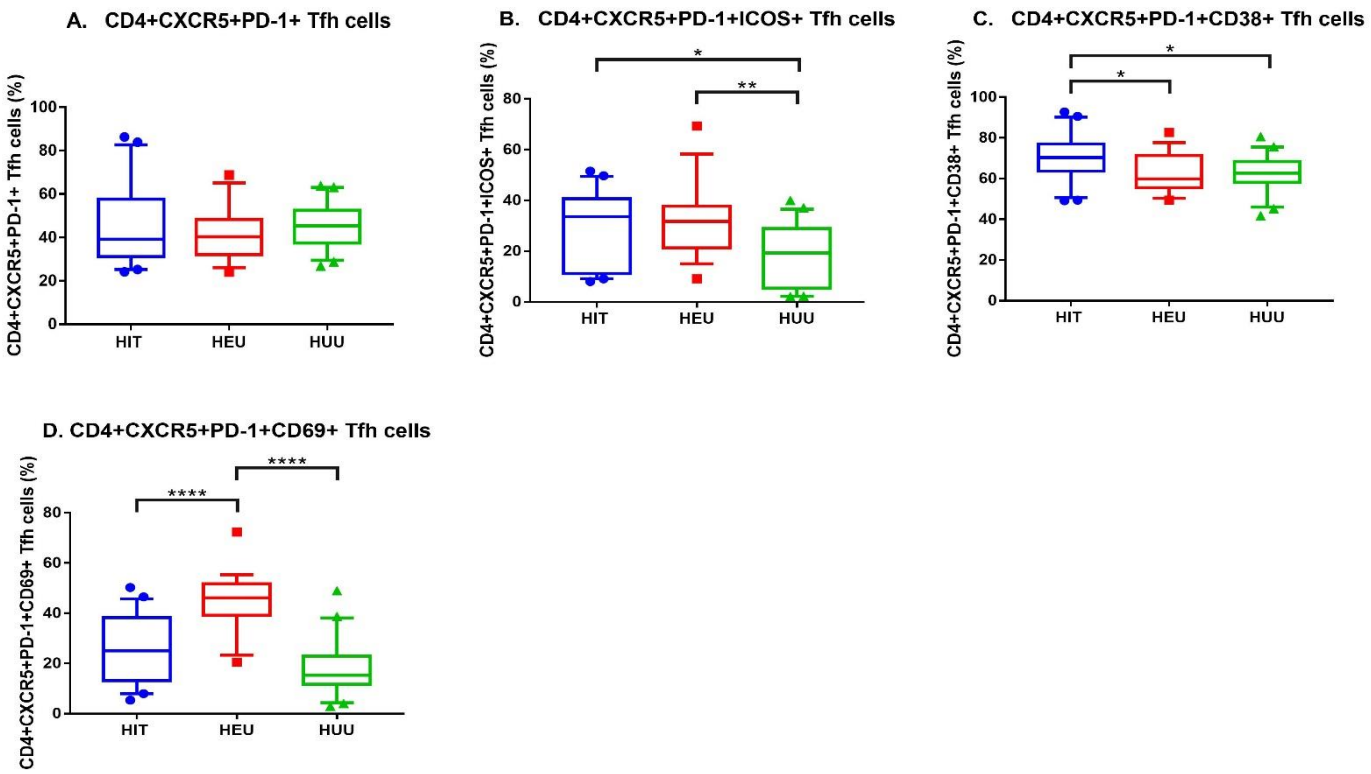

Figure 4.5: Box-and-whisker plots showing the comparison of Tfh cell populations between HIT, HEU and HUU groups.

4.1.6 CD8 Tc cells

As demonstrated in Figure 4.6A, CD8+ Tc cells were found to have a significant increased median percentage in the HIT group (median: 36.9%, IQR: 31.58 – 44.23%) in comparison to the HUU group (median: 29.35%, IQR: 24.35 – 31.4%) (p = 0.001). In this study immune activation was represented by the CD38+ and CD69+ activation of CD8 T cells and immune exhaustion by the PD-1-expressing CD8 T cells. With regards to CD38+ Tc cells, as a proportion of total CD8 Tc cells, the HIT group demonstrated a significantly higher median percentage of cells (median: 55.75%, IQR: 37.25 – 65.05%) compared to the HEU group (median: 38.1%, IQR: 32.6 – 49.8%) (p = 0.021) (Figure 4.6B). In contrast, the HEU group demonstrated a significantly higher median CD8+CD69+ T cell percentage (median: 25.7%, IQR: 16.7 – 36.6%) compared to both the HIT group (median: 15.4%, IQR: 7.37 – 20.65%) (p = 0.009) and HUU group (median: 13.55%, IQR: 9.77 – 17.85%) (p = 0.0006) (Figure 4.6C). The HUU group demonstrated a significantly lower median percentage (median: 5.22%, IQR: 2.57 – 7.96%) of CD38+CD69+ Tc cells compared to the HIT (median: 9.96%, IQR: 4.14 – 13.5%) (p = 0.042) and HEU groups (median: 10.2%, IQR: 7.03 – 16.2%) (p =

0.007) (Figure 4.6D). Lastly, as indicated in Figure 4.6E, the HIT group demonstrated a significantly higher median percentage of PD-1 Tc cells (median: 13.1%, IQR: 5.51 – 23.18%) in comparison to the HUU group (median: 6.74%, IQR: 5.13 – 8.52%) (p = 0.019).

Table 4.6: Descriptive statistics and comparison of Tc cell populations.

Cell population	Parent cell population	HIT group Median (IQR)	HEU group Median (IQR)	HUU group Median (IQR)	P-value HIT vs HEU	P-value HIT vs HUU	P-value HEU vs HUU
CD8+ Tc cells	CD3+ T cells	**36.9** (31.58 – 44.23)	**31.5** (25.5 – 37.6)	**29.35** (24.35 – 31.4)	0.064	0.001	0.16
CD8+CD38+ Tc cells	CD8+ Tc cells	**55.75** (37.25 – 65.05)	**38.1** (32.6 – 49.8)	**41.35** (33.48 – 57.8)	0.021	0.08	0.527
CD8+CD69+ Tc cells		**15.4** (7.37 – 20.65)	**25.7** (16.7 – 36.6)	**13.55** (9.77 – 17.85)	0.009	0.579	0.0006
CD8+CD38+CD69+ Tc cells		**9.96** (4.14 – 13.5)	**10.2** (7.03 – 16.2)	**5.22** (2.57 – 7.96)	0.532	0.042	0.007
CD8+PD-1+ Tc cells		**13.1** (5.51 – 23.18)	**7.03** (5.4 – 14.9)	**6.74** (5.13 – 8.52)	0.216	0.019	0.299

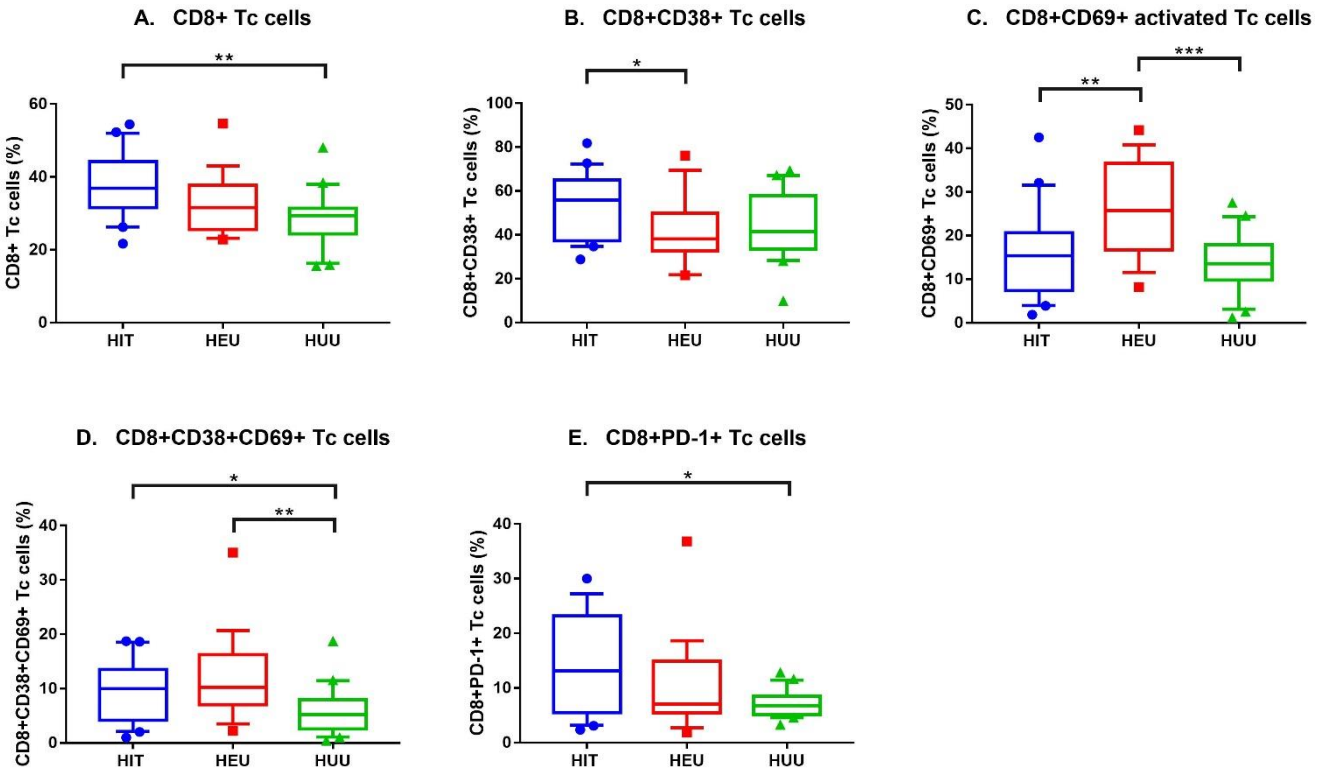

Figure 4.6: Box-and-whisker plots showing the comparison of Tc cell populations between HIT, HEU and HUU groups.

4.1.7 Follicular Tc cells

As indicated in Figure 4.7A, in regards to the follicular homing subset of CD8 T cells, CD8+CXCR5+ Tfc cells, no significant differences were found between the groups. However, for activated subsets of CXCR5+ Tfc cells, namely CD38+ Tfc cells and CD69+ Tfc cells, significant differences between groups were observed. As depicted in Figure 4.7B, the HIT group demonstrated a significantly higher percentage of CD38+ Tfc cells (median: 77.65%, IQR: 67.2 – 84.75%) compared to both the HEU (median: 65.9%, IQR: 59 – 71.9%) ($p = 0.002$) and HUU groups (median: 62.05%, IQR: 55.75 – 71.58%) ($p = 0.0004$). Whereas, the HEU group demonstrated the significantly higher median percentage of CD69+ Tfc cells (median: 34.8%, IQR: 25.7 – 42.1%) compared to both the HIT (median: 18.35%, IQR: 15.1 – 42.43%) ($p = 0.048$) and HUU (median: 13.25%, IQR: 8.38 -18.3%) ($p < 0.0001$) groups. Additionally, the median percentage of CD69+ Tfc cells was also significantly higher for the HIT group in comparison to the HUU group ($p = 0.019$) (Figure 4.7C).

Table 4.7: Descriptive statistics and comparison of follicular Tc cell populations.

Cell population	Parent cell population	HIT group Median (IQR)	HEU group Median (IQR)	HUU group Median (IQR)	P-value HIT vs HEU	P-value HIT vs HUU	P-value HEU vs HUU
CD8+CXCR5+ Tfc cells	CD8+ Tc cells	**1.74** (1.36 – 2.73)	**1.35** (1.08 – 2.28)	**1.42** (0.96 – 2.01)	0.091	0.082	0.573
CD8+CXCR5+CD38+ Tfc cells	CXCR5+ Tfc cells	**77.65** (67.2 – 84.75)	**65.9** (59 – 71.9)	**62.05** (55.75 – 71.58)	0.002	0.0004	0.347
CD8+CXCR5+CD69+ Tfc cells		**18.35** (15.1 – 42.43)	**34.8** (25.7 – 42.1)	**13.25** (8.38 – 18.3)	0.048	0.019	<0.0001

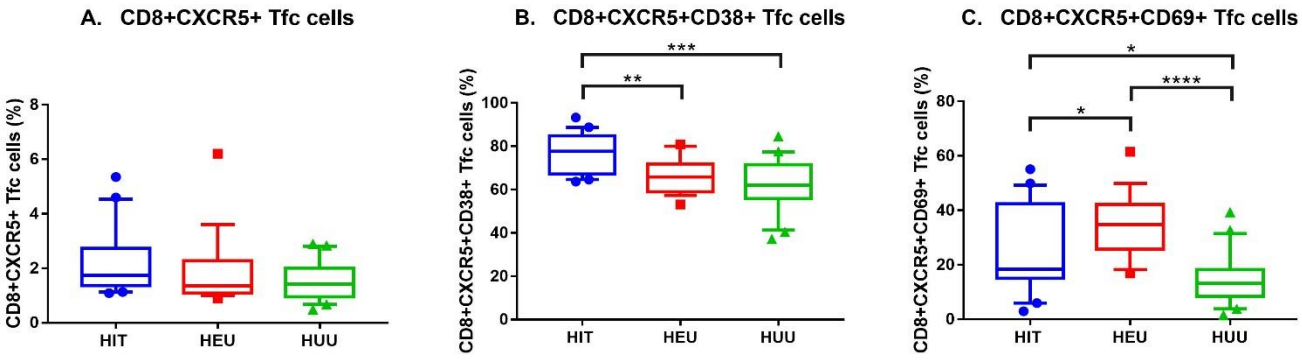

Figure 4.7: Box-and-whisker plots showing the comparison of follicular Tc cell populations between HIT, HEU and HUU groups.

4.1.8 Inflammatory cytokines

As indicated in Figure 4.8, no significant differences in IL-β were observed between the three groups. For INF-γ, the median pg/ml was significantly higher in the HEU group (median: 43.83 pg/ml; IQR: 21.23 – 67.56 pg/ml) compared to the HIT group (median: 18.59 pg/ml; IQR: 8.03 – 39.64 pg/ml) with a significance of p = 0.01. The HEU group (median: 31.43 pg/ml; IQR: 22.72 – 47.36 pg/ml) also demonstrated a significant higher median pg/ml of TNFα in comparison to the HIT group (median: 10.41 pg/ml; IQR: 9.28 – 14.22 pg/ml) with a significance of p<0.0001. In addition, the HUU group also had a significantly higher median pg/ml of TNFα (median: 20.41 pg/ml; IQR: 12.8 - 32.53 pg/ml) compared to the HIT group (p = 0.0005). In contrast, the HIT group had a much greater and significantly higher pg/ml of INF-α (median: 83.8 pg/ml; IQR: 55 – 115 pg/ml) compared to the HUU group (median: 39.1 pg/ml; IQR: 27.4 – 73.3 pg/ml) with a significance of p = 0.002. Lastly, with regards to the level of hsCRP, the HIT group demonstrated a significantly higher median ng/ml (median:1124 ng/ml; IQR: 701 – 2395 ng/ml) compared to both the HEU group (median: 395 ng/ml; IQR: 344 – 528 ng/ml) and HUU group (median: 376 ng/ml; IQR: 341 – 484 ng/ml) with a significance of p = 0.0011 and p = 0.0002, respectively.

Table 4.8: Descriptive statistics and comparison of levels of inflammatory cytokines.

Inflammatory marker	HIT group Median (IQR)	HEU group Median (IQR)	HUU group Median (IQR)	P-value HIT vs HEU	P-value HIT vs HUU	P-value HEU vs HUU
IL-1β (pg/ml)	**5.71** (2.45 – 15.6)	**13.6** (6.64 – 19)	**9.22** (6.86 – 16.5)	0.047	0.119	0.34
IFN-γ (pg/ml)	**18.59** (8.03 – 39.64)	**43.83** (21.23 – 67.56)	**23.95** (10.54 – 60.32)	0.01	0.199	0.274
TNFα (pg/ml)	**10.41** (9.28 – 14.22)	**31.43** (22.72 – 47.36)	**20.41** (12.8 – 32.53)	<0.0001	0.0005	0.064
IFN-α (pg/ml)	**83.8** (55 – 115)	**72** (27.4 – 96.5)	**39.1** (27.4 – 73.3)	0.088	0.002	0.299
hsCRP (ng/ml)	**1124** (701 – 2395)	**395** (344 – 528)	**376** (341 – 484)	0.0011	0.0002	0.646

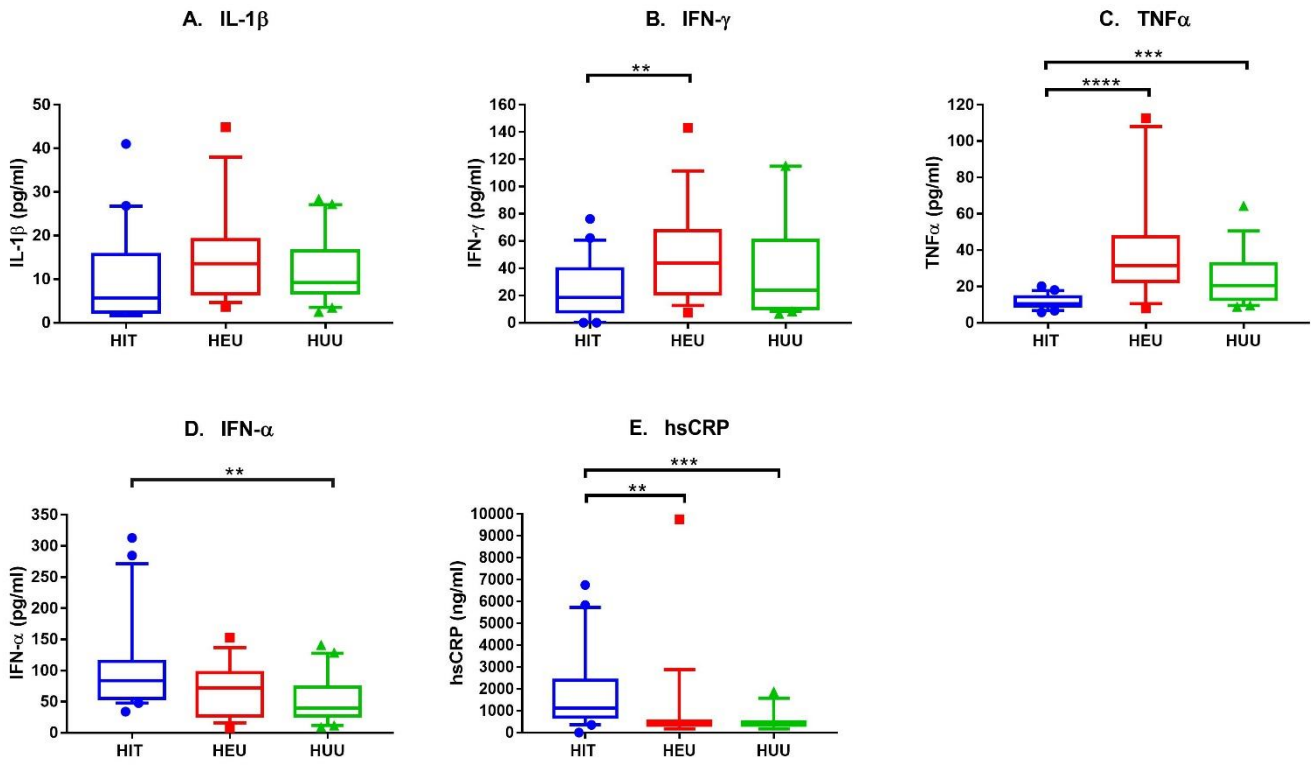

Figure 4.8: Box-and-whisker plots showing the comparison of level of inflammatory cytokines between HIT, HEU and HUU groups.

4.2 Correlative analysis of T cell populations

4.2.1 Significant correlations: CD4+CXCR5+PD-1+ Tfh cells and clinical parameters

When testing for significant correlations between CD4+CXCR5+PD-1+ Tfh cells and clinical parameters (i.e., absolute CD4 count, absolute CD8 count and CD4:CD8 ratio) for the entire study population as well as for respective groups, i.e., HIT, HEU and HUU group, no significant correlations were observed.

4.2.2 Significant correlations for entire study population: CD4+CXCR5+PD -1+ Tfh cells and other T cell subsets

As indicated in Figure 4.9, For the total study population (n = 59), a significant inverse correlation between CD4+CXCR5+PD-1+ Tfh cells and CXCR5+CD38+ Th cells (p = 0.006, r = -0.35) as well as CD4+CXCR5+PD-1+CD38+ Tfh cells (p = 0.002, r = -0.39), a subset of CD4+CXCR5+PD-1+ Tfh cells, was observed. Among CD8+ Tc cell subsets, CD4+CXCR5+PD-1+ Tfh cells negatively correlated with the following cell populations: CD8+CD69+ Tc cells (p = 0.008, r = -0.34), CD8+CD38+CD69+ Tc cells (p = 0.027, r = -0.29) and CD8+CXCR5+CD69+ Tfc cells (p = 0.014, r = -0.32). The

only positive correlation that was found to be significant was between CD4+CXCR5+PD-1+ Tfh cells and CD8+PD-1+ Tc cells ($p < 0.0001$, $r = 0.51$). Additionally, a negative correlation with CD3+CD69+ T cells, representative of total activated T cells, was observed ($p = 0.009$, $r = -0.34$).

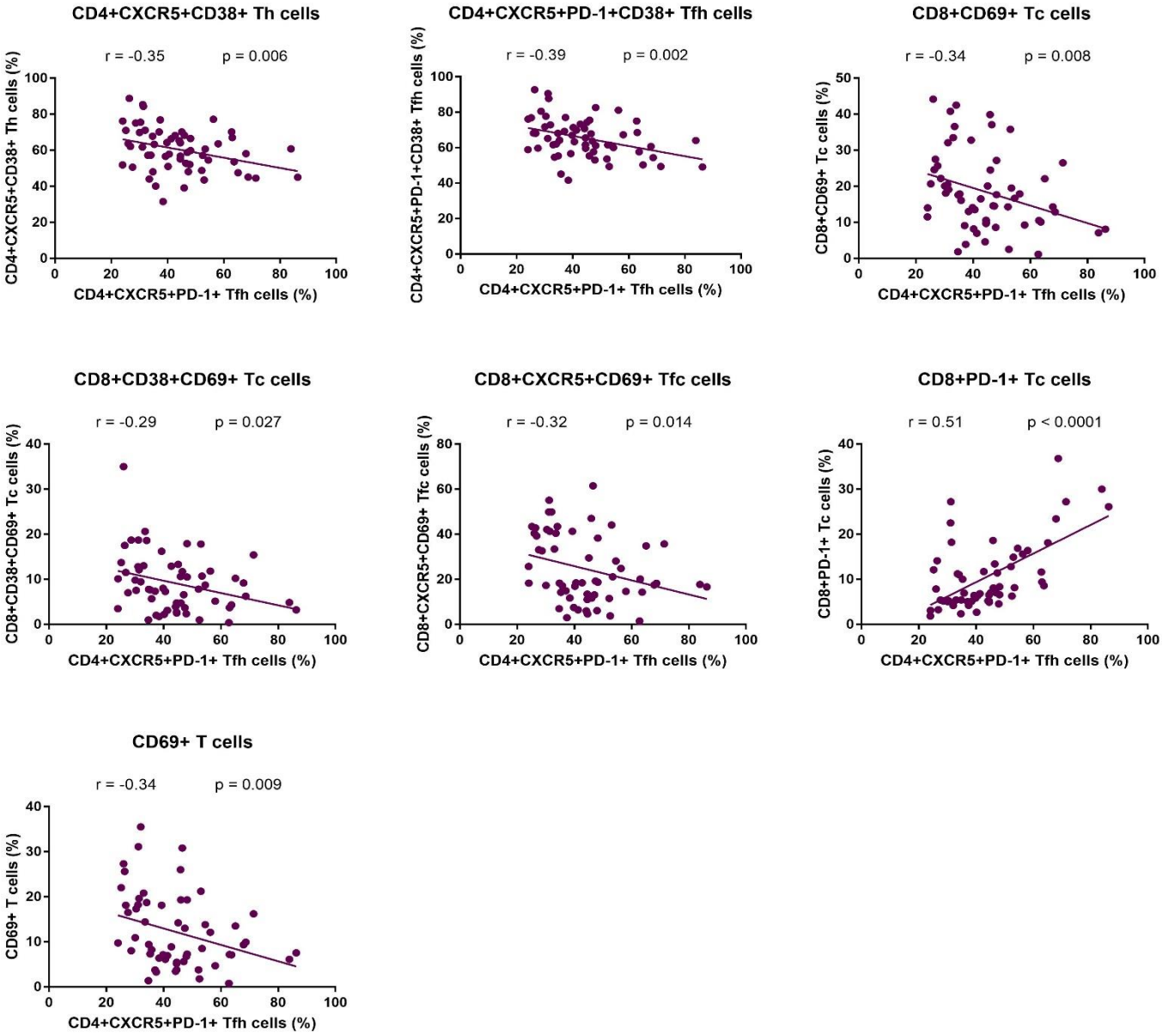

Figure 4.9: Scatter plots showing the significant correlations for entire study population: CD4+CXCR5+PD-1+ Tfh cells and other T cell subsets.

4.2.3 Significant correlations for HIT group: CD4+CXCR5+PD -1+ Tfh cells and other T cell subsets

As indicated in Figure 4.10, For the HIT group (n = 20), the majority of significant correlations between CD4+CXCR5+PD-1+ Tfh cells and other T cell populations of

interest were observed. There was a significant positive correlation with total lymphocytes ($p = 0.013$, $r = 0.55$). Although there was no significant correlation between CD4+CXCR5+PD-1+ Tfh cells and CD3+ T cells, a significant inverse correlation with activated subsets of this population, i.e., CD3+CD38+ T cells ($p = 0.012$, $r = -0.55$) and CD3+CD69+ T cells ($p = 0.023$, $r = -0.51$), were identified. CD4+CD38+ Th cells (a subset of CD3+ T cells) ($p = 0.035$, $r = -0.47$) as well as CD4+CXCR5+ Th cells (a subset of CD4+ T cells) ($p = 0.004$, $r = -0.61$) were also found to share significant inverse correlations with CD4+CXCR5+PD-1+ Tfh cells. Interestingly, there was a significant positive correlation with CD25+FOXP3+CD69+ Treg cells, an activated subset of CD4+CD25+FOXP3+ Treg cells ($p = 0.036$, $r = 0.47$). Additionally, a significant negative correlation between CD4+CXCR5+PD-1+ Tfh cells and the following CD38+ activated subsets: CD4+CXCR5+PD-1+CD38+ Tfh cells ($p = 0.005$, $r = -0.61$), CD8+ CD38+ Tc cells ($p = 0.002$, $r = -0.66$) and CD8+CXCR5+CD38+ Tfc cells ($p = 0.013$, $r = -0.54$), were observed respectively. Lastly, a significant positive correlation with CD8+PD-1+ Tc cells, representing an exhausted counterpart of CD8+ Tc cells, was found ($p = 0.043$, $r = 0.46$).

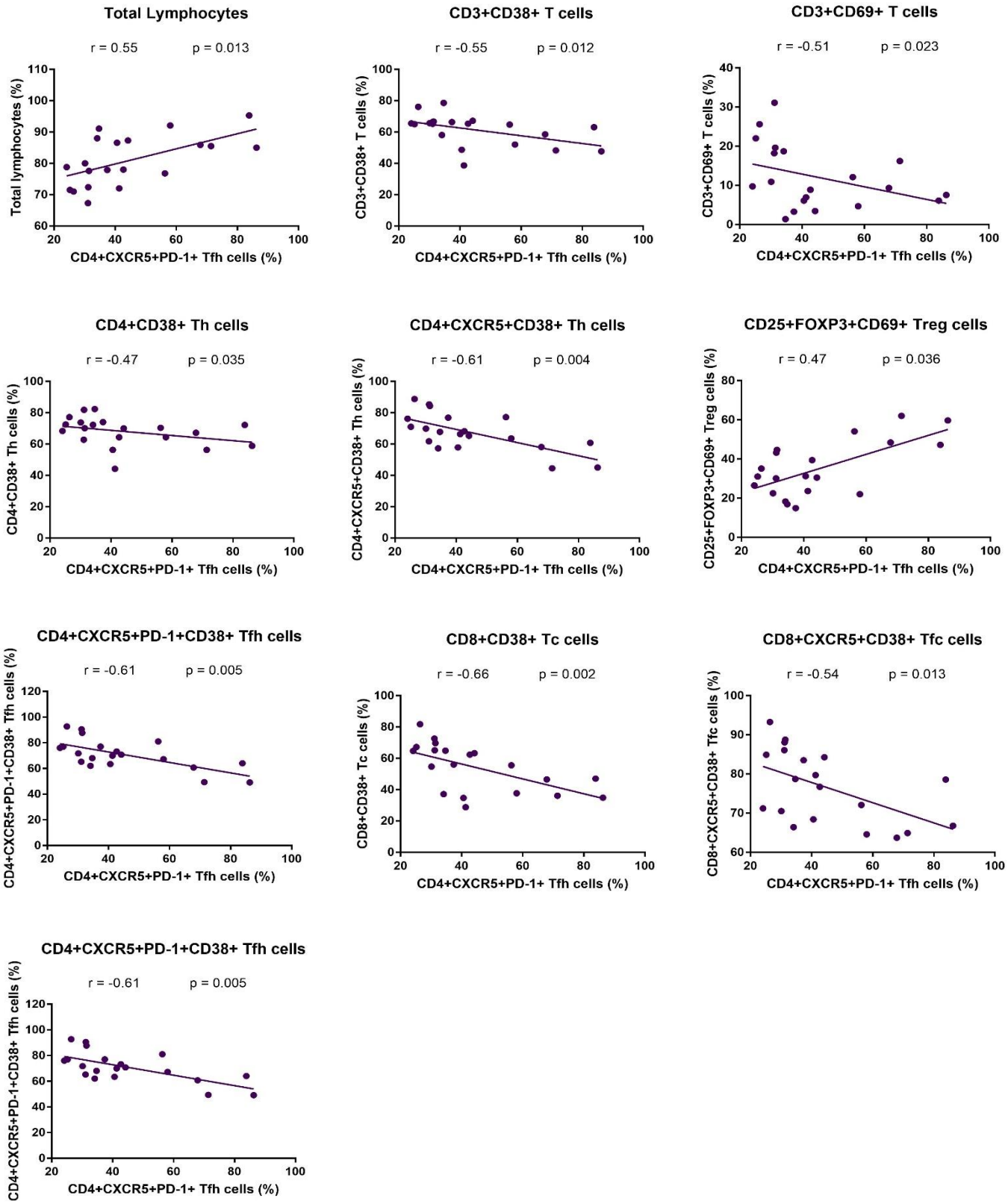

Figure 4.10: Scatter plots showing the significant correlations for HIT group: CD4+CXCR5+PD-1+ Tfh cells and other T cell subsets.

4.2.4 Significant correlations for HEU group: CD4+CXCR5+PD -1+ Tfh cells and other T cell subsets

As indicated in Figure 4.11, the HEU group (n = 19) only had two significant correlations between cell populations. CD4+CXCR5+PD-1+ Tfh cells negatively correlated with live CD3+ T cells (p = 0.029, r = -0.5) and positively correlated with CD8+PD-1+ Tc exhausted cells (p = 0.0002, r = 0.76).

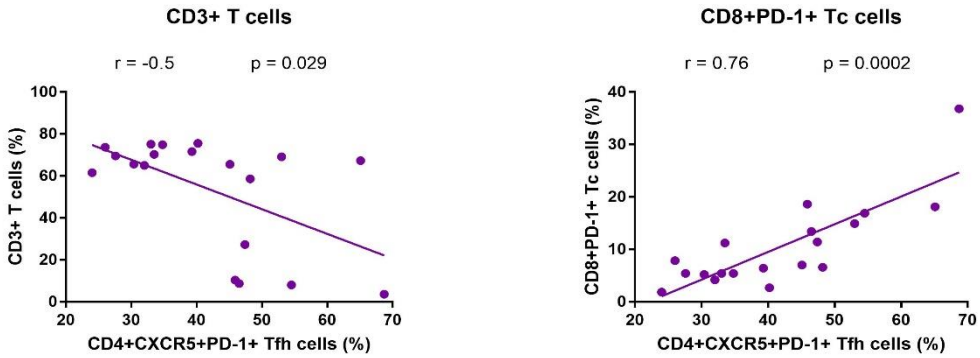

Figure 4.11: Scatter plots showing the significant correlations for HEU group: CD4+CXCR5+PD-1+ Tfh cells and other T cell subsets.

4.2.5 Significant correlations for HUU group: CD4+CXCR5+PD -1+ Tfh cells and other T cell subsets

For the HUU group (n = 20), only one significant correlation was observed: the positive correlation between CXCR5+PD-1+ Tfh cell population and CD8+PD-1+ Tc cell population, representing exhausted CD8 T cells (p = 0.009, r = 0.57) (Figure 12).

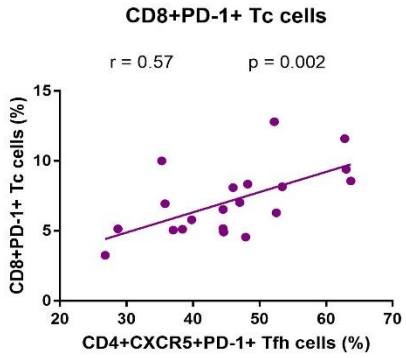

Figure 4.12: Scatter plot showing the significant correlation for HUU group: CD4+CXCR5+PD-1+ Tfh cells and CD8+PD-1+ Tc cells.

4.2.6 Significant correlations: Inflammatory cytokines

When testing for significant correlations between CD4+CXCR5+PD-1+ Tfh cells and inflammatory cytokines, namely IL-1β, IFN-γ, TNFα, IFN-α and hsCRP, within each group (i.e., HIT, HEU and HUU) and the entire study population no significant correlations were observed. However, in regards to the ICOS-expressing subset of CD4+CXCR5+PD-1+ Tfh cells (i.e., CD4+CXCR5+PD-1+ICOS+ Tfh cells), a positive correlation with IL-1β was observed (p = 0.041, r = 0.46) (Figure 4.13A). Additionally, the HIT group demonstrated a significant negative correlation between CD4+CXCR5+PD-1+ICOS+ Tfh cells and hsCRP (p = 0.049, r = -0.45) (Figure 4.13B). For the entire study population (HIT, HEU and HUU groups combined), similar to the HIT group, there was also a significant positive correlation between CD4+CXCR5+PD-1+ICOS+ Tfh cells and IL-1β (p = 0.024, r = 0.29) (Figure 4.13C).

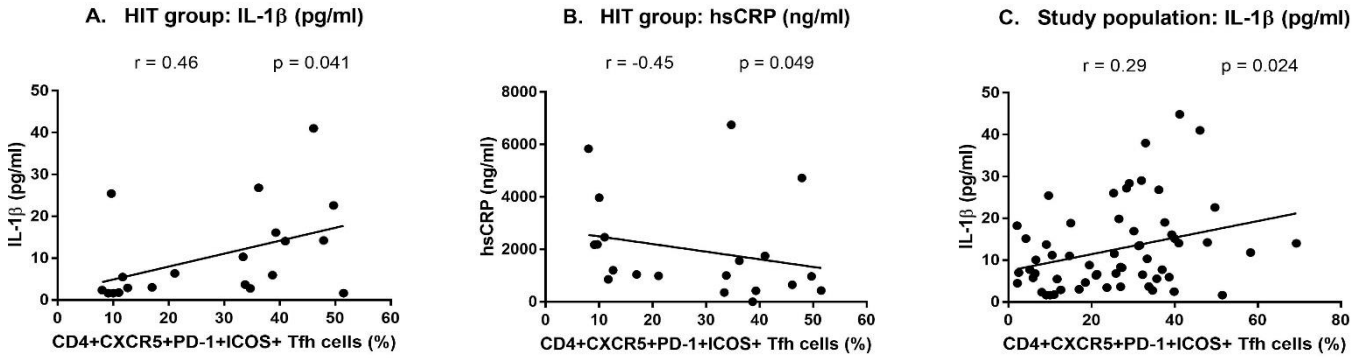

Figure 4.13: Scatter plots showing the significant correlations between CD4+CXCR5+PD-1+ICOS+ Tfh cells and inflammatory cytokines.

4.3 Graphical comparison of Tfh cell populations in groups

Depicted below are representative flow cytometric dot plots of Tfh cell populations (i.e., CD4+CXCR5+PD-1+ Tfh cells and CD4+CXCR5+PD-1+ICOS+ Tfh cells) from an individual representative sample of each group.

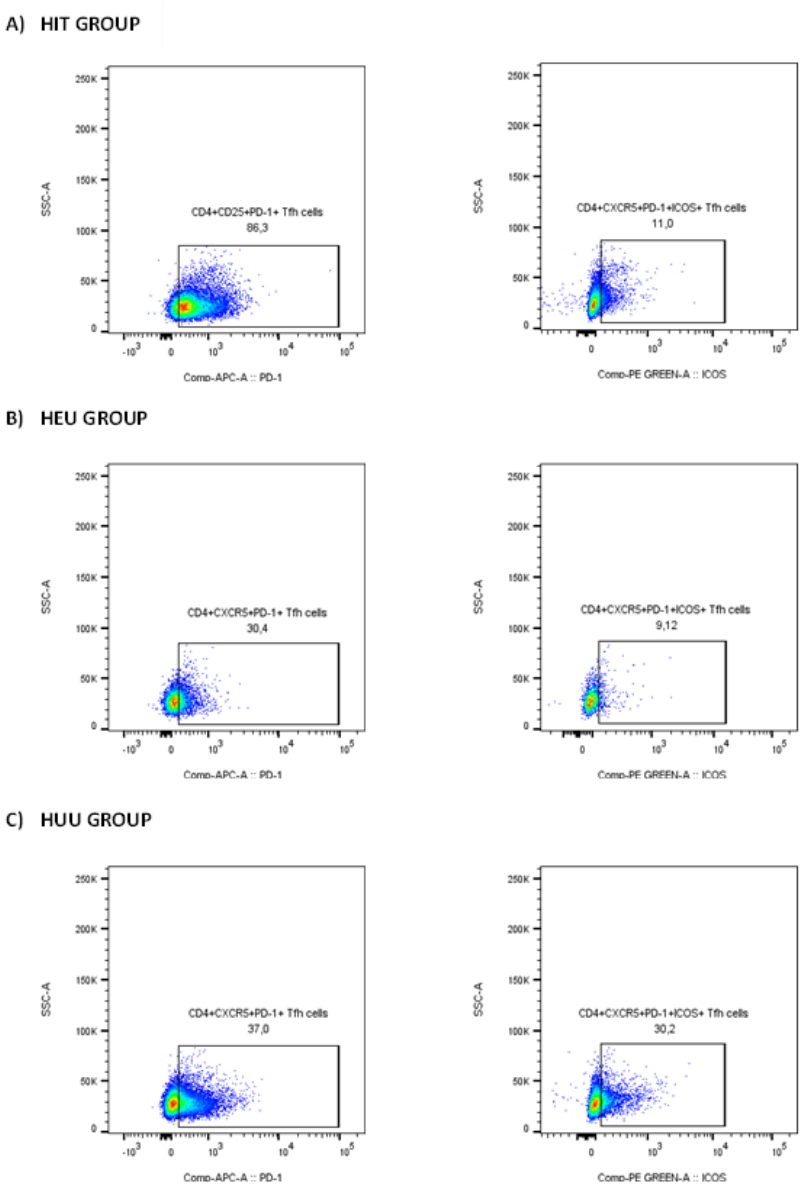

Figure 4.14: Flow cytometric dot plots of CD4+CXCR5+PD-1+ Tfh cells and CD4+CXCR5+PD-1+ICOS+ Tfh cells in HIT, HEU and HUU groups. Dot plots were generated in FlowJo (version 10.3). In the plot each dot represents a single cell and where they cluster indicates a distinct cell population. Red and yellow areas are where the cells are densest (i.e., highest percentage of cells). Squares within the plot represent region gates designed to discriminate between marker-specific positive and negative cells.

Chapter 5 – Discussion

This study demonstrated a significant expansion of Tfh cells (characterised as CD4+CXCR5+PD-1+ICOS+) within the HIT and HEU groups compared to the control HUU group. Even though no significant difference in the total Tfh cells (characterised as CD4+CXCR5+PD-1+) was found between the three groups, several significant inverse correlations between this cell population and activated T cell subset populations were observed. This finding suggested that increased levels of immune activation may lead to a reduction in the population of circulating Tfh cells. Overall, significantly higher levels of T cell activation were observed in the HIT and HEU groups. Generally, the HIT group demonstrated significantly higher levels of CD38+ T cell activation whereas the HEU group demonstrated significantly higher levels of CD69+ T cell activation. A direct correlation between CD4+CXCR5+PD-1+ Tfh cells and PD-1+ Tc (i.e., an indicator of immune exhaustion) was also demonstrated within the total study population and each group individually. Suggesting that whereas levels of immune activation negatively regulate Tfh cells, levels of immune exhaustion positively regulate the frequency of Tfh cells. CD4+CXCR5+PD-1+ICOS+ Tfh cells was also shared a significant positive correlation with IL-1β (i.e., inflammatory cytokine) within the total study population as well as the HIT group, suggesting that an expansion of Tfh cells within HIT and HEU children is contributed to in part by levels of inflammation.

HIV is characterised by extreme immune system dysfunction and a disruption in T cell homeostasis (Cao et al., 2016). In infants when treatment is not administered early on it causes a rise in mortality and morbidity (Shalekoff, 2021)

A major consequence of HIV infection is the depletion of CD4 T cells. HIV selectively targets, infects and rapidly proliferates within CD4 T cells causing their impairment and death. Without the initiation of antiretroviral treatment, patients become susceptible to severe opportunistic infections. Therefore, immune function is typically measured by CD4 T cell count in the context of HIV infection (WHO, 2022). It provides a reliable indication of immunological status and is the main parameter used for HIV management and guidance of clinical treatment. Although there was no significant difference in the absolute CD4 T cell count between groups, and each group had a relatively normal median CD4 T cell count (normal range is approximately 500 – 1400

cells/µl), the HUU group demonstrated the overall highest median of cells/µl. The relative normalisation of CD4 T cell count demonstrated by the HIT group is most likely the outcome of early antiretroviral treatment initiation and successful viral suppression, followed by continuous use throughout life. In contrast to the decline of CD4 T cells, CD8 T cells are expanded in untreated HIV-infection as a response to viral replication. The normalisation of CD8 T cell count is rarely seen, regardless of optimal CD4 T cell count recovery, after long-term treatment (Cao et al., 2016).

The comparison of the absolute count CD8 T cell count between the three groups showed that the HIT group demonstrated a significantly higher median of cells/µl than the HEU and HUU group. Increased levels of CD8 T cell count have been associated with an increased risk of developing non-AIDS-related clinical syndromes, such as cardiovascular disease and malignancies, independent of the normalisation of CD4 T cell count (Cao et al., 2016).

Even though long-term antiretroviral treatment leads to a moderate reduction in CD8 T cell expansion, the early initiation of therapy is responsible for reducing antigenic stimulation and contributes in part to the CD8 T cell normalisation (Cao et al., 2016). This was demonstrated in the results for HIT and HEU children for whom median CD8 T cell count was relatively normal (normal range is approximately 150 – 1000 cells/µl).

Generally, HIV-negative individuals have more CD4 than CD8 T cells whereas for HIV-positive untreated individuals, whose immune systems become weaker over time, the ratio of CD4:CD8 count decreases. The normal CD4:CD8 ratio range for HIV-negative individuals is between 0.9 and 1.9, meaning there is approximately 1 to 2 CD4 T cells for every CD8 T cell. For all the groups the CD4:CD8 ratio fell within the normal range, however it was significantly lower in the HIT group in comparison to the HEU and HUU groups. Based on the results generated in this study, there was no association between clinical parameters (i.e., CD4 T cell count, CD8 T cell count and CD4:CD8 ratio) and Tfh cells (phenotypically characterised as CD4+CXCR5+PD-1+).

Advancing on to the phenotypic investigations, the goal of this study was to characterise peripheral Tfh cells (based on the expression of CD4, CXCR5, PD-1 and additionally ICOS) and compare the differences in frequency for HIT, HEU and HUU children in the South African setting. The relationship between Tfh cells and other lymphocyte populations of interest was also investigated to gain a deeper

understanding of the individual roles and dynamics between immune cell populations in relation to HIV infection. Additionally, to gain insight into the associations between Tfh cells and immune activation (and exhaustion) as well as inflammation, which are key factors of HIV immunopathology.

The percentage of CD4 T cells is considered to reflect CD4 T cell count relative to other immune cells. It has been suggested that it is a more stable measure of immune status compared to CD4 count, which tends to fluctuate and needs to be tested for several times over a period of time in order to identify a trend. A normal range of the percentage of CD4 T cells is between 25 – 65% for an HIV-negative individual (i-base, 2022).

In this study, although the percentage of CD4 T cells fell within the normal range for each group, the percentage of CD4+ T cells was found to be significantly higher in the HUU group in comparison to the HIT group. Suggesting that even though normalisation of the percentage of CD4 cells is achieved with early ART, it does not mirror that of a healthy uninfected individual.

Tfh cells are a specialised subset of CD4 T cells that primarily function to aid B cells within GCs and are crucial for the generation of T cell-dependent Ab responses. In recent years, peripheral Tfh cells have gained profound interest as the functional and phenotypic counterpart of circulating Tfh cells since they are easily accessible and act as possible biomarkers for long-lasting humoral immunity (Sánchez-Vargas & Mathew, 2019).

Interestingly, no significant difference was observed between the three groups with regards to the proportion of CD4+CXCR5+PD-1+ Tfh cells. This may be an indication that the proportion of CD4+CXCR5+PD-1+ Tfh cells is relatively similar among early treated HIV-infected children or HIV-exposed uninfected children and uninfected unexposed children as a result of the initiation of treatment against HIV early in life.

In contrast, the ICOS+ subset of Tfh cells (phenotypically characterised as CD4+CXCR5+PD-1+ICOS+) was significantly lower in the HUU group compared to the HIT and HEU groups. The HIT group especially demonstrated a significantly increased proportion of ICOS+ Tfh cells in comparison to the HUU group. Disruption of the Tfh cell compartment has been previously documented in HIV infected children irrespective of antiretroviral treatment however it is noticeably reduced as a result of

the early initiation of ART and consequent reduction in viral load (Shalekoff et al., 2021).

As peripheral blood was used to determine the frequency of cell populations, the low proportion of CD4+CXCR5+PD-1+ Tfh cells in HIT children may be an indication of the preferential localisation of Tfh cells from peripheral blood to lymphoid follicles. Several studies have demonstrated that Tfh cells constitute a major reservoir for latent HIV infection and escape Ag-specific CD8 T cell immune clearance by migrating to and seeking sanctuary within lymphoid follicles.

ICOS plays a key role in follicular localisation and facilitates the interaction of Tfh and B cells within GCs of lymphoid follicles. In healthy individuals, these Tfh cells are rare and low in number. In this study, CXCR5+PD-1+ICOS+ Tfh cells were found to be expanded in the HIT and HEU group in comparison to the HUU group.

The expansion of CXCR5+PD-1+ICOS+ Tfh cells within the HIT group could be connected to the preferential differentiation of CD4+ Th cells into Tfh cells during HIV infection. Abnormal increases in Tfh cell proportions have been associated with the spontaneous development of GCs and generation of autoantibodies (Chen et al., 2019).

Treg cells, another subset of C4 T cells (phenotypically characterised as CD4+CD25+FOXP3+) function to supress and restrain Th cell and Tc cell responses during infection to prevent autoimmunity and inflammation. Although no significant differences in the frequency of total Treg cells was observed between the three groups, several significant differences were identified for activated (CD38+ and CD69+) and follicular-homing (CXCR5+) subsets.

The proportion of CD38+ Treg cells was significantly higher in the HIT group compared to the other two groups. This heightened activation of Treg cells illustrates the need for immune control during HIV infection. In contrast, the HUU group demonstrated a significantly lower proportion of CD69+ Treg cells in comparison to the HIT and HEU groups. In addition, CD69+ Treg cells shared an inverse correlation with Tfh cells within the HEU group. Treg cells are responsible for immune regulation and execute this by limiting the spread of virus by activated infected T cells (Kleinman et al., 2018).

In regards to the follicular-homing subset of Treg cells, CXCR5+ Treg (Tfr) cells were significantly expanded in the HIT group in comparison to both the HEU and HUU group. Tfr cells play a role in impairing the function of Tfh cells (Kleinman et al., 2018). The finding of activated follicle homing cells may point to this as a source for some of the immune activation demonstrated in HIT children.

Dynamic responses of CD8 T cells are crucial for the effective control of viral replication (Lu et al., 2021). In this study it was observed that the proportion of CD8+ T cells was significantly expanded in the HIT group compare to the HUU group.

In the course of immune responses to infection, CD8 T cells that are Ag-specific (i.e., effector cytotoxic T cells) ordinarily do not enter B-cell follicles. However, the latest research has identified a population of CXCR5-expressing follicular CD8 T cells (i.e., Tfc cells) that are able to home to B-cell follicles where they target and eliminate infected Tfh and B cells during acute and chronic infections (Chen et al., 2019). In this study, no significant difference in the proportion of CXCR5+ Tfc cells was observed. However, activated subsets of CD38+ Tfc and CD69+ Tfc were found to be significantly expanded in the HIT group and HEU group, respectively. The HIT group also demonstrated a significantly higher proportion of both CD38+ Tfc and CD69+ Tfc compared to the HUU group.

Additionally, the proportion of CD4+CXCR5+PD-1+ Tfh cells inversely correlated with CD38 Tfc cells within thin the HIT group and CD69 Tfc cells within the total study population. This suggests that activated Tfc cell subsets function to target and reduce the number of Tfh cells, potentially reducing the size of the HIV reservoir to which infected Tfh cells contribute to. Additionally, since the excessive expansion of Tfh cells contributes to autoantibody production Tfc cells are of particular interest in the development of strategies to control autoimmunity incurred during HIV infection (Chen et al., 2019).

One of the hallmark characteristics of HIV immunopathology is the abnormally enhanced activation of immune cells. There are several indicators that can be used to measure levels of immune activation, however certain studies have shown that the expression of CD38 is the preferred predictor of disease progression for HIV infection (Lu et al., 2021). In regards to the activation of immune cells, characterised by the expression of CD38 and CD69 expression, the results of this study demonstrated

generally significantly higher percentages of CD38+ cell populations within the HIT group and CD69+ cells populations within the HEU group, respectively.

In this study, CD38+ Tc cells were significantly expanded in the HIT group compared to the HEU group and was negatively correlated with Tfh cells for the HIT group. CD69+ Tc cells were significantly expanded in the HEU group and negatively correlated with Tfh cells for both the whole study population as well as for the HIT group.

The HUU group demonstrated a lower proportion of dual-expression CD38+CD69+ Tc cells in comparison to the other groups. This cell population also shared an inverse correlation with Tfh cells for the entire study population.

The positive correlation observed between CD4+CXCR5+PD-1+ Tfh cells and PD-1+ Tc cells was found for each group individually as well as for the entire study population as a whole. Suggesting an association between Tfh cells and immune exhaustion. The HIT group had an increased frequency of PD-1+ Tfh cells in comparison to the HUU group. Several studies suggested that the high expression of PD-1 on Ag-specific CD8 T cells is an indicator of cellular exhaustion and that the inhibition of PD-1 and PD-L1 engagement enhances the functional capacity of these cells, with regards to proliferation and cytokine production, in response to infection (Sauce et al., 2007; Ahn et al., 2018). The exhaustion of Ag-specific CD8 T cells is a consequence of persistent antigen stimulation and immune cell activation that is frequently demonstrated in chronic infection, especially that of HIV infection. A lack of controlled replication may lead to an expansion of latently infected cells, contributing to a growing HIV reservoir.

Chronic immune activation and inflammation persists in HIV-infected individuals regardless of successful ART. The continued presence of viral antigens encourages immune activation and inflammation, which leads to the upregulation of proinflammatory cytokines and contributes to dysregulation in the T cell compartment. In addition, uncontrolled immune activation and inflammation is linked to an increased risk for developing non-AIDS co-morbidities (Zicari et al., 2019).

In this study, the levels of several proinflammatory cytokines were compared between groups. The increased level of inflammatory cytokines INF-α and hsCRP within the HIT group as well as the positive correlation between inflammatory cytokine, IL-1β and CD4+CXCR5+PD-1+ICOS+ Tfh cells, suggests that the expansion of Tfh cells is

contributed to, in part, by inflammation. This suggests that despite therapy and viral suppression there is ongoing innate stimulation (inflammation). The inflammation could be driven by persistent viral replication – or other factors such as intestinal barrier dysfunction (leaky gut). Increased mortality and morbidity have been linked to sustained inflammation within HIV-positive individuals, which plays a role in various pathologies (i.e., neurocognitive disorders, changes in the state of coagulation and vascular impairment) (Pérez et al., 2019).

Overall, this study showed an increase in the Tfh cell population in HIT children as well as persistent immune activation and inflammation. The additional expansion of follicular homing cells (Tfc and Treg cells) indicated that some lymphoid tissue processes were occurring. This may be an indirect indication of activity within lymph node/tissue reservoirs, where in the low levels of viral transcription and translation leads to innate and adaptive immune stimulation and expansion of follicle homing cells to regulate process. The findings need to be studied further – and an analysis of B cells (due to their relationship to Tfh cells) and NK cells (as key innate effectors) would be beneficial.

Over the past decade there have been many advances in research regarding Tfh cells. To a large extent there has been an interest in Tfh cell populations as a target for therapeutic interventions directed at human autoimmune diseases, especially that of HIV. Additionally, several studies have highlighted benefits of understanding Tfh cell-associated biology for vaccine development and enhancement (Crotty, 2019).

It has been suggested that Tfh cell populations monitored from peripheral blood and could be used as a prospective tool for measuring vaccine efficacy (Pissani & Streeck, 2014). However, because the definitive phenotype of Tfh cells in peripheral blood is controversial compared to established GC Tfh cells, it is difficult to determine what role Tfh cells play in HIV latency using only peripheral blood (Miles & Connick, 2016).
A deeper understanding of the dynamics of Tfh cells in the context of HIV may contribute to the development of immunotherapies for the elimination of HIV in viral reservoirs and reduction of immune dysregulation in HIV-infected children.

Study limitations and future recommendations

Several limitations were encountered in the course of this study. Due to the lack of stored available samples for selection a larger sample size could not be used. Although, the sample size (n = 59) used in this study did suffice to indicate some significant differences between groups and correlations between cell populations, a larger sample size many have demonstrated greater significance.

As cryopreserved samples were limited, only a certain number of events (i.e., 200 000 events) could be acquired during data acquisition. If more samples for each participant were available, a greater number of events could have been acquired which would have been beneficial for downstream gated populations (e.g., CD38- and CD69-expressing CD4+CXCR5+PD-1+ICOS+ Tfh cell populations) which are rare and proportionally low.

Furthermore, this study analysed peripheral Tfh cells as counterparts of GC Tfh cells. The analysis of GC Tfh cells from human lymphoid tissue could have yielded a more accurate depiction of differences between the three cohorts and associations with other cell populations. However, the invasive nature of accessing human lymphoid tissue (i.e., lymph node biopsies) comes with several ethical and practical constraints and was therefore not a realistic possibility for this study.

Lastly, several studies have associated Tfh cell dysregulation with hypergammaglobulinemia during HIV infection. Since plasma for each sample was also collected, it would be had been interesting to investigate IgG antibody levels within these cohorts to determine whether there is a link between Tfh cells and IgG antibody levels and how this translates to the development of hypergammaglobulinemia.

Chapter 6 – Conclusions and Future Perspectives

Research into the elimination of HIV is continually expanding and therefore the need for assays that efficiently measure the disease burden within ARV-treated infected patients has increased (Strain & Richman, 2013). This is especially relevant for children infected through vertical transmission, who's immature immune systems develop in the presence of HIV, and who may develop non-AIDS co-morbidities later in life due to low levels of persistent immune activation and inflammation.

This study phenotypically characterised and quantified a number of T cell populations (including follicular homing subsets in addition to Tfh cells) in three well-defined and matched groups in order to assess the dynamic relationships between Tfh cells and other T cell populations and assess the impact of immune activation (and exhaustion) as well as inflammation within HIV-infected and exposed children.

By determining the relative proportions of CD38 and CD69-expresing (i.e., markers of activation) T cells, this study demonstrated generally high levels of CD38+ T cell activation within early treated HIV-infected children and CD69+ T cell activation in HIV-exposed uninfected children, respectively. In addition, the finding that several activated T cell subsets (incl. activated Tc and Tfc cells) inversely correlated with total Tfh cells suggested that increased levels of immune activation could lead to a decline in Tfh cell populations. This highlighted the impact of immune activation has on the frequency of Tfh cells.

Immune exhaustion is the result of continuous, persistent immune activation and is common in chronic HIV infection. Through the assessment of immune exhaustion, this study demonstrated that the proportion of Tfh cells was directly linked to the proportion of exhausted Tc cells. Furthermore, it was proved that immune activation and inflammation persists in early treated HIV-infected and HIV-exposed children regardless of successful ART. Additionally, levels of inflammation are a contributing factor in the expansion of Tfh cells within HIT children.

As a result, this study provided a deeper insight into the relationships between Tfh cells populations and other T lymphocyte populations that play a significant role in

immune responses against HIV infection within HIV infected and HIV exposed children. Furthermore, it assessed the differences in proportions of T cell populations that have been shown to play a significant role in HIV immunopathology.

A number of cell populations assessed in this study are of particular interest for vaccine strategies and targeted immunotherapy against HIV infection. Through the suppression of Tfh cell populations, it may be possible to reduce levels of immune activation and inflammation that likely occurs as a result of action of effect CD8 T cells and Tregs against the expansion and dysregulation of the Tfh cell compartment during HIV infection.

References

Afran, L., Garcia Knight, M., Nduati, E., Urban, B. C., Heyderman, R. S., & Rowland-Jones, S. L. (2014). HIV-exposed uninfected children: A growing population with a vulnerable immune system? In *Clinical and Experimental Immunology* (Vol. 176, Issue 1, pp. 11–22). https://doi.org/10.1111/cei.12251

Ahn, E., Araki, K., Hashimoto, M., Li, W., Riley, J. L., Cheung, J., Sharpe, A. H., Freeman, G. J., Irving, B. A., & Ahmed, R. (2018). Role of PD-1 during effector CD8 T cell differentiation. *Proceedings of the National Academy of Sciences of the United States of America*, *115*(18), 4749–4754. https://doi.org/10.1073/pnas.1718217115

Alvarez, P., Mwamzuka, M., Marshed, F., Kravietz, A., Ilmet, T., Ahmed, A., Borkowsky, W., & Khaitan, A. (2017). Immune activation despite preserved CD4 T cells in perinatally HIV-infected children and adolescents. *PLoS ONE*, *12*(12). https://doi.org/10.1371/journal.pone.0190332

Bourke, C. D., Gough, E. K., Pimundu, G., Shonhai, A., Berejena, C., Terry, L., Baumard, L., Choudhry, N., Karmali, Y., Bwakura-Dangarembizi, M., Musiime, V., Lutaakome, J., Kekitiinwa, A., Mutasa, K., Szubert, A. J., Spyer, M. J., Deayton, J. R., Glass, M., Geum, H. M., … Prendergast, A. J. (2019). Cotrimoxazole reduces systemic inflammation in HIV infection by altering the gut microbiome and immune activation. *Science Translational Medicine*, *11*(486). https://doi.org/10.1126/scitranslmed.aav0537

Cao, W., Mehraj, V., Kaufmann, D. E., Li, T., & Routy, J. P. (2016). Elevation and persistence of CD8 T-cells in HIV infection: The Achilles heel in the ART era. *Journal of the International AIDS Society*, *19*(1). https://doi.org/10.7448/IAS.19.1.20697

Chen, Y., Yu, M., Zheng, Y., Fu, G., Xin, G., Zhu, W., Luo, L., Burns, R., Li, Q. Z., Dent, A. L., Zhu, N., Cui, W., Malherbe, L., Wen, R., & Wang, D. (2019). CXCR5+PD-1+ follicular helper CD8 T cells control B cell tolerance. *Nature Communications*, *10*(1). https://doi.org/10.1038/s41467-019-12446-5

Clerici, M., Saresella, M., Colombo, F., Fossati, S., Sala, N., Bricalli, D., Villa, M. L., Ferrante, P., Dally, L., & Vigano', A. (2000). *T-lymphocyte maturation abnormalities in uninfected newborns and children with vertical exposure to HIV*. www.bloodjournal.org

Cossarizza, A., Chang, H., Radbruch, A., Andr, I., Martin, B., Garc, M. D., & Wing, J. (2017). *Guidelines for the use of flow cytometry and cell sorting in immunological studies*. 1584–1797. https://doi.org/10.1002/eji.201646632

Crotty, S. (2019). T Follicular Helper Cell Biology: A Decade of Discovery and Diseases. In *Immunity* (Vol. 50, Issue 5, pp. 1132–1148). Cell Press. https://doi.org/10.1016/j.immuni.2019.04.011

Deeks, S. G., Kitchen, C. M. R., Liu, L., Guo, H., Gascon, R., Narváez, A. B., Hunt, P., Martin, J. N., Kahn, J. O., Levy, J., McGrath, M. S., & Hecht, F. M. (2004). Immune activation set point during early HIV infection predicts subsequent CD4+ T-cell changes independent of viral load. *Blood*, *104*(4), 942–947. https://doi.org/10.1182/blood-2003-09-3333

Demers, K. R., Reuter, M. A., & Betts, M. R. (2013). *CD8 + T-cell effector function and transcriptional regulation during HIV pathogenesis*.

Eggena, M. P., Barugahare, B., Jones, N., Okello, M., Mutalya, S., Kityo, C., Mugyenyi, P., & Cao, H. (2005). Depletion of Regulatory T Cells in HIV Infection Is Associated with Immune Activation. *The Journal of Immunology*, *174*(7), 4407–4414. https://doi.org/10.4049/jimmunol.174.7.4407

Ekali, G. L., Jesson, J., Enok, P. B., & Leroy, V. (2019). Effect of in utero exposure to HIV and antiretroviral drugs on growth in HIV-exposed uninfected children: A systematic review and meta-analysis protocol. In *BMJ Open* (Vol. 9, Issue 6). BMJ Publishing Group. https://doi.org/10.1136/bmjopen-2018-023937

Fahey, L. M., Wilson, E. B., Elsaesser, H., Fistonich, C. D., McGavern, D. B., & Brooks, D. G. (2011). Viral persistence redirects CD4 T cell differentiation toward T follicular helper cells. *Journal of Experimental Medicine*, *208*(5), 987–999. https://doi.org/10.1084/jem.20101773

Gensous, N., Charrier, M., Duluc, D., Contin-Bordes, C., Truchetet, M.-E., Lazaro, E., Duffau, P., Blanco, P., & Richez, C. (2018). T Follicular Helper Cells in Autoimmune Disorders. *Frontiers in Immunology*, *9*(1637), 1–18. https://doi.org/10.3389/fimmu.2018.01637

Gulzar, N., & Copeland, K. F. T. (2004). CD8+ T-Cells: Function and Response to HIV Infection. In *Current HIV Research* (Vol. 2).

Hoffmann, M., Pantazis, N., Martin, G. E., Hickling, S., Hurst, J., Meyerowitz, J., Willberg, C. B., Robinson, N., Brown, H., Fisher, M., Kinloch, S., Babiker, A., Weber, J., Nwokolo, N., Fox, J., Fidler, S., Phillips, R., & Frater, J. (2016). Exhaustion of Activated CD8 T Cells Predicts Disease Progression in Primary HIV-1 Infection. *PLoS Pathogens*, *12*(7), 1–19. https://doi.org/10.1371/journal.ppat.1005661

i-base. (2022).1.9 Interpreting CD4 results: CD4 count and CD4 percentage. Treatment training manual. Retrieved from https://i-base.info/ttfa/section-1/9-interpreting-cd4-results-cd4-count-and-cd4-percentage/.

King, C., Tangye, S. G., & Mackay, C. R. (2008). T Follicular Helper (T_{FH}) Cells in Normal and Dysregulated Immune Responses. *Annual Review of Immunology*, *26*(1), 741–766. https://doi.org/10.1146/annurev.immunol.26.021607.090344

Kinter, A., Mcnally, J., Riggin, L., Jackson, R., Roby, G., & Fauci, A. S. (2007). *Suppression of HIV-specific T cell activity by lymph node CD25 regulatory T cells from HIV-infected individuals*. www.pnas.orgcgidoi10.1073pnas.0611423104

Kitchen, S. G., Jones, N. R., LaForge, S., Whitmire, J. K., Vu, B.-A., Galic, Z., Brooks, D. G., Brown, S. J., Kitchen, C. M. R., & Zack, J. a. (2004). CD4 on CD8(+) T cells directly enhances effector function and is a target for HIV infection. *Proceedings of the National Academy of Sciences of the United States of America*, *101*(23), 8727–8732. https://doi.org/10.1073/pnas.0401500101

Kleinman, A. J., Sivanandham, R., Pandrea, I., Chougnet, C. A., & Apetrei, C. (2018). Regulatory T cells as potential targets for HIV cure research. In *Frontiers in Immunology* (Vol. 9, Issue APR). Frontiers Media S.A. https://doi.org/10.3389/fimmu.2018.00734

Leong, Y. A., Atnerkar, A., & Yu, D. (2017). Human immunodeficiency virus playing hide-and-Seek: Understanding the TFHcell reservoir and proposing strategies to overcome the follicle sanctuary. *Frontiers in Immunology*, *8*(MAY), 622. https://doi.org/10.3389/fimmu.2017.00622

Leong, Y. A., Chen, Y., Ong, H. S., Wu, D., Man, K., Deleage, C., Minnich, M., Meckiff, B. J., Wei, Y., Hou, Z., Zotos, D., Fenix, K. A., Atnerkar, A., Preston, S., Chipman, J. G., Beilman, G. J., Allison, C. C., Sun, L., Wang, P., … Yu, D. (2016). CXCR5+ follicular cytotoxic T cells control viral infection in B cell follicles. *Nature Immunology*, *17*(10), 1187–1196. https://doi.org/10.1038/ni.3543

Lindqvist, M., van Lunzen, J., Soghoian, D. Z., Kuhl, B. D., Ranasinghe, S., Kranias, G., Flanders, M. D., Cutler, S., Yudanin, N., Muller, M. I., Davis, I., Farber, D., Hartjen, P., Haag, F., Alter, G., Schulze zur Wiesch, J., & Streeck, H. (2012). Expansion of HIV-specific T follicular helper cells in chronic HIV infection. *Journal of Clinical Investigation*, *122*(9), 3271–3280. https://doi.org/10.1172/JCI64314

Linterman, M. A., & Hill, D. L. (2016). Can follicular helper T cells be targeted to improve vaccine efficacy? *F1000Research [version 1 ; referees : 3 approved] Referee Status : 5*(0). https://doi.org/10.12688/f1000research.7388.1

Linterman, M. A., Pierson, W., Lee, S. K., Kallies, A., Kawamoto, S., Rayner, T. F., Srivastava, M., Divekar, D. P., Beaton, L., Hogan, J. J., Fagarasan, S., Liston, A., Smith, K. G. C., & Vinuesa, C. G. (2011). Foxp3+ follicular regulatory T cells control the germinal center response. *Nature Medicine*, *17*(8), 975–982. https://doi.org/10.1038/nm.2425

Lu, L., Wang, J., Yang, Q., Xie, X., & Huang, Y. (2021). The role of CD38 in HIV infection. In *AIDS Research and Therapy* (Vol. 18, Issue 1). BioMed Central Ltd. https://doi.org/10.1186/s12981-021-00330-6

Luo, Z., Li, Z., Martin, L., Hu, Z., Wu, H., Wan, Z., Kilby, M., Heath, S. L., Huang, L., & Jiang, W. (2017). Increased natural killer cell activation in HIV Infected immunologic non-responders correlates with CD4+ T cell recovery after antiretroviral therapy and viral suppression. *PLoS ONE*, *12*(1). https://doi.org/10.1371/journal.pone.0167640

McCarty, B., Mwamzuka, M., Marshed, F., Generoso, M., Alvarez, P., Ilmet, T., Kravietz, A., Ahmed, A., Borkowsky, W., Unutmaz, D., & Khaitan, A. (2018). Low Peripheral T Follicular Helper Cells in Perinatally HIV-Infected Children Correlate With Advancing HIV Disease. *Frontiers in Immunology*, *9*. https://doi.org/10.3389/fimmu.2018.01901

Miles, B., & Connick, E. (2016). T FH in HIV Latency and as Sources of Replication-Competent Virus. In *Trends in Microbiology* (Vol. 24, Issue 5, pp. 338–344). Elsevier Ltd. https://doi.org/10.1016/j.tim.2016.02.006

Miyamoto, M., Pessoa, S. D., Ono, E., Machado, D. M., Salomão, R., Succi, R. C. de M., Pahwa, S., & de Moraes-Pinto, M. I. (2010). Low CD4+ T-cell levels and B-cell apoptosis in vertically HIV-exposed noninfected children and adolescents. *Journal of Tropical Pediatrics*, *56*(6), 427–432. https://doi.org/10.1093/tropej/fmq024

Moukambi, F. F., Rodrigues, V., Fortier, Y., Rabezanahary, H., Borde, C. C., Krust, B., Andreani, G., Silvestre, R., Petrovas, C., Laforge, M., & Estaquier, J. J. (2017). CD4 T follicular helper cells and HIV infection: Friends or enemies? *Frontiers in Immunology*, *8*(FEB), 4–11. https://doi.org/10.3389/fimmu.2017.00135

Mouquet, H. (2017). Hunting Down the HIV-1 Reservoir: A Starring Role for Antibodies? In *Immunity* (Vol. 46, Issue 4, pp. 527–529). Cell Press. https://doi.org/10.1016/j.immuni.2017.04.001

Muema, D. M., Macharia, G. N., Olusola, B. A., Hassan, A. S., Fegan, G. W., Berkley, J. A., Urban, B. C., & Nduati, E. W. (2017). Proportions of circulating follicular helper T cells are reduced and correlate with memory B cells in HIV-infected children. *PLoS ONE*, *12*(4), 1–11. https://doi.org/10.1371/journal.pone.0175570

Nielsen, S. D., Jeppesen, D. L., Kolte, L., Clark, D. R., Sørensen, T. U., Dreves, A. M., Ersbøll, A. K., Ryder, L. P., Valerius, N. H., & Nielsen, J. O. (2001). Impaired progenitor cell function in HIV-negative infants of HIV-positive mothers results in decreased thymic output and low CD4 counts. *Blood*, *98*(2), 398–404. https://doi.org/10.1182/blood.V98.2.398

Nilsson, J., Boasso, A., Velilla, P. A., Zhang, R., Vaccari, M., Franchini, G., Shearer, G. M., Andersson, J., & Chougnet, C. (2006). HIV-1-driven regulatory T-cell

accumulation in lymphoid tissues is associated with disease progression in HIV/AIDS. *Blood*, *108*(12), 3808–3817. https://doi.org/10.1182/blood-2006-05-021576

Perdomo-Celis, F., Taborda, N. A., & Rugeles, M. T. (2017). Follicular CD8+ T Cells: Origin, function and importance during HIV infection. In *Frontiers in Immunology* (Vol. 8, Issue SEP). Frontiers Media S.A. https://doi.org/10.3389/fimmu.2017.01241

Pérez, P. S., Romaniuk, M. A., Duette, G. A., Zhao, Z., Huang, Y., Martin-Jaular, L., Witwer, K. W., Théry, C., & Ostrowski, M. (2019). Extracellular vesicles and chronic inflammation during HIV infection. In *Journal of Extracellular Vesicles* (Vol. 8, Issue 1). Taylor and Francis Ltd. https://doi.org/10.1080/20013078.2019.1687275

Pissani, F., & Streeck, H. (2014). Emerging concepts on T follicular helper cell dynamics in HIV infection. In *Trends in Immunology* (Vol. 35, Issue 6, pp. 278–286). Elsevier Ltd. https://doi.org/10.1016/j.it.2014.02.010

Puthanakit, T., Saphonn, V., Ananworanich, J., Kosalarasksa, P., Hansudewechakul, R., Vibol, U., et al. Early versus deferred antiretroviral therapy for children older than 1 year infected with HIV (PREDICT): a multicentre, randomised, open-label trial. *The Lancet Infectious Diseases, 12*(12): 933-41. https://doi.org/10.1016/s1473-3099(12)70242-6

Read, K. A., Powell, M. D., & Oestreich, K. J. (2016). T follicular helper cell programming by cytokine-mediated events. In *Immunology* (Vol. 149, Issue 3, pp. 253–261). Blackwell Publishing Ltd. https://doi.org/10.1111/imm.12648

Ruffin, N., HongThang, P., Rethi, B., Nilsson, A., & Chiodi, F. (2012). The impact of inflammation and immune activation on B cell differentiation during HIV-1 infection. *Frontiers in Immunology*, *2*(JAN). https://doi.org/10.3389/fimmu.2011.00090

Sánchez-Vargas, L. A., & Mathew, A. (2019). Peripheral follicular helper T cells in acute viral diseases: A perspective on dengue. In *Future Virology* (Vol. 14, Issue 3, pp. 161–169). Future Medicine Ltd. https://doi.org/10.2217/fvl-2018-0197

Sauce, D., Almeida, J. R., Larsen, M., Haro, L., Autran, B., Freeman, G. J., & Appay, V. (2007). *PD-1 expression on human CD8 T cells depends on both state of differentiation and activation status*.

Shalekoff, S., Loubser, S., Dias, B. D. C., Strehlau, R., Shiau, S., Wang, S., He, Y., Abrams, E. J., Kuhn, L., & Tiemessen, C. T. (2021). Normalization of B Cell Subsets but Not T Follicular Helper Phenotypes in Infants With Very Early Antiretroviral Treatment. *Frontiers in Pediatrics*, *9*. https://doi.org/10.3389/fped.2021.618191

Siliciano, R. F., & Greene, W. C. (2011). HIV latency. *Cold Spring Harbor Perspectives in Medicine*, *1*(1). https://doi.org/10.1101/cshperspect.a007096

Strain, M. C., & Richman, D. D. (2013). New assays for monitoring residual HIV burden in effectively treated individuals. *Current Opinion in HIV and AIDS* (Vol. 8, Issue 2, pp. 106–110). https://doi.org/10.1097/COH.0b013e32835d811b

The INSIGHT START Study Group (2015). Initiation of Antiretroviral Therapy in Early Asymptomatic HIV Infection. *N Engl J Med, 373(9):* 795-807. https://doi.org/10.1056/NEJMoa1506816

Titanji, K., de Milito, A., Cagigi, A., Thorstensson, R., Grützmeier, S., Atlas, A., Hejdeman, B., Kroon, F. P., Lopalco, L., Nilsson, A., & Chiodi, F. (2006a). Loss of memory B cells impairs maintenance of long-term serologic memory during HIV-1 infection. *Blood*, *108*(5), 1580–1587. https://doi.org/10.1182/blood-2005-11-013383

UNAIDS. (2020). UNAIDS DATA 2021. Retrieved from https://www.unaids.org/en/resources/documents/2020/unaids-data.

UNAIDS. (2021). UNAIDS DATA 2021. Retrieved from https://www.unaids.org/en/resources/documents/2021/2021_unaids_data.

Violari A., Cotton, M. F., Gibb, D. M., Babiker, A. G., Steyn, J., Madhi, S. A., et al. (2008) Early antiretroviral therapy and mortality among HIV-infected infants. *N Engl J Med, 359(21)*: 2233-44. https://doi.org/10.1056/NEJMoa0800971

WHO. (2022). HIV. Newsroom Fact Sheets. Retrieved from https://www.who.int/news-room/fact-sheets/detail/hiv-aids.

Xu, B., Wang, S., Zhou, M., Huang, Y., Fu, R., Guo, C., Chen, J., Zhao, J., Gaskin, F., Fu, S. M., & Yang, N. (2017). The ratio of circulating follicular T helper cell to follicular T regulatory cell is correlated with disease activity in systemic lupus erythematosus. *Clinical Immunology*, *183*, 46–53. https://doi.org/10.1016/j.clim.2017.07.004

Yu, D., & Ye, L. (2018). A Portrait of CXCR5+ Follicular Cytotoxic CD8+ T cells. In *Trends in Immunology* (Vol. 39, Issue 12, pp. 965–979). Elsevier Ltd. https://doi.org/10.1016/j.it.2018.10.002

Zhang, J., Liu, W., Wen, B., Xie, T., Tang, P., Hu, Y., Huang, L., Jin, K., Zhang, P., Liu, Z., Niu, L., & Qu, X. (2019). Circulating CXCR3+ Tfh cells positively correlate with neutralizing antibody responses in HCV-infected patients. *Scientific Reports*, *9*(1). https://doi.org/10.1038/s41598-019-46533-w

Zicari, S., Sessa, L., Cotugno, N., Ruggiero, A., Morrocchi, E., Concato, C., Rocca, S., Zangari, P., Manno, E. C., & Palma, P. (2019). Immune activation, inflammation, and non-AIDS co-morbidities in HIV-infected patients under long-term ART. In *Viruses* (Vol. 11, Issue 3). MDPI AG. https://doi.org/10.3390/v11030200

Appendix A

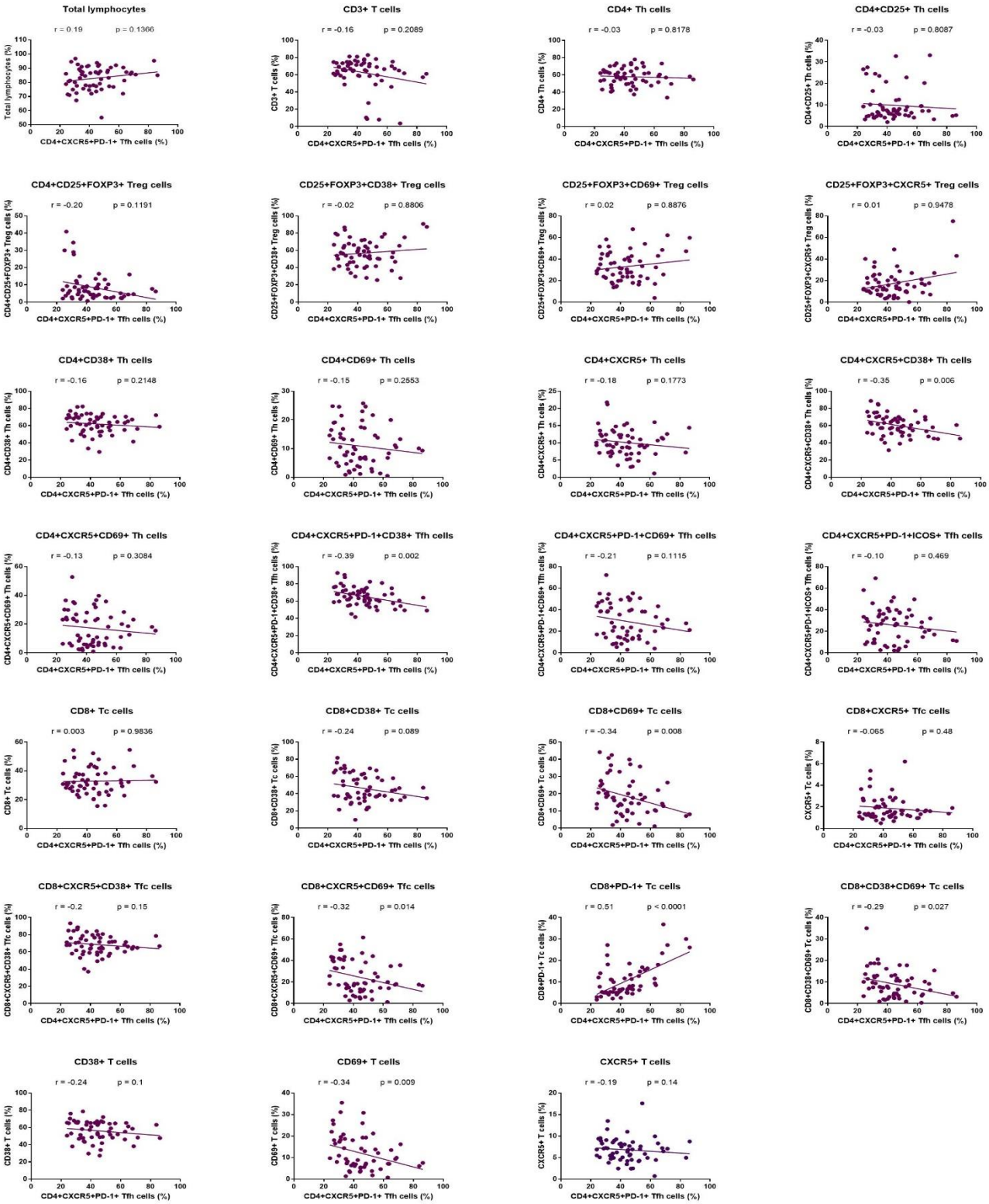

Figure A: Scatter plots showing the total correlations between CD4+CXCR5+PD-1+ Tfh cells and other T cell subsets.